Elettra Sincrotrone Trieste

Utilizzo della luce di Sincrotrone nell'imaging pre-clinico

Giuliana Tromba

SYnchrotron **R**adiation for **ME**dical **P**hysics (SYRMEP) beamline

Elettra - Sincrotrone Trieste

Elettra
Sincrotrone
Trieste

Outline

- Introduction to Synchrotron Radiation (SR)
- Advantages of using SR for biomedical imaging
- SR X-rays imaging techniques
  - K-edge subtraction imaging
  - *Phase sensitive* techniques
- Some applications

What is Synchrotron Radiation?

- Synchrotron Radiation (SR) is the electromagnetic radiation emitted by charged particles when they are accelerated radially.
- SR is produced in electron accelerators using 'bending magnets' and the so-called 'insertion devices' (undulators and wigglers)
- SR is extracted from the accelerators and transported to the experimental stations using vacuum pipes

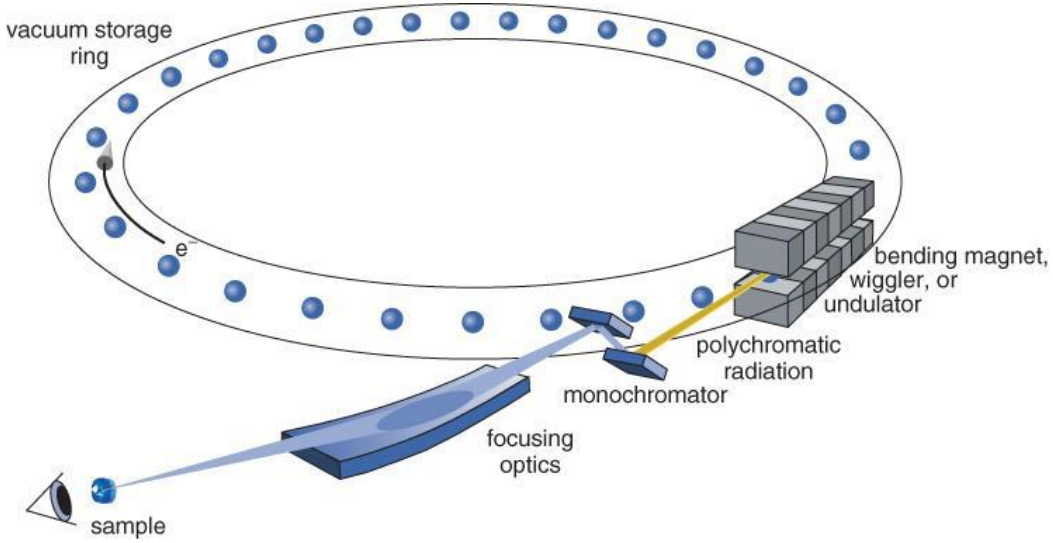

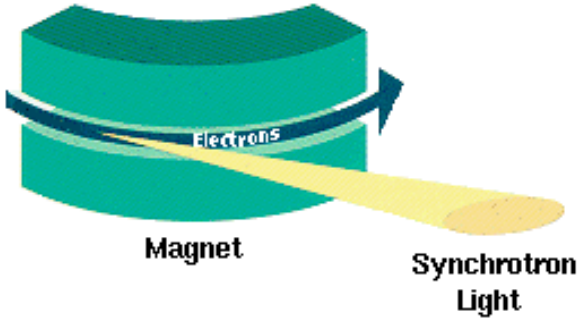

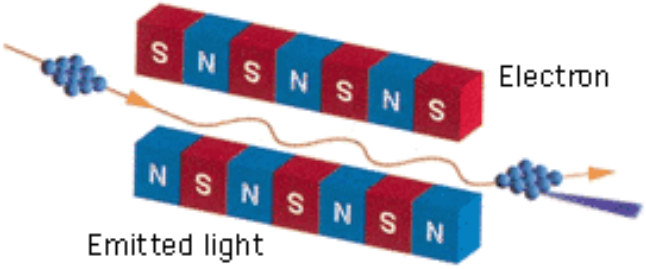

Elettra Sincrotrone Trieste

Skeme of a synchrotron facility

- Accelerators complex composed by Pre-injector, Booster, Storage ring
- Several beamlines operate simultaneously

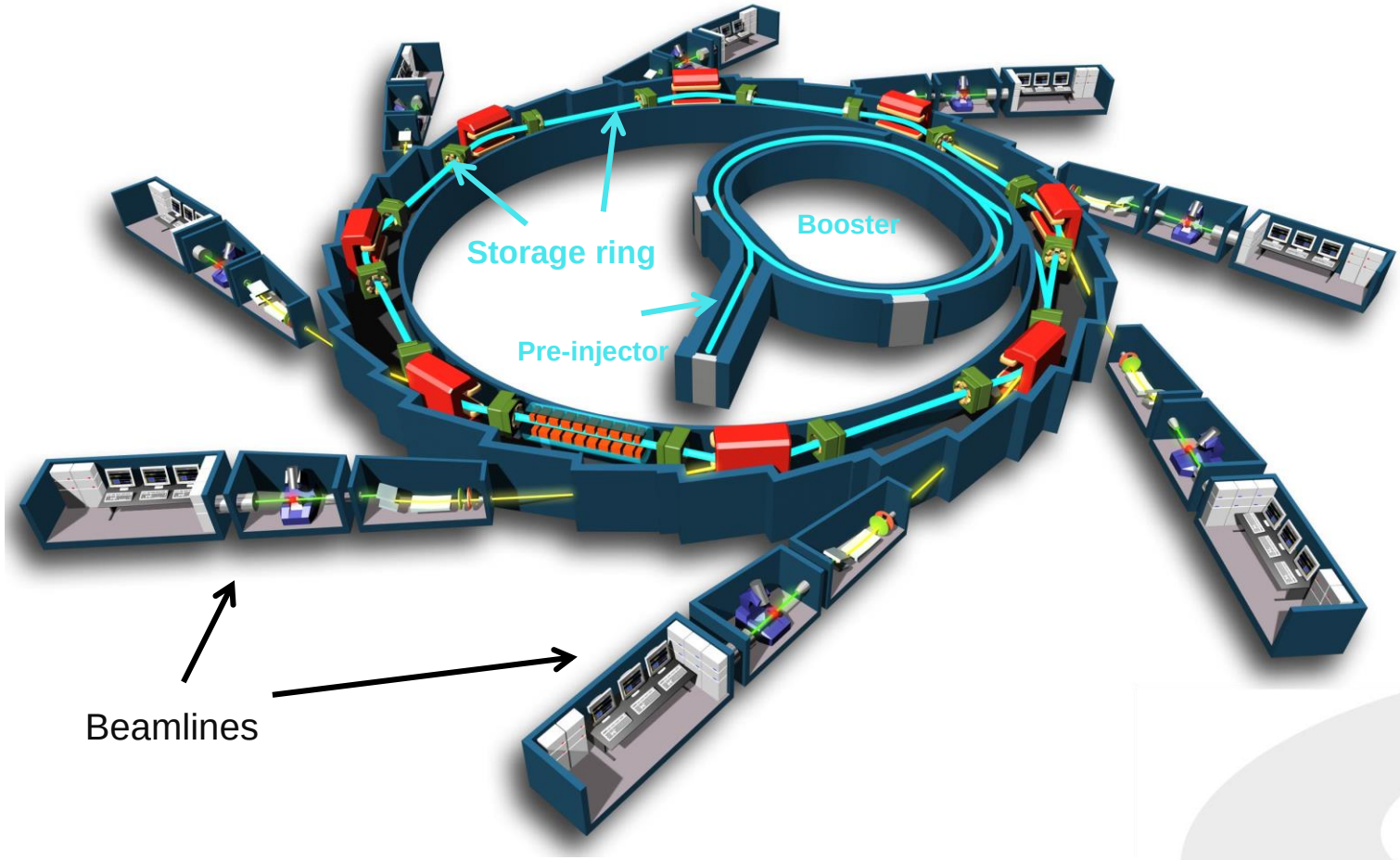

Advantages of SR for biomedical imaging

Monochromaticity allows for:

- *optimization* of X-ray energy according to the specific case under study (dose reduction)
- quantitative CT evaluations
- no beam hardening
- convenient use of contrast agent (**K-edge subtraction imaging**)

Spatial coherence

- Phase contrast overcomes the limitation of conventional radiology (it enables the applications of ***phase contrast techniques***)
- It brings to a dose reduction
- Improved contrast resolution, edges enhancement
- Use of phase retrieval algorithms to separate phase from absorption contribution

High fluxes

- Short exposure time
- Dynamic studies….

Collimation

- parallel beams, scatter reduction
- beam shaping (micro-beams)

Elettra
Sincrotrone
Trieste

SR X-rays imaging techniques

1) K-edge subtraction imaging

Exploiting the monochromaticity of SR…

K-edge Subtraction (KES) Imaging

1. Contrast agent: Iodine, or Gadolinium, etc.
2. Two Images are acquired: just Above (A) and just Below (B) the K-edge of Contrast agent
3. From image processing : Iodine and Tissue images can be separated

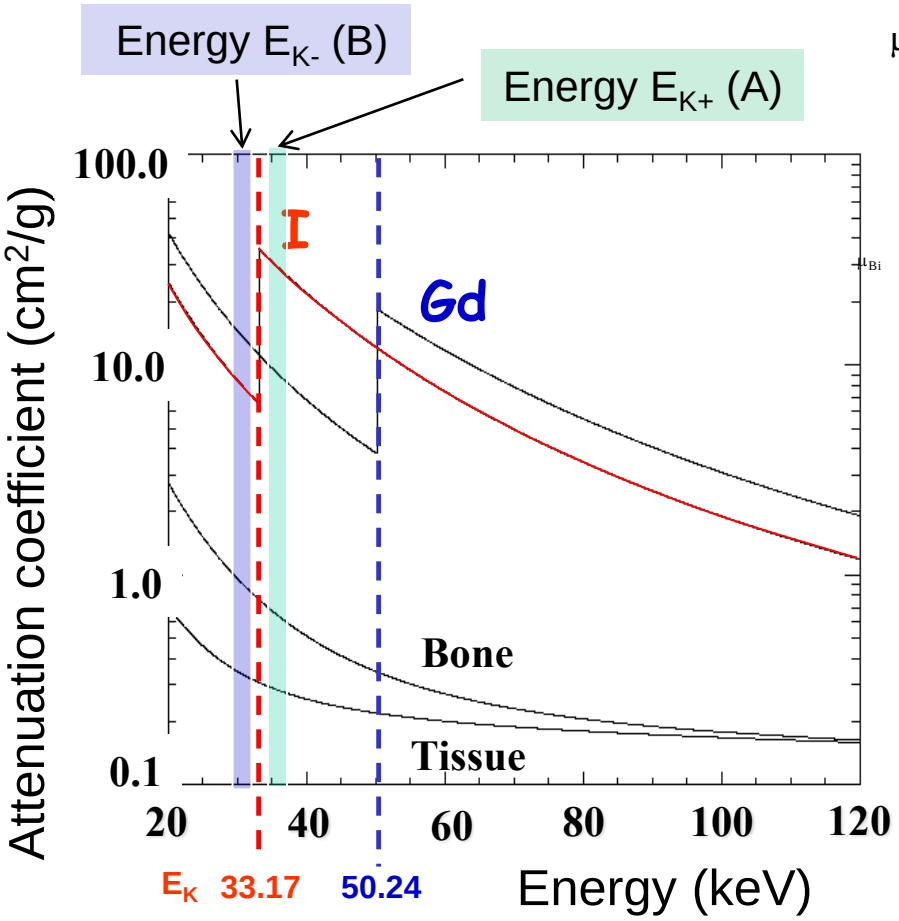

μ_{xy} : Attenuation coefficients : x = energies (A or B), y = material (tissue (t) or iodine (i)).

$$x_i = \frac{\mu_{Bi}\ln(A) - \mu_{Ai}\ln(B)}{\mu_{Bi}\mu_{At} - \mu_{Ai}\mu_{Bt}}$$

$$x_t = \frac{\mu_{Bi}\ln(A) - \mu_{Ai}\ln(B)}{\mu_{Bi}\mu_{At} + \mu_{Ai}\mu_{Bt}}$$

Elettra
Sincrotrone
Trieste

K-Edge absorption imaging: applications

- Coronary angiography (clinical research protocol)
- Bronchography/lungs imaging (pre-clinical – animal model)

Application to coronary angiography

Diagnosis of coronary diseases: detection of narrowing of arterial lumen (stenosis) in coronary arteries down to 1 mm diameter.

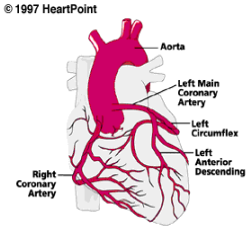

Conventional angiography:

- ☺ Excellent method for primary diagnosis
- ☺ Combination of diagnosis and intervention (angioplasty) possible
- ☹ Intra-arterial catheterization and injection of contrast agent (iodine)
- ☹ Invasive method with non-negligible risk (e.g. death 0.2%; myocardial infarct 0.3%)

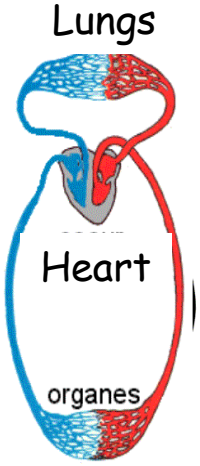

Transvenous Injection with SR

Conventional imaging: Arterial Injection

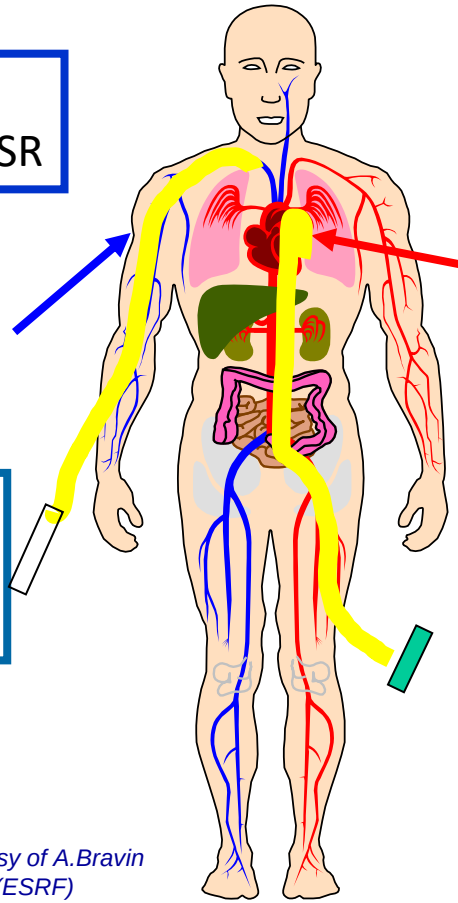

Catheter Arm Vein

Catheter in the Coronary Artery

Selective Opacification
Iodine concentration
350 mg/ml

Invasive

Circulation → Dilution
Iodine concentration : 10 mg/ml
Less invasive
Superposition

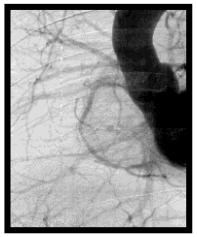

Courtesy of A.Bravin (ESRF)

Coronary angiography trial outcomes

- SR Angiography showed best spatial resolution of minimally-invasive techniques.
- No complications (64 patients).
- Possibility to clearly see intra-stent stenosis.
- The technique allows the detection of in-stent restenosis (ISR) on the Right Coronary Artery (RCA), for the Left Anterior Descending Artery (LAD) the diagnosis is difficult because of the superposition with the left ventricle or the aorta.
- Sensitivity (rate of true positive) and specificity (rate of true negative):
  79% sensitivity and 92% specificity for the RCA
  45% sensitivity and 98% specificity for the LAD

View of the RCA in a patient with stents

Tissue SR image with stent visualization | Iodine SR image | Iodine conventional angiography image

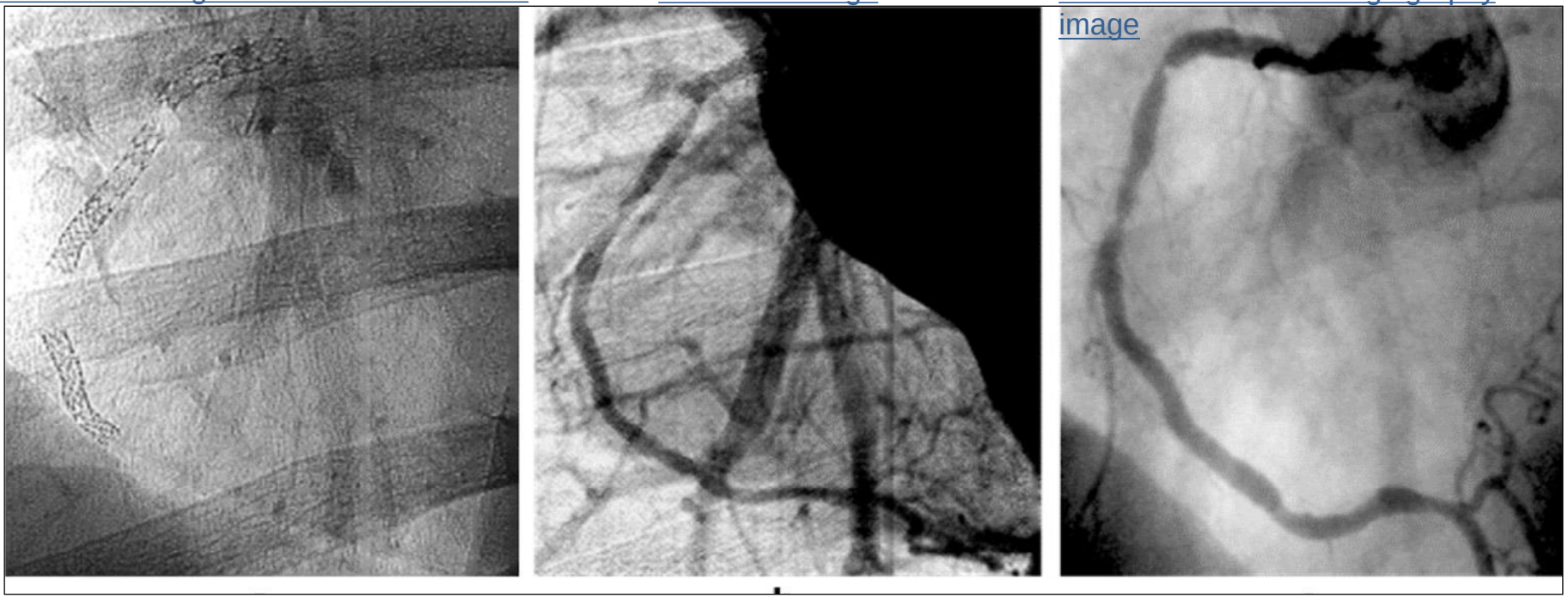

Bertrand B et al., Comparison of synchrotron radiation angiography with conventional angiography for the diagnosis of in-stent restenosis after percutaneous transluminal coronary angioplasty. Eur Heart J 2005;26.

Bronchography - CT imaging at ESRF

Dual Line Ge Detector
w: 150 mm, 350 μm pitch, beam thickness 700 μm
Used contrast agent: Xenon (gas)

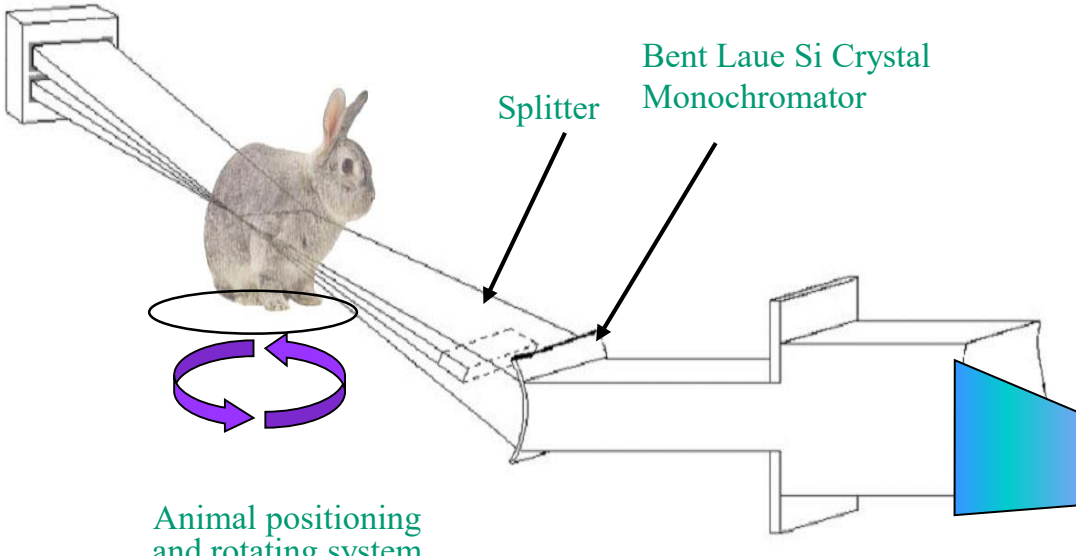

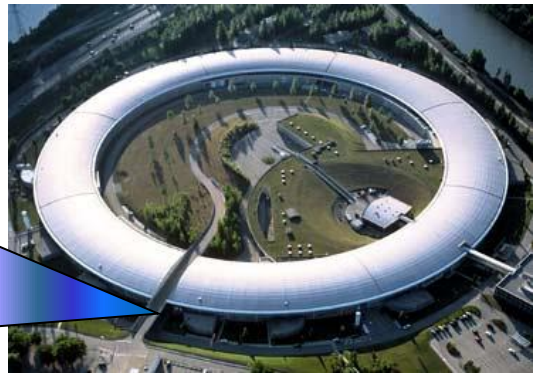

Image Processing

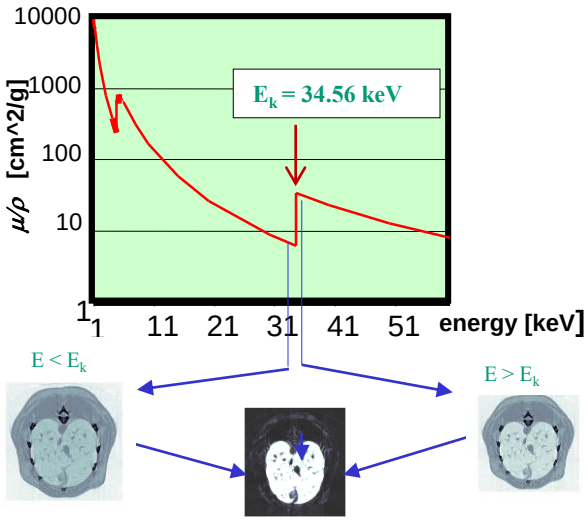

Projection Images
In Vivo Rabbit Lung
Xenon K-edge Imaging

Lung ventilation studies
Presence of ventilation heterogeneities

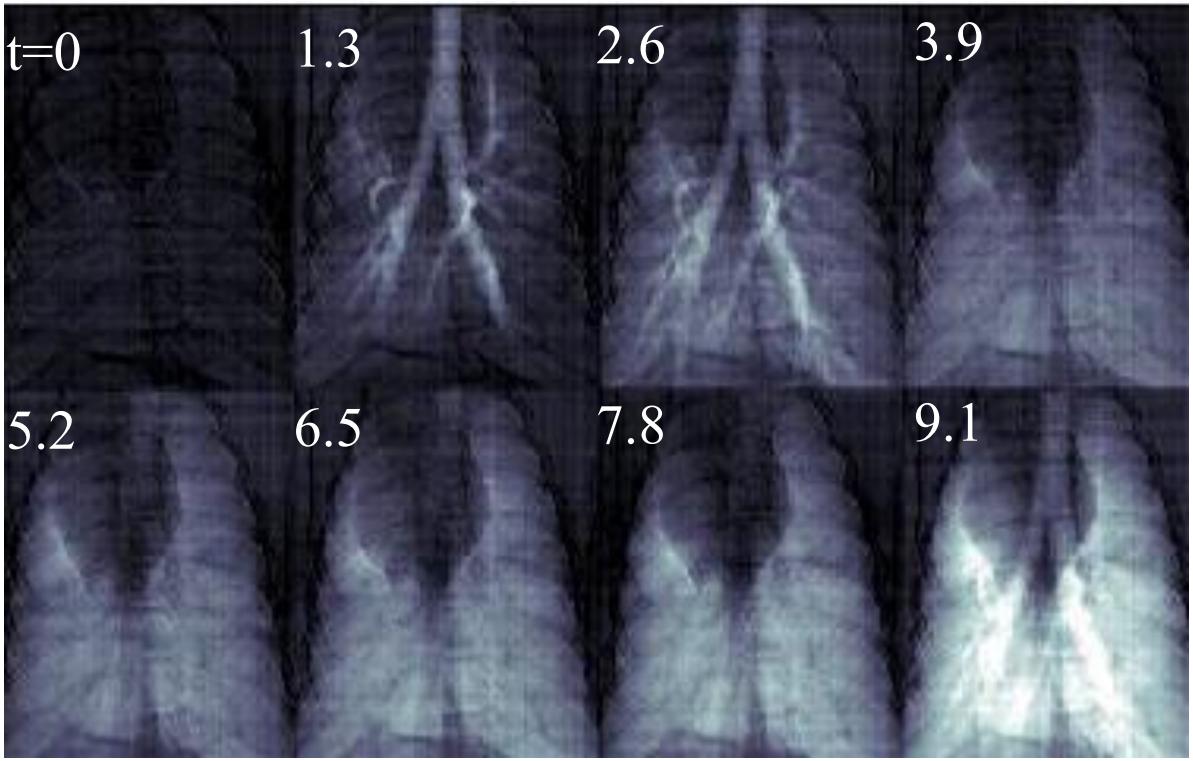

Time between images = 1.3 sec

Courtesy of A.Bravin (ESRF)

Effects on lungs ventilation induced by different treatments on healthy or asthmatic animals

Experimental asthma studies have been carried out to study allergic reactions by using **ovalbumine-sensitized rabbit model**. These reactions were compared with asthma reactions caused by non-specific drug provocation (Methacholine, Mch). Mch caused **airway narrowing** mainly on the central large airways, while ovalbumine induces **a predominantly peripheral and heterogeneous lung response**.

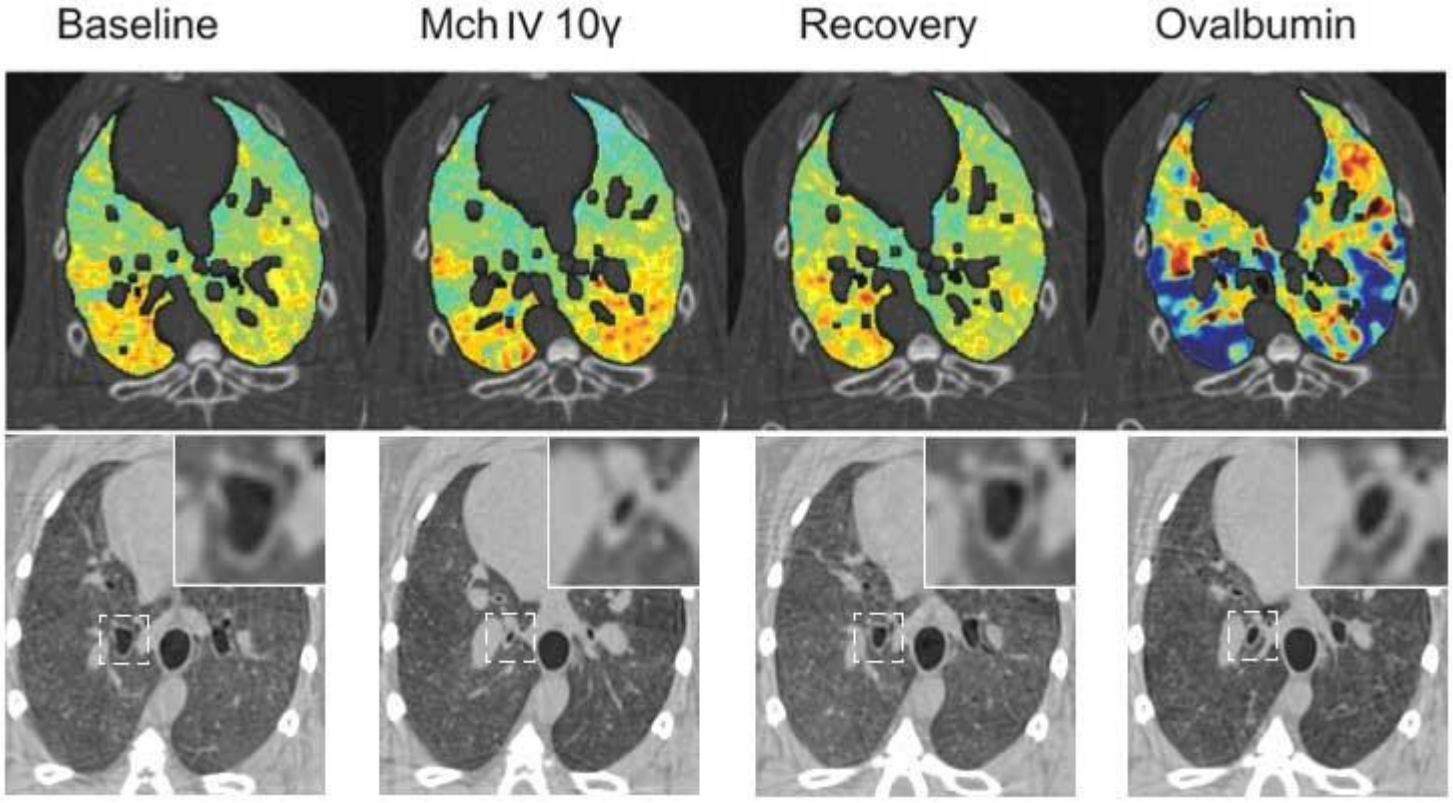

Upper part: **images of specific ventilation** in a sensitized rabbit at baseline, during Mch infusion, upon recovery and after Ovalbumine allergen provocation. Lower part: **absorption CT slices** showing changes in the central airway cross-sectional area at the different experimental stages in one representative animal. Magnifications of the indicated square areas are shown in the right-upper corners.

Courtesy of S.Bayat (INSERM-Univ. Grenoble)

 Bayat S. et al:, Am J Respir Crit Care Med.180(4) (2009).

Quantitative imaging of contrast agent: aerosol particle deposition

- To evaluate the inhaled aerosol particle distribution and targeting in the lung, knowledge of **regional deposition**, **lung morphology** and **regional ventilation**, is needed
- KES imaging was used to quantitatively map the regional deposition of **iodine labelled aerosol particles**
- 2 X-ray beams tuned at slightly different energies above and below the K-edge, of Xe (34.6 keV) or Iodine (33.2 keV)
- Two CT scans are simultaneously acquired during the inhalation of stable Xe gas or iodine-stained aerosol particles. The density due to the contrast element (Xe, I) can be separated from that of tissue, in each image.
- **"Xe-density" or "I-density" images allow the direct quantitative measurement of these elements within the airways.**
- **A "tissue-density" image obtained from the same data allows the assessment of lung morphology.**

Iodine Aerosol Depositionn *In Vivo* Rabbit

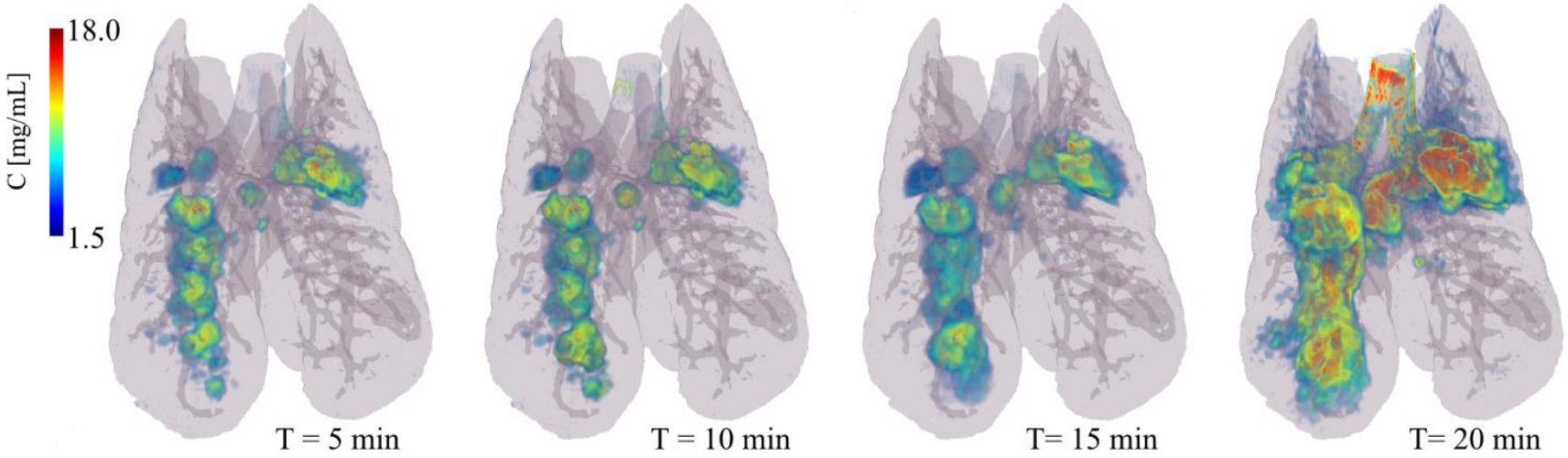

- Aerosol particles with 3 µm mass median aerodynamic diameter -> inhomogenous deposition !
- Comprehensive technique for studying biodistribution of inhaled drugs/pollutants

Courtesy of S.Bayat (INSERM-Univ. Grenoble)

Porra L. et al. Scientific Reports. 2018:8:3519

Phase sensitive techniques (PHase Contrast (PHC) imaging)

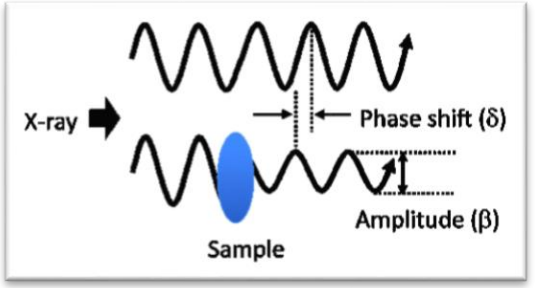

- X-ray interaction with matter is ruled by the **refractive index** (**n**). In the complex representation, it is composed by two parts: $n = 1 - \delta + i\beta$
  - The immaginary part (β), related to absorption properties of the material, determines the wave amplitude variation.
  - The real part (δ) defines the phase shifts effects induced by the material on the incoming wave

Linear attenuation of X-rays: $\mu = 4\pi\beta/\lambda$ (λ = X-ray wavelength)
Transmitted beam intensity: $I = I_0\, e^{-\mu t}$ (I_0 = incident intensity)
Phase shifts: $\phi = -2\pi\delta t/\lambda$ (t=sample thickness)

- Conventional imaging relies on **X-ray absorption** (measure of Amplitude variation)
- If X-ray source is highly coherent (like SR) also phase shifts of coherent X-rays can be measured
- **Phase contrast imaging** is based on the detection of **phase shifts** occurring to X-rays crossing the sample

Propagation based imaging (PBI) - Simplest approach – no optical element needed. Image contrast arises from interference among parts of the wavefront differently deviated (or phase shifted) by the sample.
Edge enhancement effects, different regimes according to the selected sample-to-detector distance.

Scheme of PBI

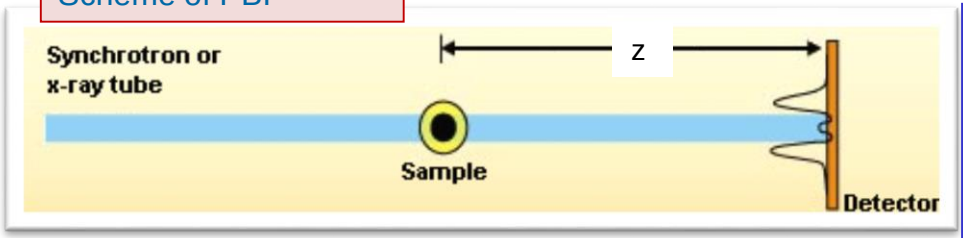

PHC regimes

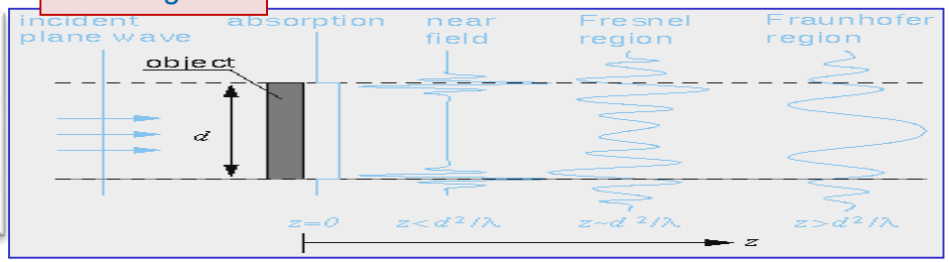

Elettra
Sincrotrone
Trieste

Edge enhancement effects

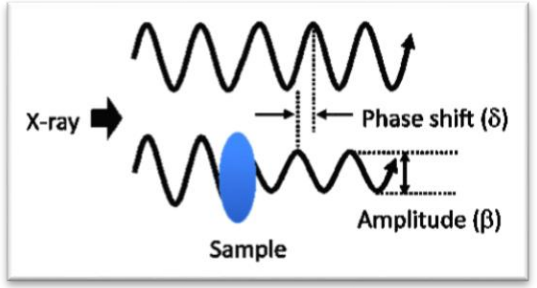

Absorption (z = 0)

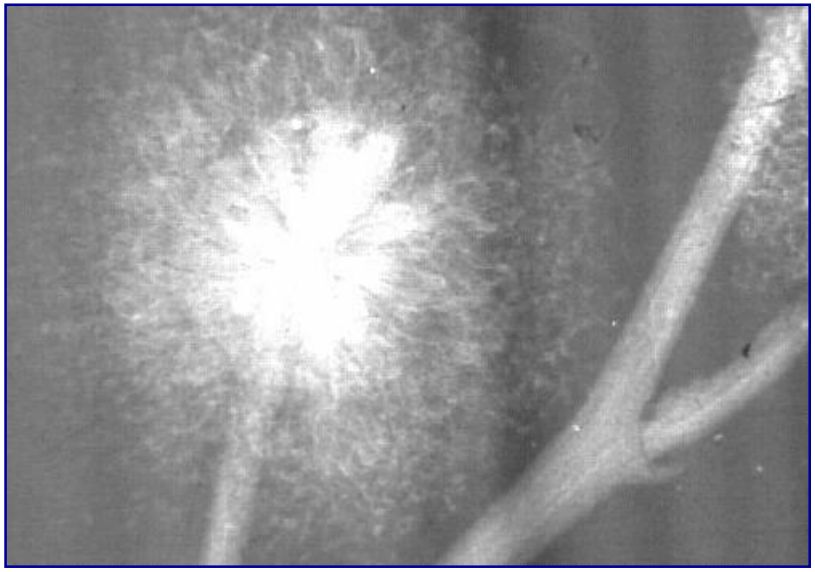

Near field (z = 50 cm)

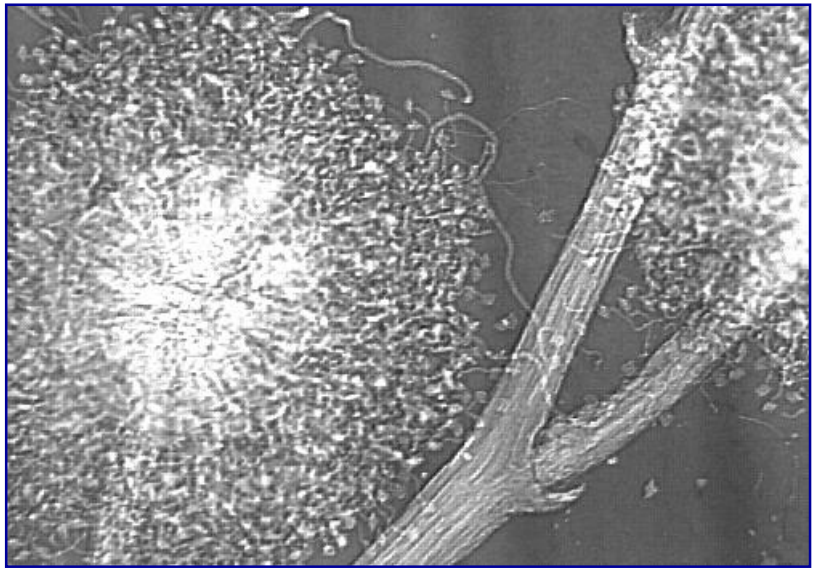

Edge enhancements effects – trend with X-ray energy

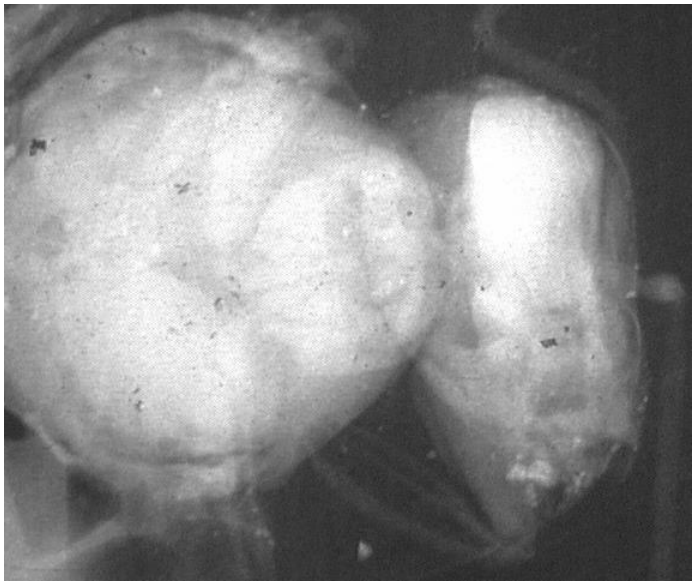

10 keV

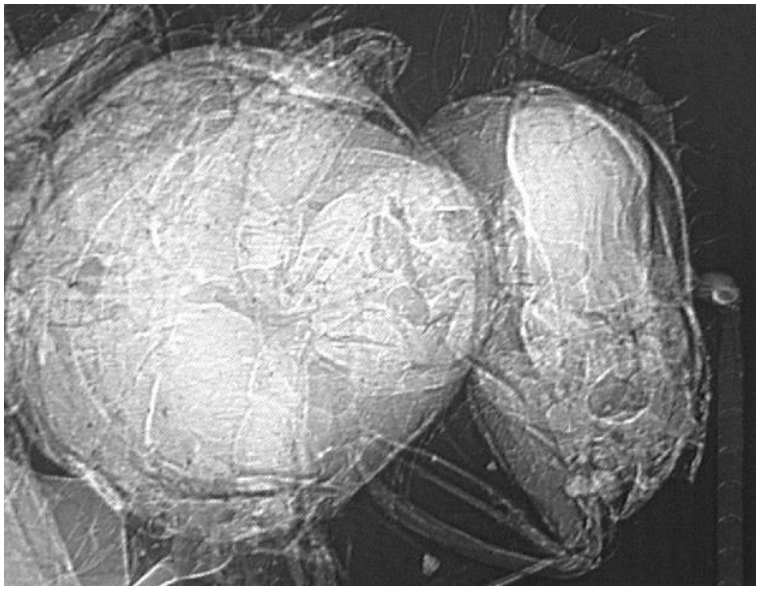

Absorption

Phase Contrast

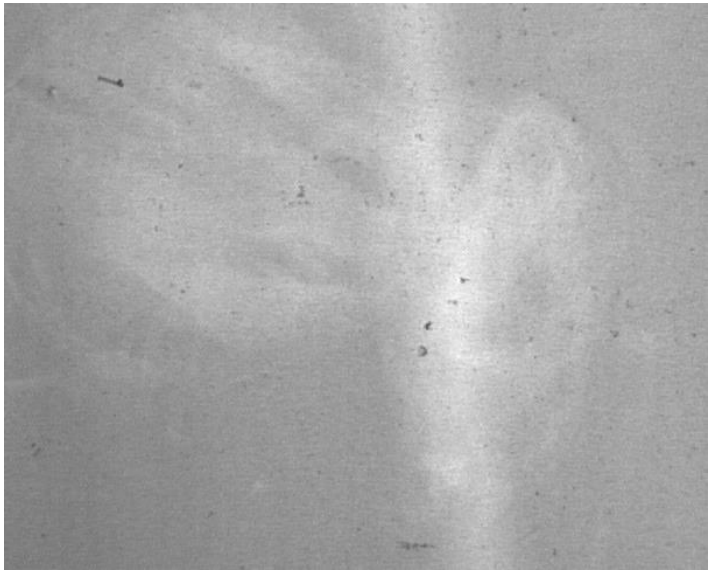

20 keV

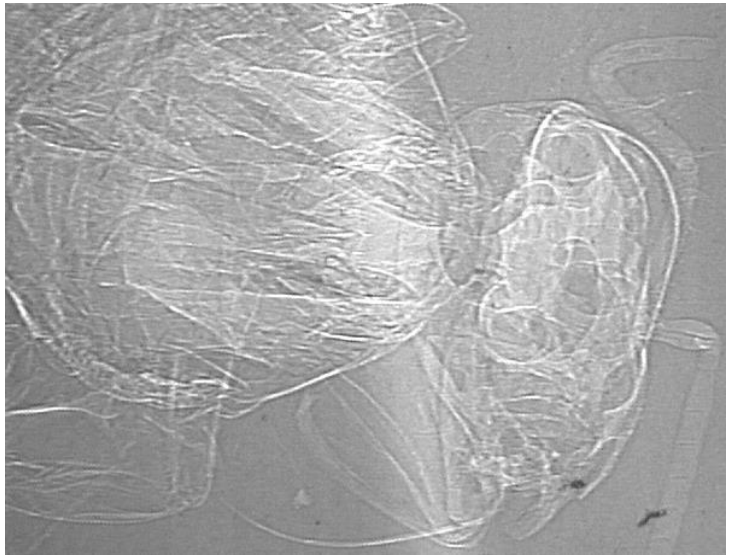

Edge enhancement effect and use of phase retrieval algorithms

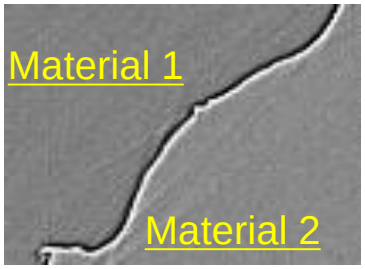

Edge between two materials with negligible absorption

An “edge” image obtained by PBI imaging does not resolve unambiguously the structure of the imaged sample

Complex refractive index: $n = 1 - \delta + i\beta$

phase — attenuation

Instead of “edge contrast” we would like “area contrast” (ideally a map of δ)
The approach to get the “area contrast” is called *phase retrieval* and two main approches exist:

- **Holotomography** - (P. Cloetens et al., ESRF) - quantitative approach with identification of material components, it requires multiple distances acquisition
- **Single-distance** – approximated, working on homogeneus materials in the near field conditions has the advantage to require acquisition at one distance (D. Paganin – Monash Univ.) – preferable for biomedical imaging

Edge contrast – PHC

Area contrast

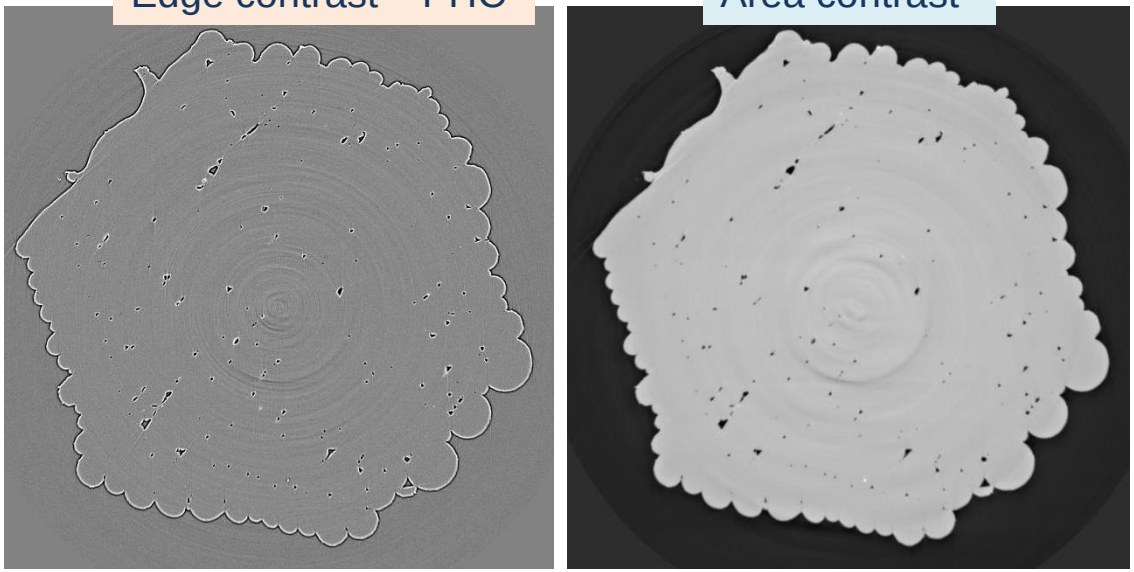

Typical edge enhancement features of PHC

Application of phase retrieval (Single distance algorithm)

*Paganin D., et al., J Microsc **206**, 33–40 (2002).*

P. Cloetens et al., Appl. Phys. Lett. 75, 2912 (1999)

PHC imaging: other approaches

Methods exploiting the particle nature of photons – measure of X-ray refraction angles

Analyzer Based Imaging

Use of perfect crystals to select angular directions of X-rays exiting the sample

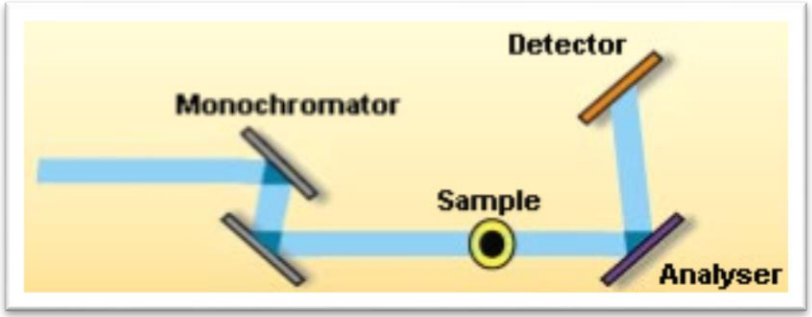

Coded Apertures

Use of coded apertures (masks) to select refraction angles

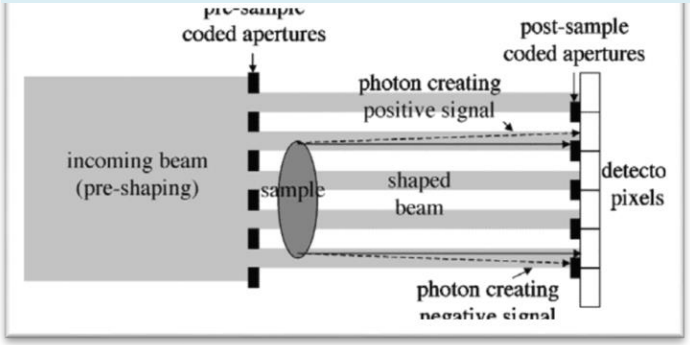

Interferometric approaches - waves are superimposed in order to extract information - direct measure of phase shifts introduced by the sample

Crystal Interferometry

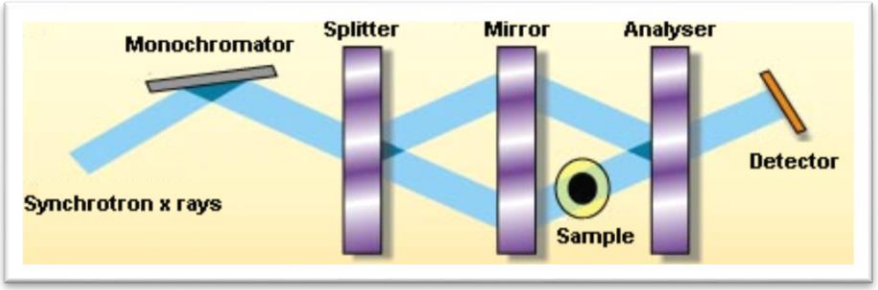

Grating interferometry

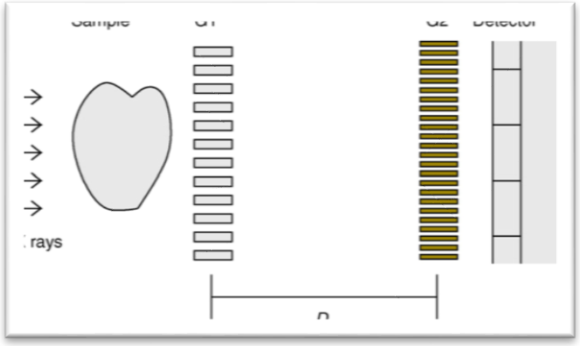

Analyzer Based Imaging (ABI)

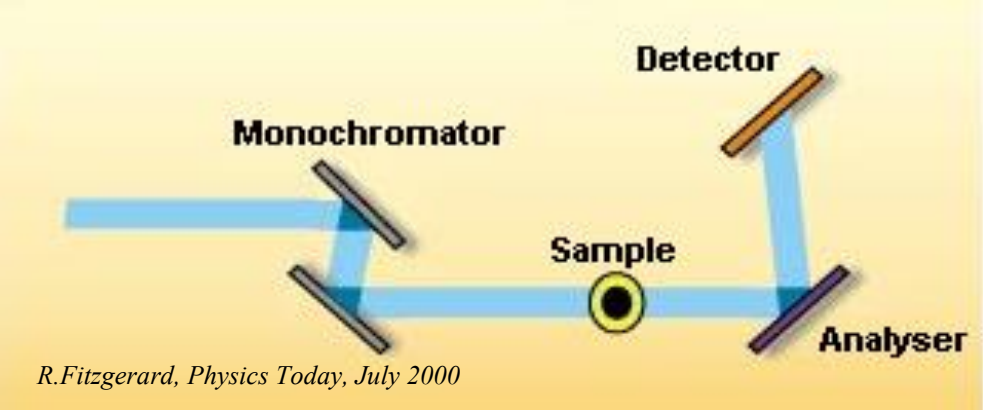

- A perfect crystal is used as an angular filter to select angular emission of X-rays. The filtering function is the rocking curve (FWHM: 1-20 μrad)
- Image formation with ABI is sensitive to a variation of δ in the sample. Indeed, **refraction angle is roughly proportional to the gradient of δ**
- Analyzer and monochromator aligned -> X-ray scattered by more than some tens μrad are rejected
- Small misalignments -> investigation of phase shift effects
- With greater misalignments the primary beam is almost totally rejected and pure refraction images are obtained
- Sensitive to $\nabla\Phi(x,y)$
- The technique requires the beam monochromaticity.

Podurets K. M. et al., Sov. Phys. Tech. Phys. 34(6), 1989
V. N. Ingal and E. A. Beliaevskaya, J. Phys. D: Appl. Phys. 28, 1995
Chapman D et al., Phys. Med. Biol. 42, 1997

ABI images for different analyzer positions

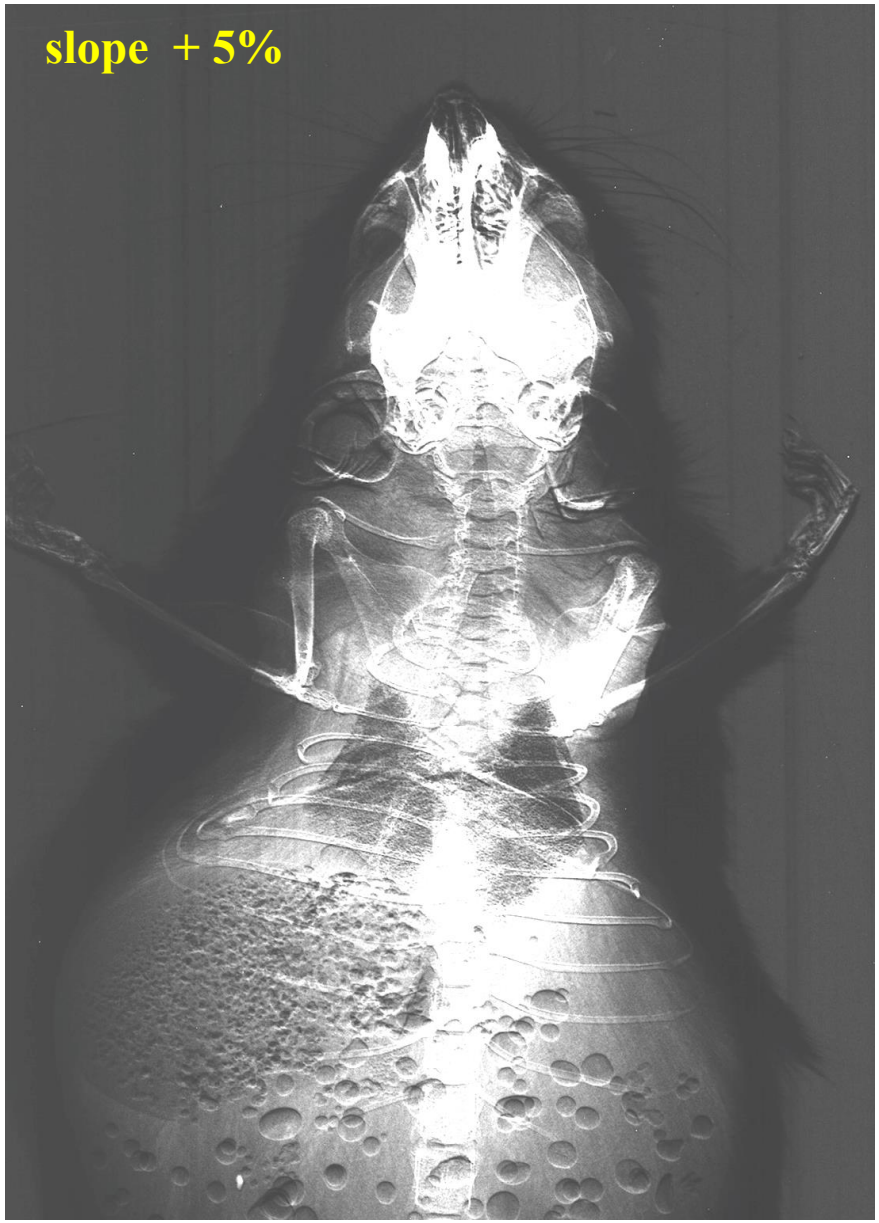

Apparent absorption and refraction images

Apparent absorption

Refraction image

Elettra
Sincrotrone
Trieste

Applications

Multiscale imaging for biomedical research

- "In vitro" imaging: high resolution morphological studies (es. micro-CT studies of tissues, organs, biomaterials - virtual histology)
  High resolution required, main limitation is radiation damage, typical pixel size:0.6-4 µm
- Imaging of small animals, tissues and organs (Pre-clinical research): applied for different purposes in the development of ***animal models*** *(ex vivo, in-vivo)*
  Research protocols, pixel size: 4.5 - 9 µm (ex-vivo) up to 100 µm (in-vivo).
- Potential applications to patients (Clinical imaging)
  *Need to **limit** radiation dose. Strict research protocol for selected patients. Find best compromise between dose and image quality, pixel sizes : 50 – 100 µm*

Increase of dose and spatial resolution

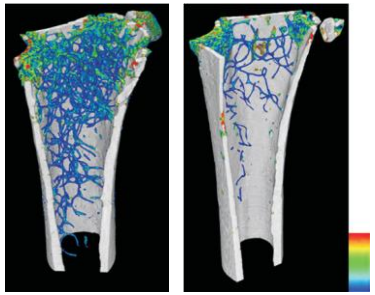

High resolution Phase Contrast imaging

- "In vitro" imaging: high resolution morphological studies (es. micro-CT studies of tissues, organs, biomaterials - virtual histology)
  High resolution required, main limitation is radiation damage

  - Virtual histology
    - Breast lesions
    - Imaging of atherosclerotic plaques (PBI and GI)
  - PBI potentials in tissues visualization
  - Use of staining and Phase Retrieval algorithm
  - Dose reduction with PHC Imaging

Virtual histology of breast malignant lesions

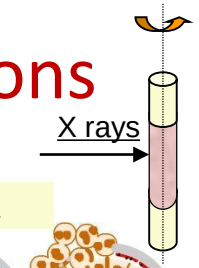

Use of high resolution microCT as complementary tool of histology

- Unstained sample embedded in paraffine (3–4 mm)
- White/pink scan, 0.9–1.2 μm pixel size
- sample–detector dist. = 19 cm, application of PHR

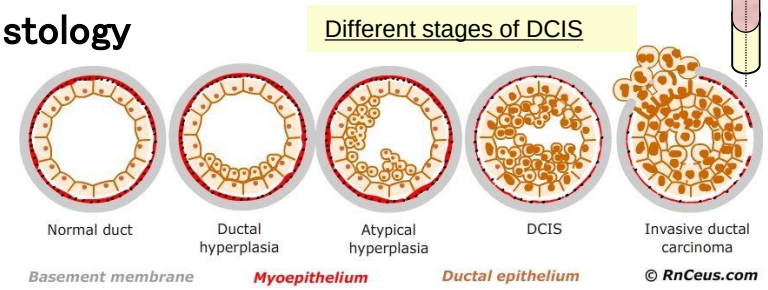

In situ cribriform Ductal Carcinoma (DCIS)

a) classical histological slice stained with haematoxylin and eosin, b) μCT slice

https://cdn.knightlab.com/libs/juxtapose/latest/embed/index.html?uid=cb428a40-d914-11e7-b263-0edaf8f81e27

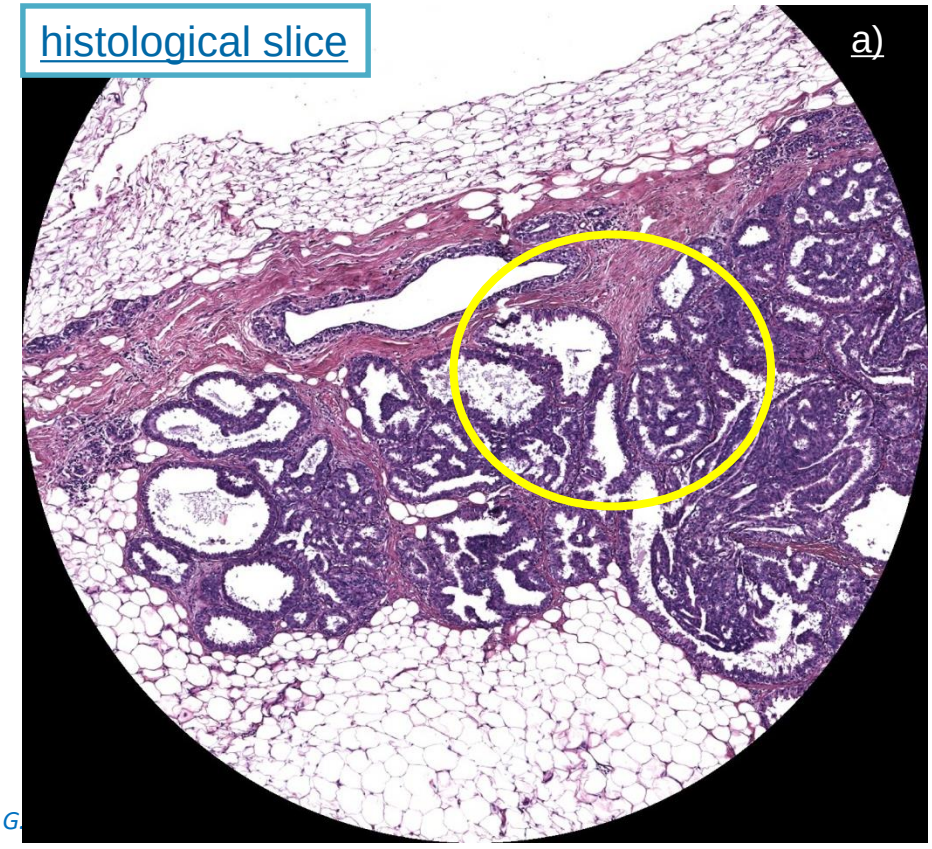

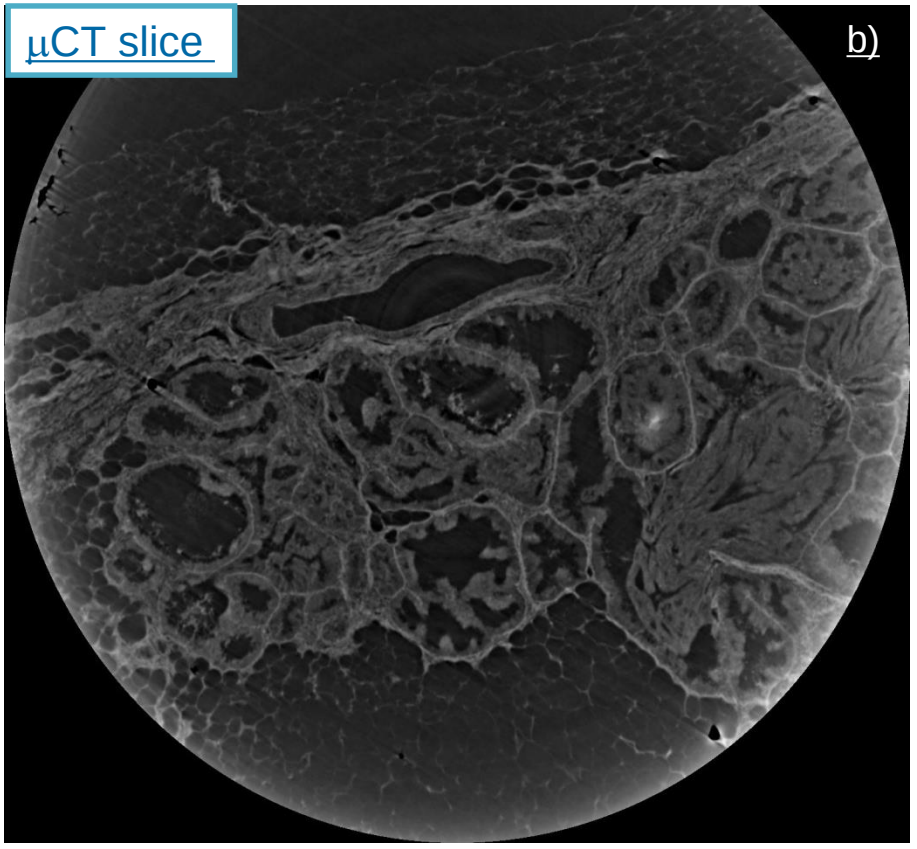

Breast malignant lesion: duct detail

histological slice - detail

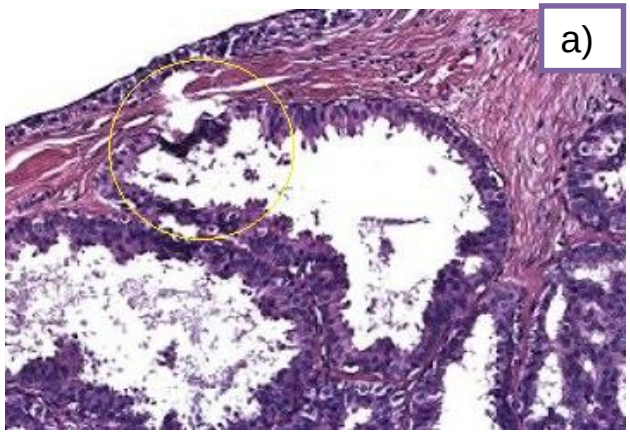

μCT slice - detail

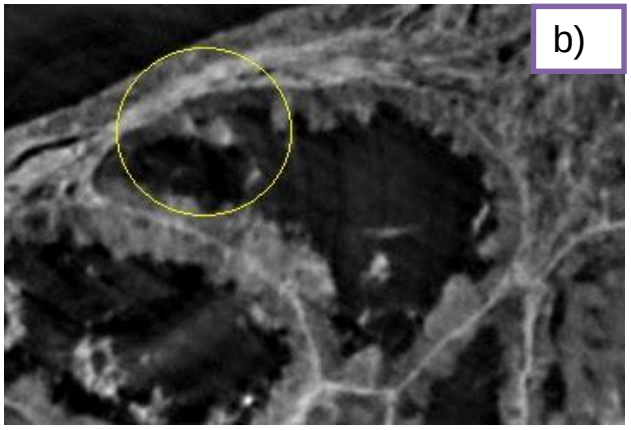

Close-up of a duct including micro-calcifications (yellow circle). On μCT image (b) calcifications are well visible, on the histology image (a) they are completely lost due to the cutting process causing an hyperchromasia (dark purple zone inside the circle).

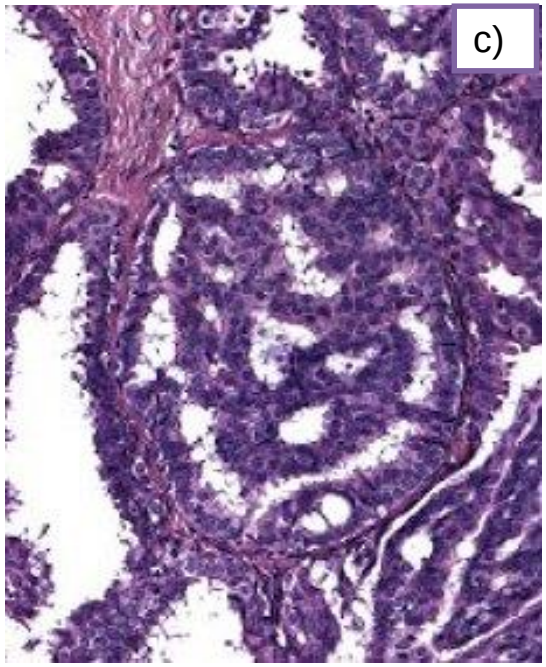

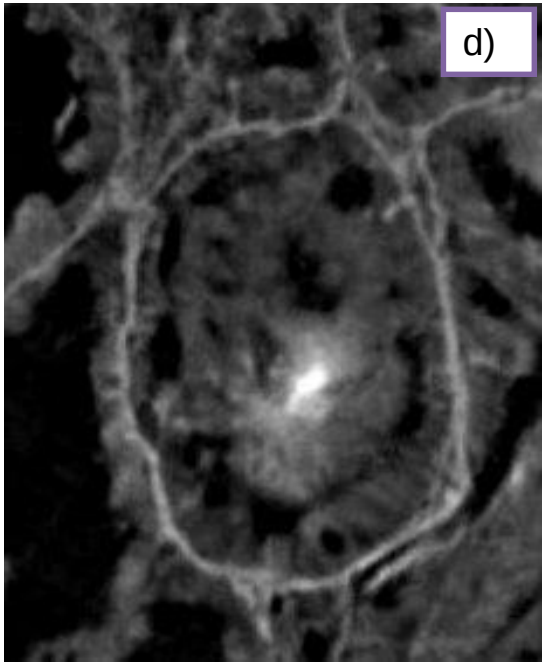

Duct with typical cribriform features. Basement membrane and calcification better visible in in d)

PBI μCT can be helpful for:

- deciding the cutting orientation of the histology
- evaluate presence of microcalcifications
- highlight interfaces (membranes, etc.)

Virtual histology: visualizing atherosclerosis plaques in mice using PBI

Animal model: atherosclerotic mouse

Apolipoprotein E-deficient (apo) mouse (deficient transgenic mice demonstrates a strong tendency to develop hyper-cholesterolemia)

Aim: evaluate the capability of **µ**CT to highlight the formation of atherosclerotic plaques in normal and Apo mice - All mice were fed with a high fat diet for 70 days.

Combination of soft tissue staining by phosphotungstic acid (PTA)* and sample embedding in paraffin or agarose gel allows direct overlay of **µ**CT data sets and microscopy after immunochemical staining

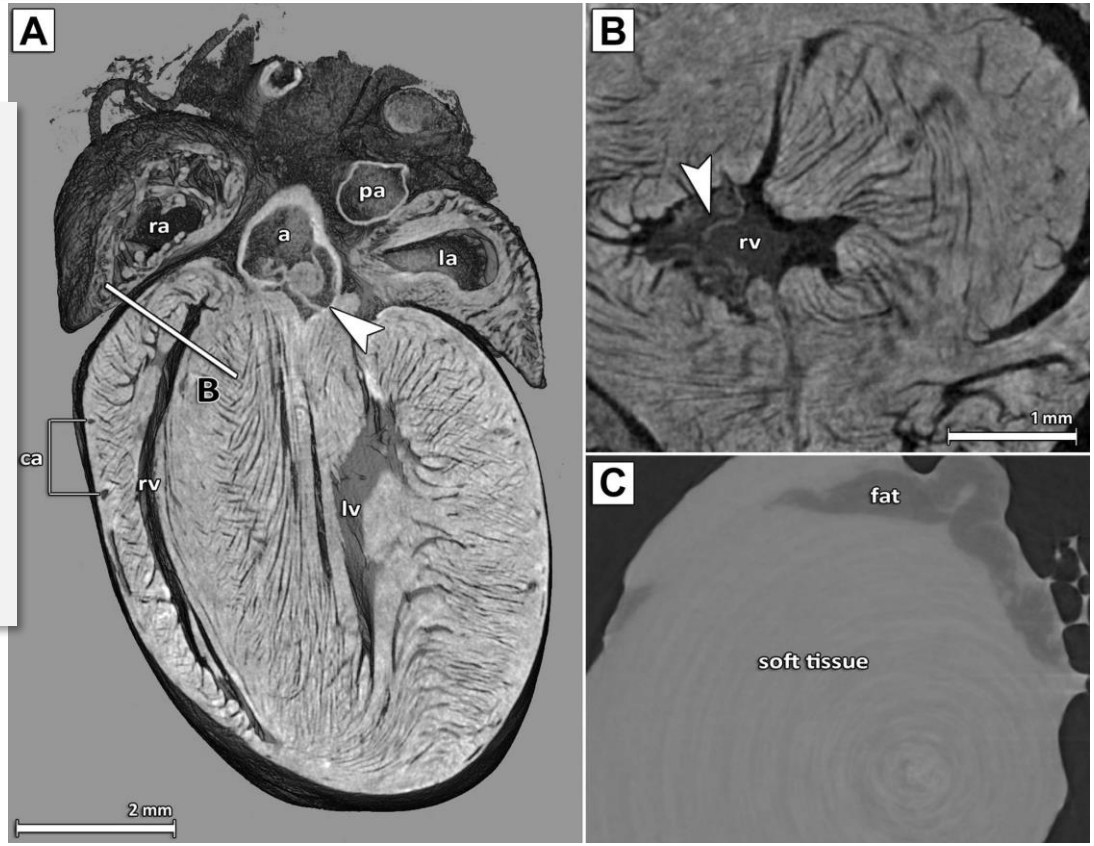

(A) Virtual cut through a volume rendering- Details of the anatomical structures: the right atrium (ra), the left atrium (la), the right and left ventricle (rv, lv), some coronary arteries (ca), the aorta (a) and the aortic valve (white arrow head) and the pulmonary artery (pa). The PTA staining allows for identification of the orientation of the muscle fibre bundles**. (B) Detailed view of the PTA stained right ventricle shown in (A)**. The position and orientation of the virtual cut section shown here is indicated by the line 'B' in panel (A). **(C) Image of the right ventricle area of an unstained heart**, it shows no contrast apart from a difference between fatty and soft-tissue.

**B.Metscher, BMC Physiology 2009,*

Dullin C et al., PLoS ONE 12(2): e0170597 (2017)

Comparing CT slice with histology

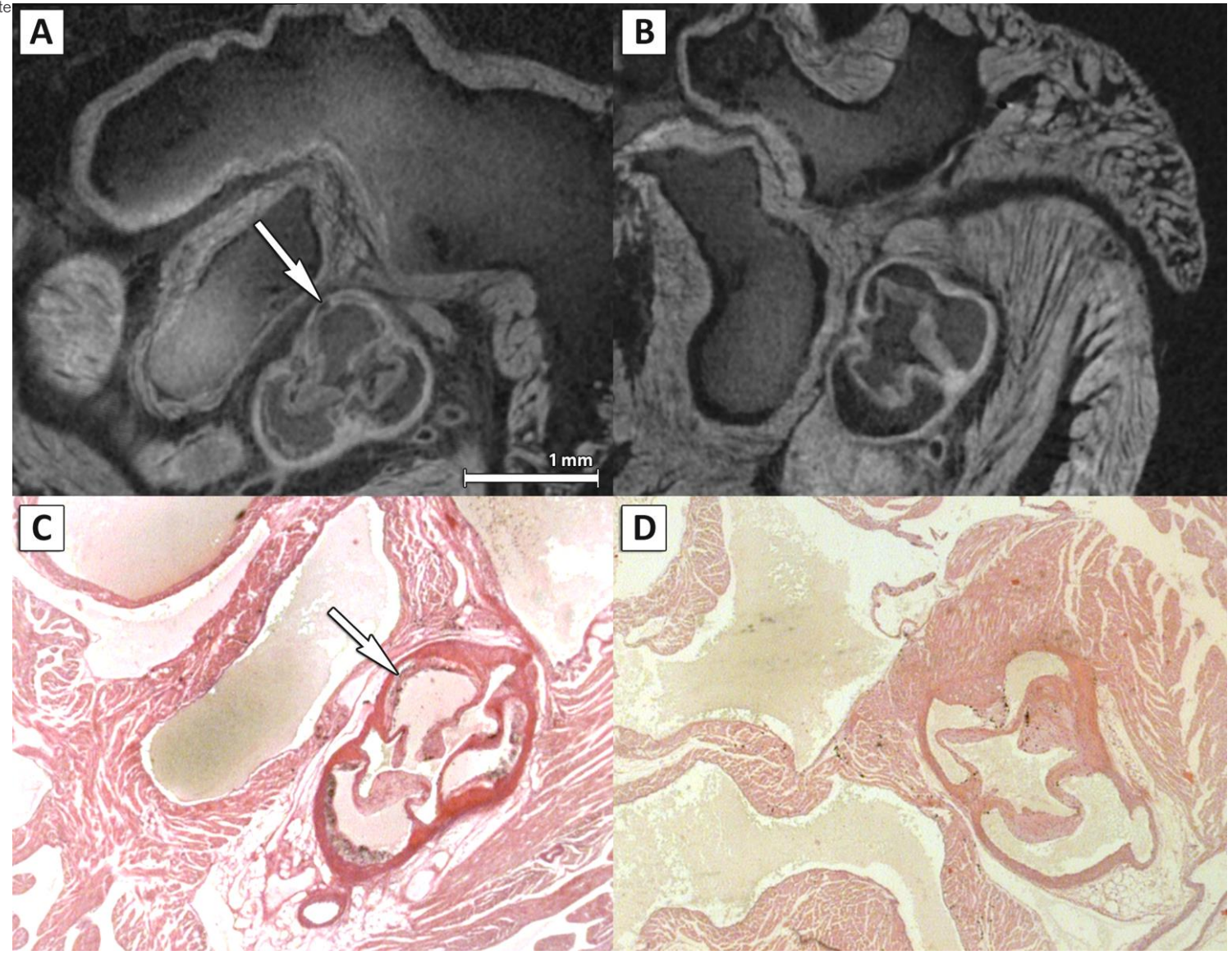

no additional shrinkage or distortion by re-embedding the tissue in resin

Dullin C et al., PLoS ONE 12(2): e0170597 (2017)

Use of staining and Phase Retrieval algorithm - Imaging of PTA stained mouse heart embedded in paraffin

Standard FBP reconstruction

Application of Phase retrieval algorithm

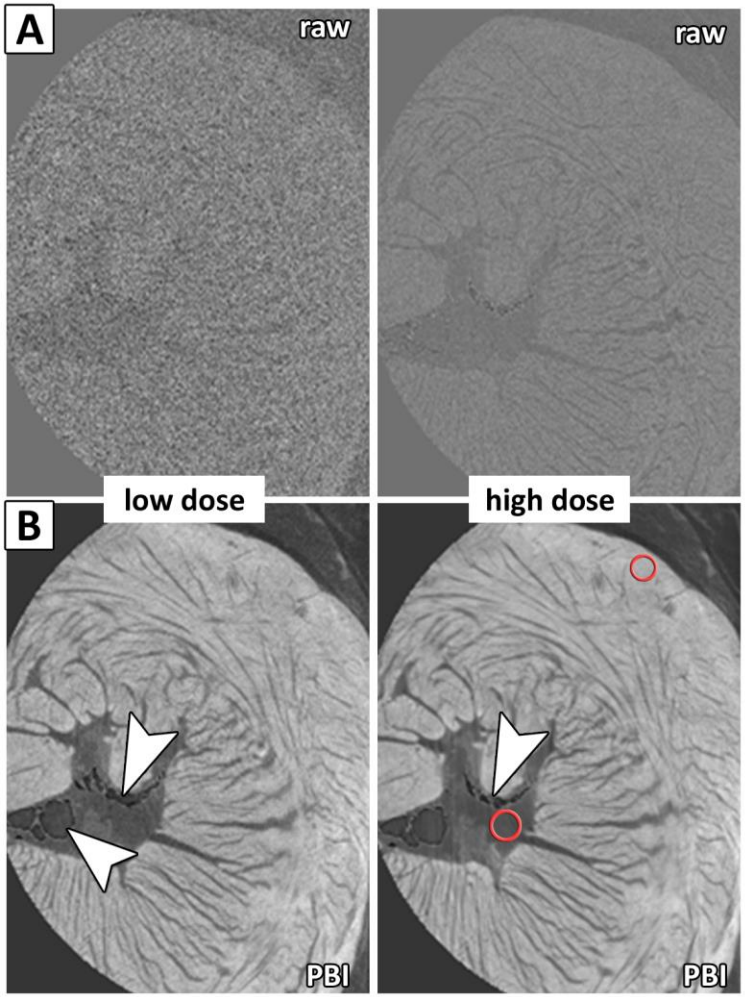

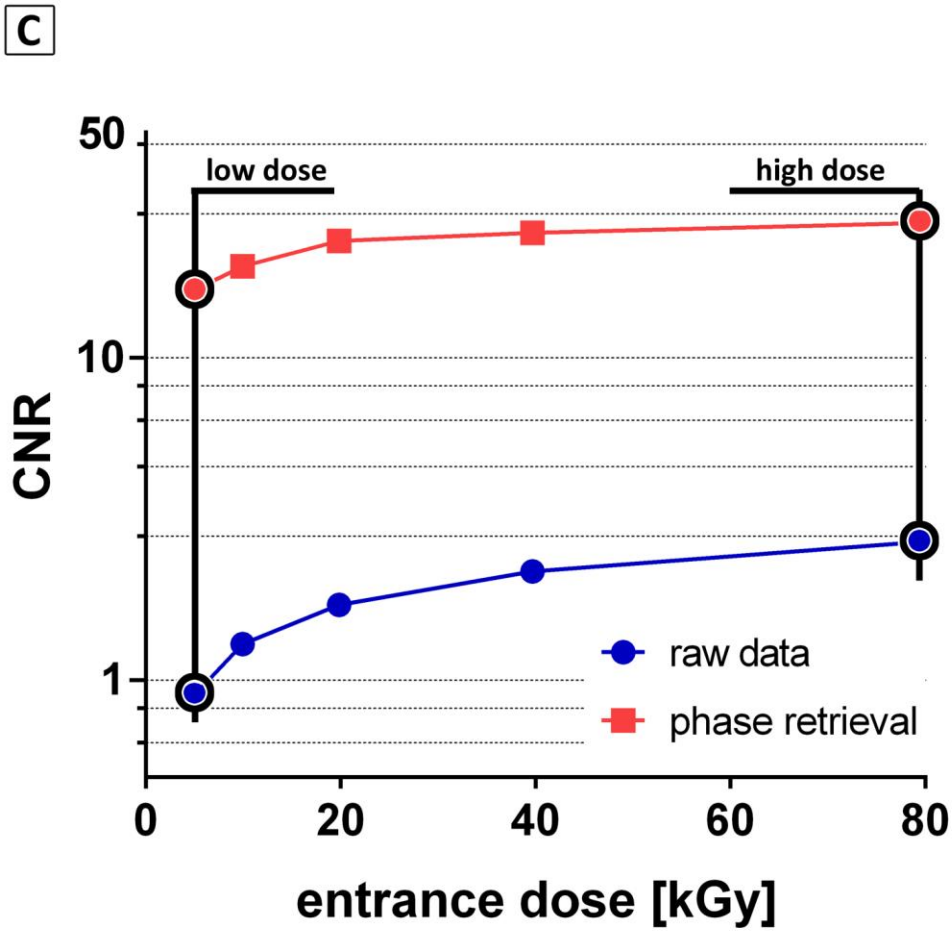

Metscher, Brian D. *BMC physiology* 9.1 (2009): 1

PBI + phase retrieval dramatically **increases** contrast-to-noise ratio in PTA stained mouse hearts -> possible **dose reduction** or **shorter acquisition times**

Iodine (I2), chromium (chrom alaun) in comparison with PTA

Mouse lungs stained with different staining embedded in paraffin, voxel size = 2.6 µm

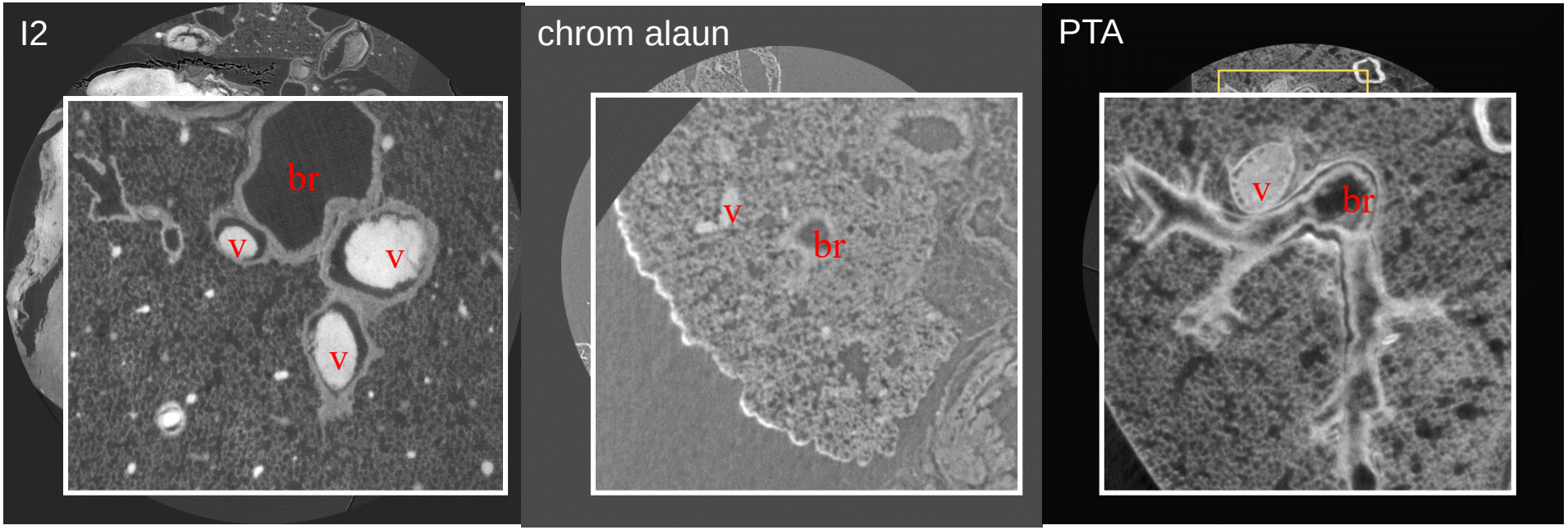

The detailed views ct edures allow a precise delineation d l chi (br) and vessel walls (v). Wit els e blood is strongly stained, all re ract.

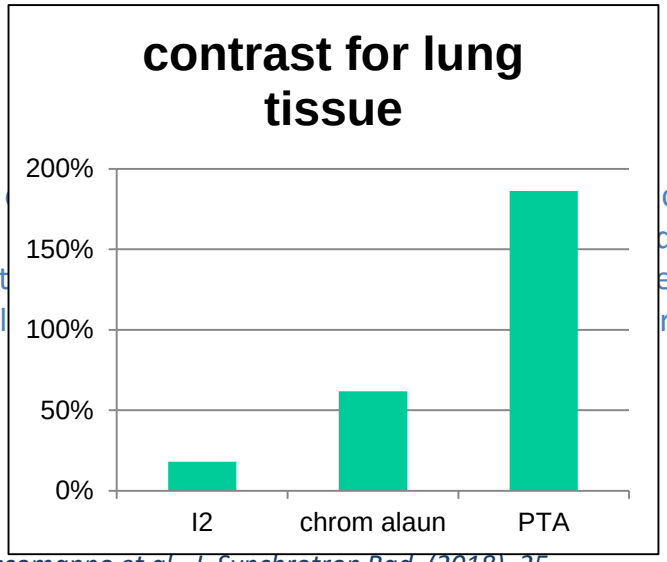

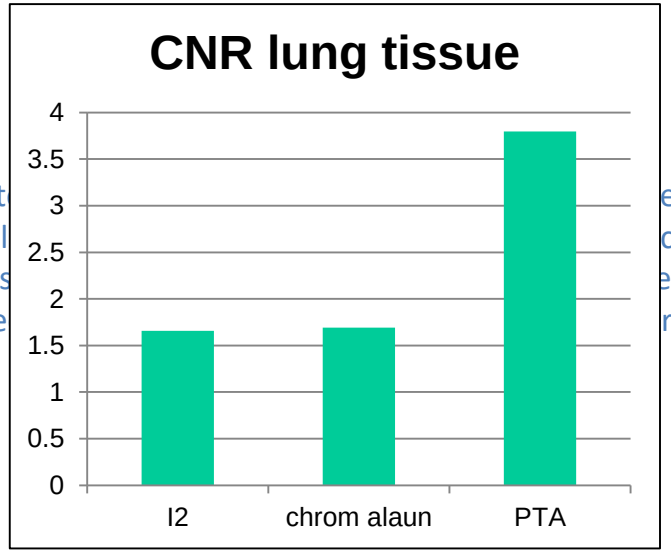

M.Saccomanno et al., J. Synchrotron Rad. (2018). 25

PBI potentials in tissues visualization - Imaging of mouse brain embedded in paraffin

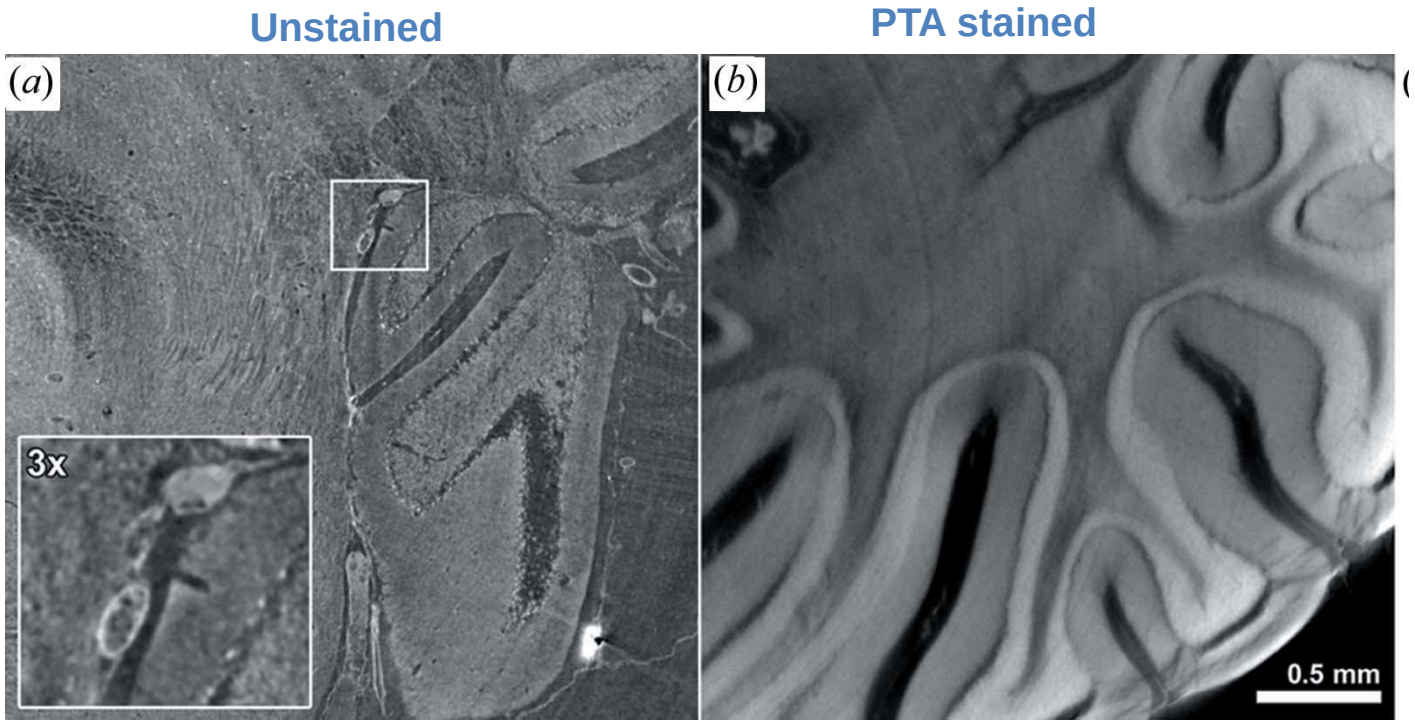

- Comparable area within the cerebellum (a) Unstained, b) PTA stained).
- In (a) the structure of the cerebellum of the unstained brain is better distinguishable.
- The different anatomical structures of the cerebellum of the PTA stained brain are also visualized in (b), but only at a limited level of detail in comparison with (a).

The use of PBI and phase retrieval allow an accurate morphological characterization of the sample visualization without the need of staining

M.Saccomanno et al., J. Synchrotron Rad. (2018) 25

Pre-clinical imaging

- Imaging of small animals, tissues and organs: applied for different purposes in the development of ***animal models*** *(ex vivo, in-vivo)*
  Research protocols, pixel size: 4.5 - 9 µm (ex-vivo) up to 100 µm (in-vivo).

  - Lungs imaging: 2D and 3D, structure and function
  - Imaging of brain

2D dynamic Imaging of lungs Function & morphology (I)

- Animal model: rabbit pups
- Imaged pups with PBI, either before the first breath (fetus) and at fixed intervals after birth (up to 2h)

Effects of Ventilation on Lung Liquid Clearance at Birth

Aim: to observe lung aeration on a breath-by-breath basis.

Exp. time: 80 ms
Interval: 0.8 s
Skin Dose: ~ 0.15mGy/f
Pixel Size: 22.5 µm
E = 25 keV

Kitchen, M. J., et al., Phys. Med. Biol., 53(21), 6065-77 (2008).

Elettra
Sincrotrone
Trieste

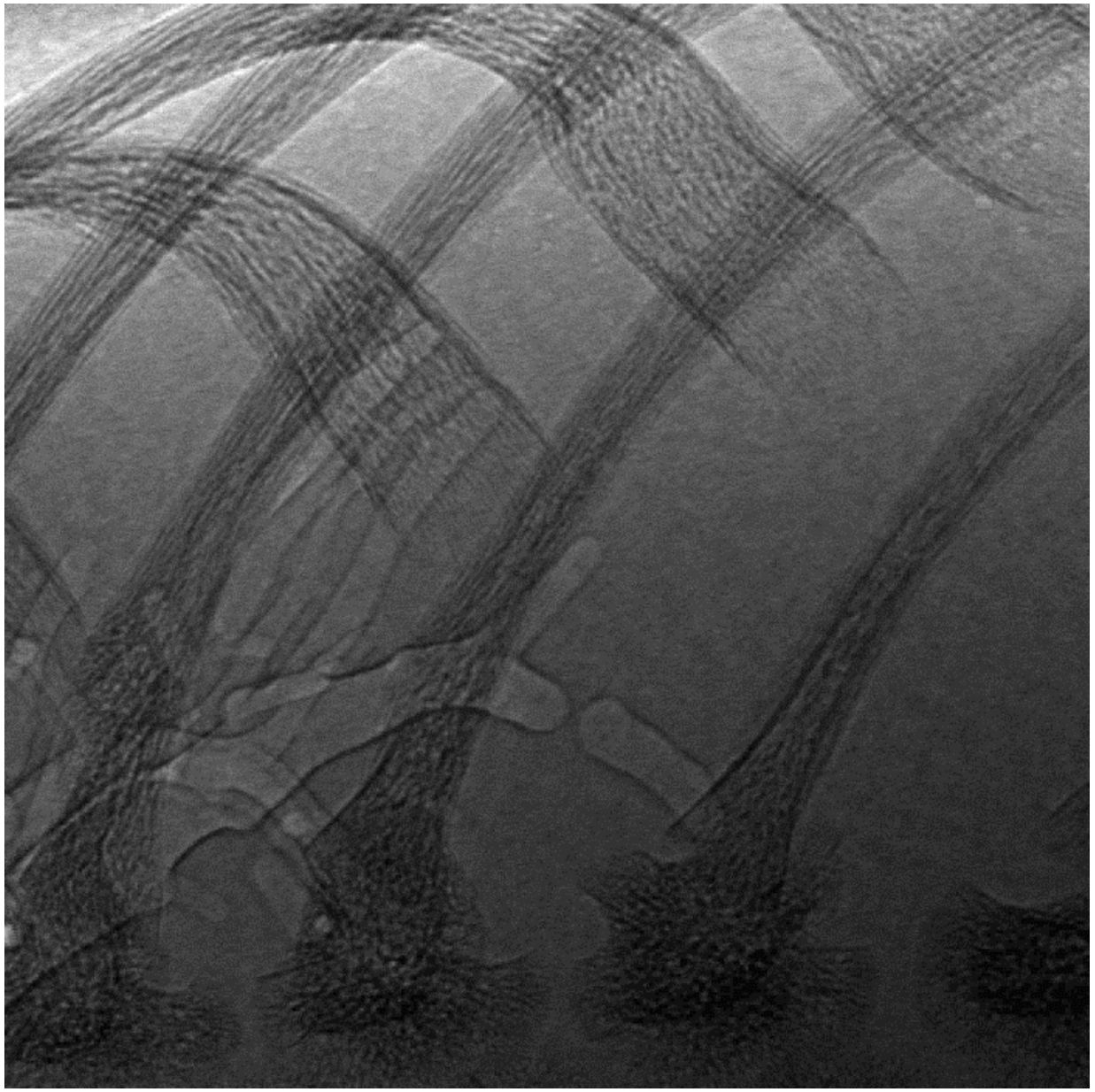

Imaging protocol: use of macrophages with double staining

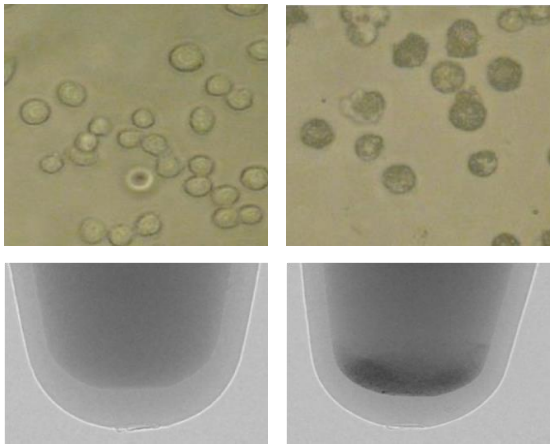

Unlabeled MΦ Ba labeled MΦ

- Animal model of allergic asthma induced by ovalbumin based on balb/c mice
- Aim: evaluate the potential of SR-based technique for **functional** and **morphological** imaging of mice lungs
- Available techniques: optical imaging and PBI micro-CT
- Use of immortalized Murine Alveolar Macrophage Cell line (MΦ) with double staining:
  - Barium sulfate (clinical contrast agent) for microCT
  - DiD fluorescent dye for optical imaging.

In vivo validation of homing of MΦto inflammation sites. Images performed 24 hours after MΦ administration.

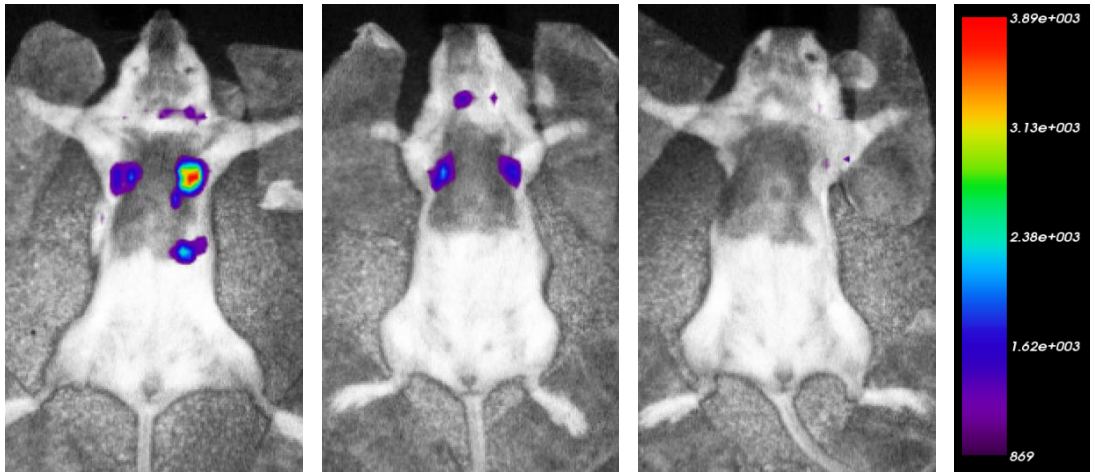

Asthmatic mouse treated with MΦ

Normal mouse treated with MΦ

Native mouse untreated

Macrophages were adminstered intra tracheally 48 hours after asthma induction

MEDIZINISCHE UNIVERSITÄT WIEN

cbm cluster in biomedicine

UNIVERSITÄTSMEDIZIN GÖTTINGEN UMG

P3AGI Public Private Partnership for Asthma Imaging and Genomics

SEVENTH FRAMEWORK PROGRAMME

G. Tromba

PBI potentials in tissues visualization II - Imaging of inflammation in asthmatic mice

- Animal model of allergic asthma induced by ovalbumin based on balb/c mice
- Murine Alveolar Macrophage Cells stained with Barium sulfate (Guerbet, F)
- Macrophages adminstered intra tracheally 48 hours after asthma induction

No PHR

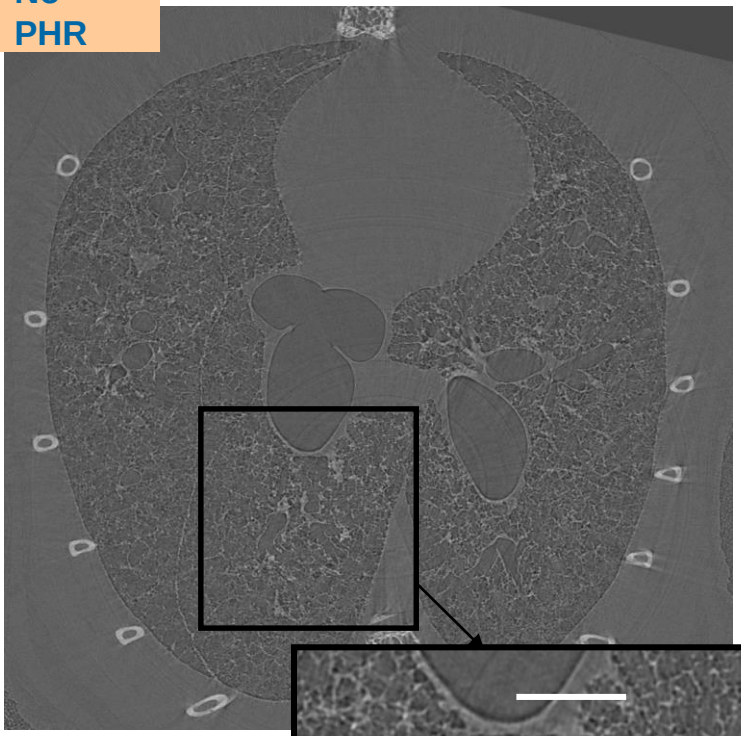

Lung slice

E=22 keV
PHC dist = 30 cm
Pixel size = 9 μm

Clear separation of tissue, Ba and bones signals with PHR

PHR (single dist.)

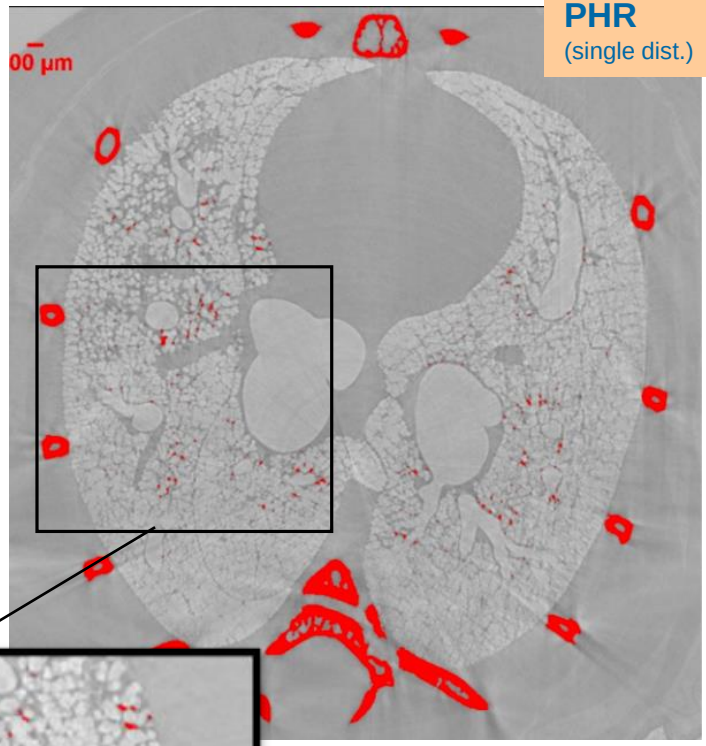

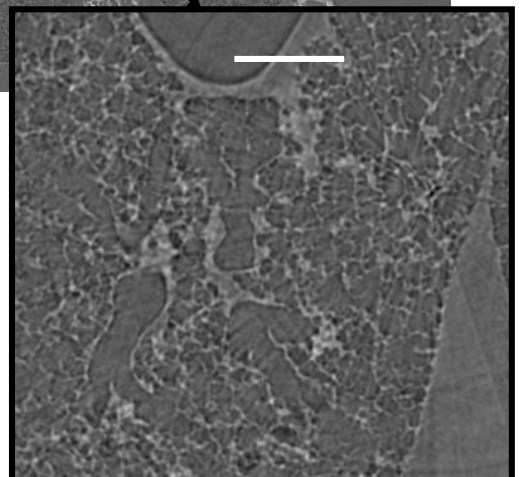

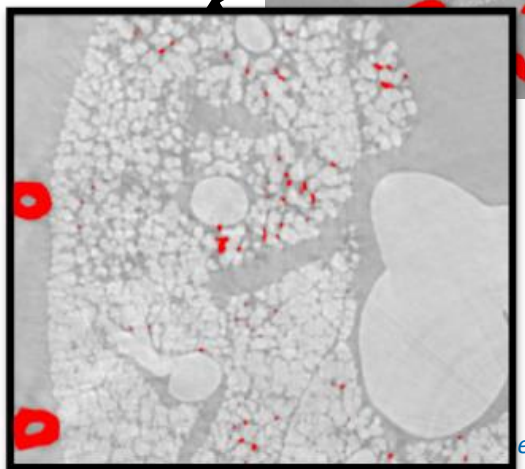

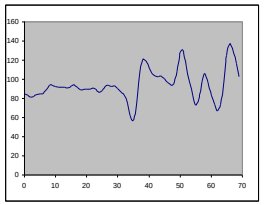

Edge enhancement effects due to PHC

Bones
Barium

C. Dullin et al, J. of Synchrotron Radiation 22(1) (2015)

Visualization of labeled macrophages

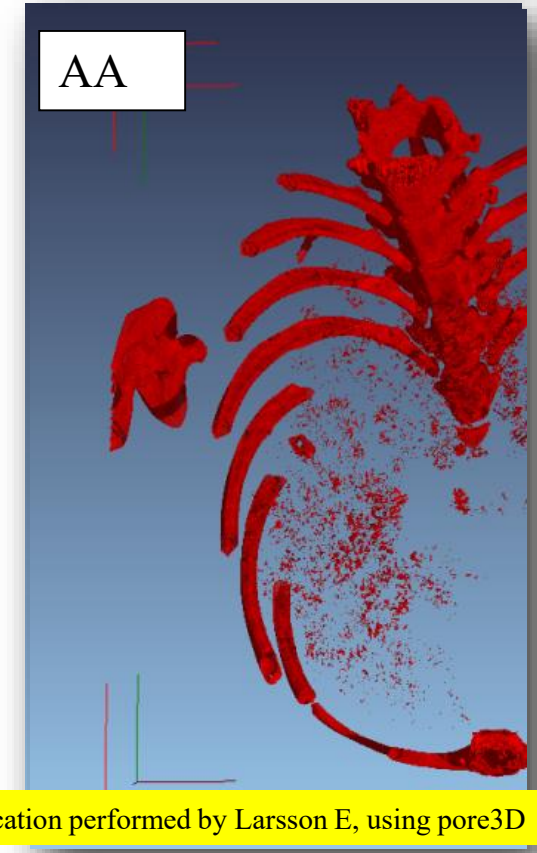

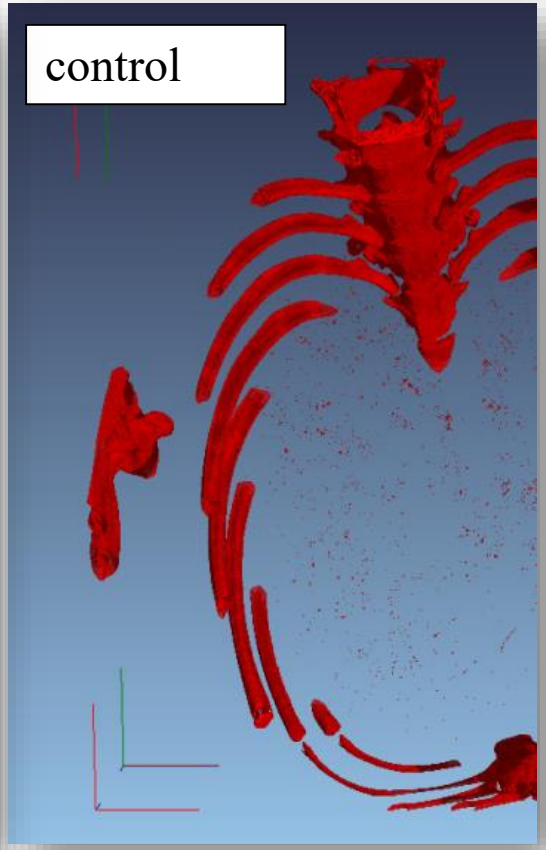

Quantification performed by Larsson E, using pore3D

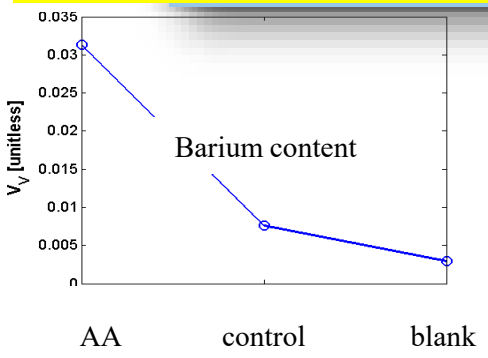

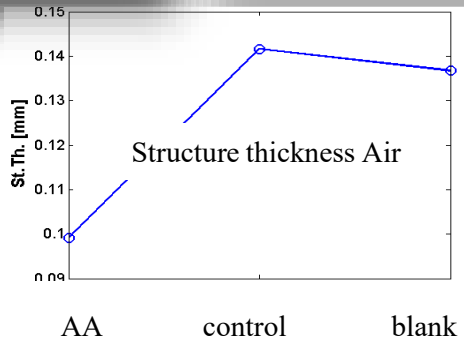

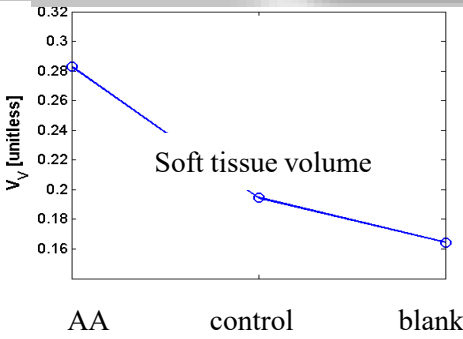

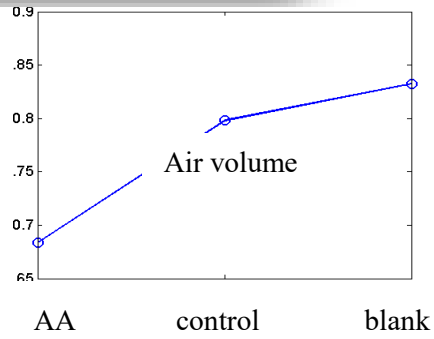

C. Dullin et al, J. of Synchrotron Radiation 22(1) (2015)

VOI of soft lung tissue

Soft Tissue (green), Macrophages with barium (red), Medial axis/skeleton (blue)

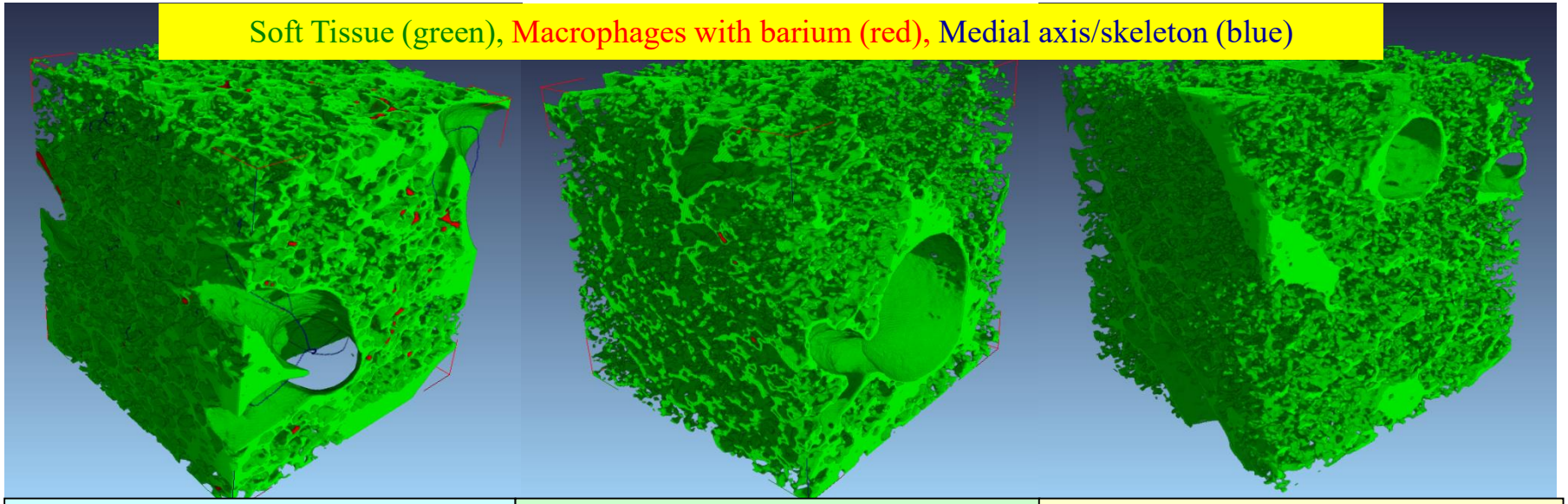

a) asthmatic mouse treated with macrophages labeled by Barium	b) healthy mouse treated with macrophages labeled by Barium	c) control: healthy mouse untreated (no Barium)

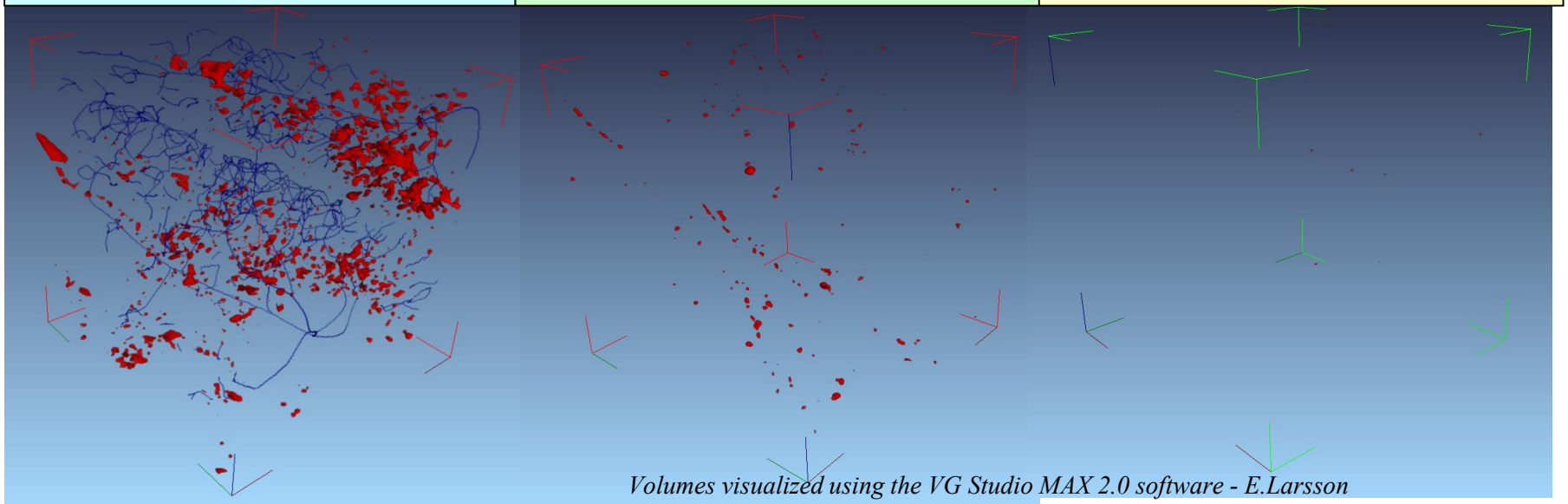

Volumes visualized using the VG Studio MAX 2.0 software - E.Larsson

Elettra Sincrotrone Trieste

Dynamic measure of **X-ray Absorption function** (Xaf) XAFs of a healthy control mouse (**blue**), an asthmatic mouse (**red**) and a dexamethasone treated mouse (**green**).

UNIVERSITÄTSMEDIZIN GÖTTINGEN : UMG

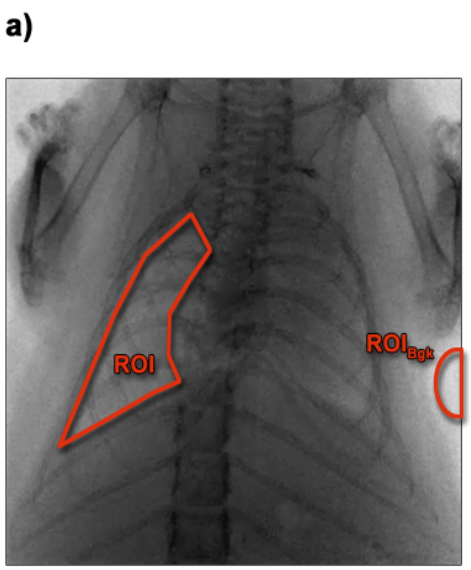

radiograph of the mouse chest

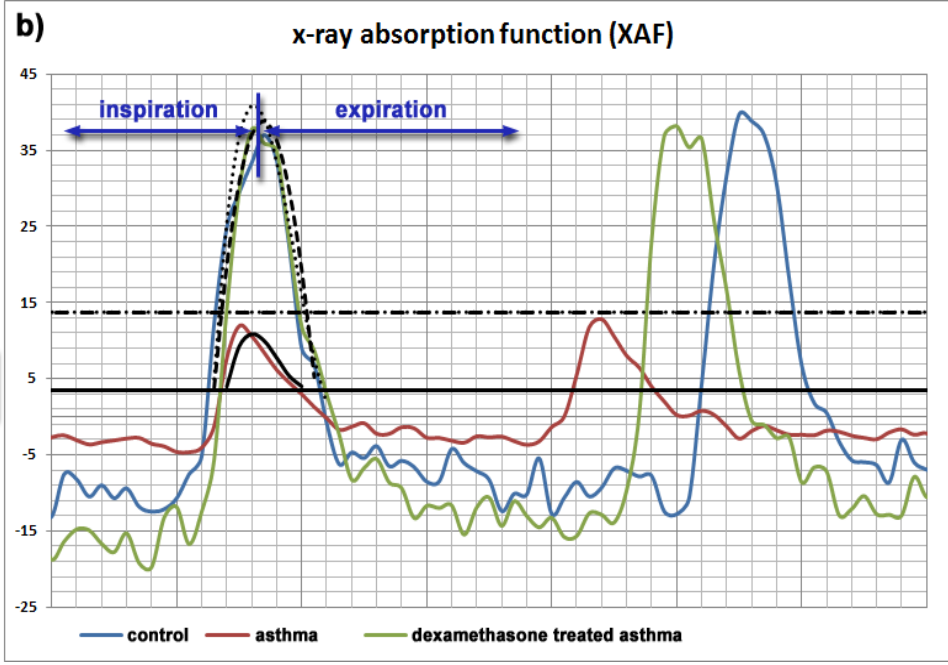

C. Dullin, et al.:, Scientific Reports | 6:36297 | 2016

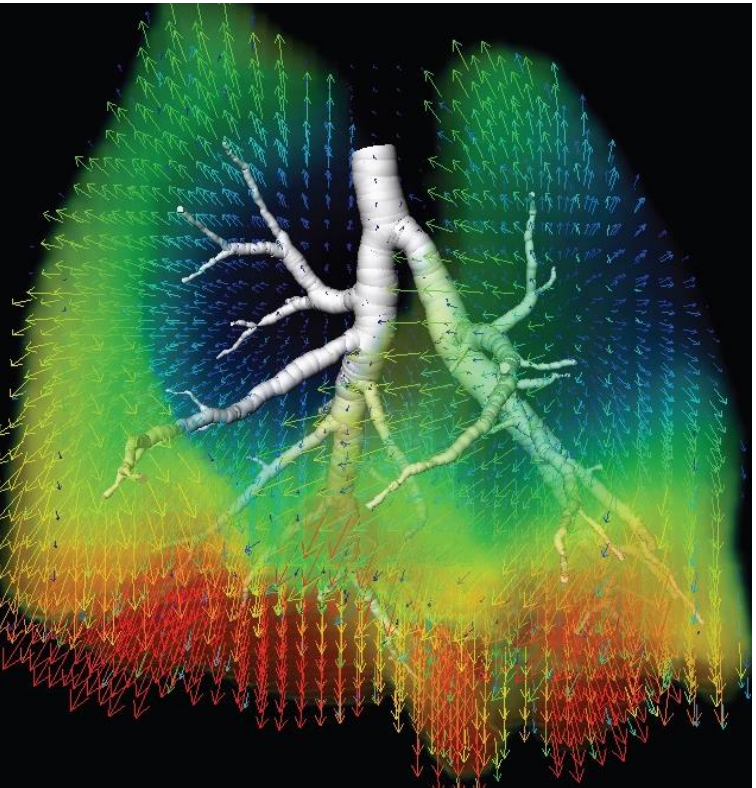

Measure of Lung function

X-ray velocimetry - 3D map of mouse lung tissue velocity during inspiration. The vectors represent tissue velocity direction, and the colours represent velocity magnitude.

SPring-8

S. Dubsky, A. Fouras, Advanced Drug Delivery Reviews 85 (201

Elettra Sincrotrone Trieste

Brain studies

Technique:	FPI + contrast agent (Au nano particles)
Purpose:	tracking tumor development
Modality:	micro-CT *ex-vivo* imaging on mice
	(recent development: first *in-vivo* experiment)

Technique:	Grating Interferometry (GI)
Purpose:	animal model of Alzheimer disease
Modality:	micro-CT *in vitro* imaging of mice brains

Cell tracking brain tumors in rats

C6 glioma cells were cultured and some of the cultures were exposed to colloidal **Gold Nano Particles** (GNP) for 22 hrs.

Cells were implanted into the brain of adult male Wistar rats with animal under anesthesia.

The animals were sacrificed two weeks later.

The detection of labeled cells is **enhanced by the higher absorption of gold** with respect to tissue and by PHC effects.

Aims for cell tracking:

- to monitor the dynamic of tumour growth
- to follow the migration of tumour cells
- to understand the metastasis spread dynamic

E = 24 keV

Num. proj. = 720, Pixel size =14μm

Histologies – 2 weeks after implant.

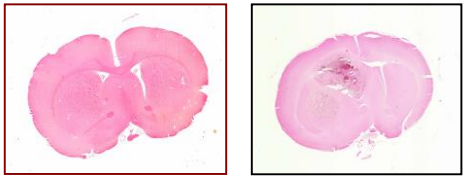

Healthy | Brain with C6 cells

C,J,Hall et al., Eur. J. of Radiol., Volume 68, Issue 3 (2008)

3D rendering of 3 mm height skull portion

A1 and A2: Tumor with 300,000 cells – not labelled

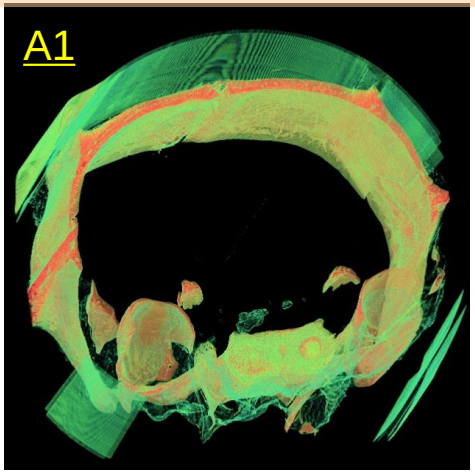

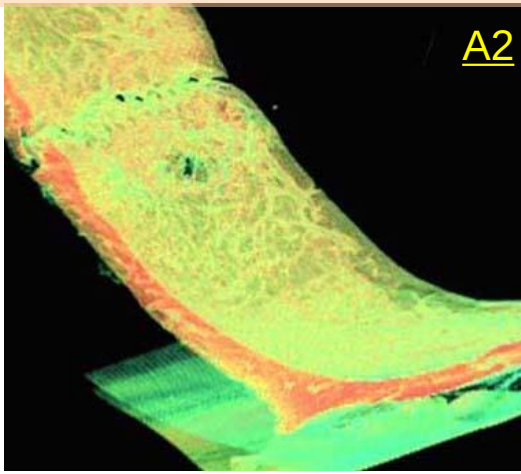

B 1 and B 2: Tumor with 300,000 colloidal gold-loaded cells

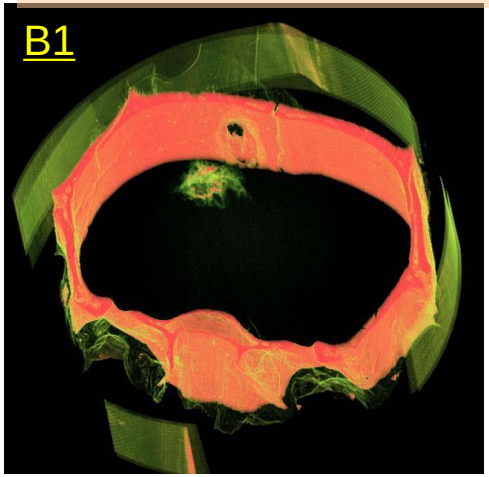

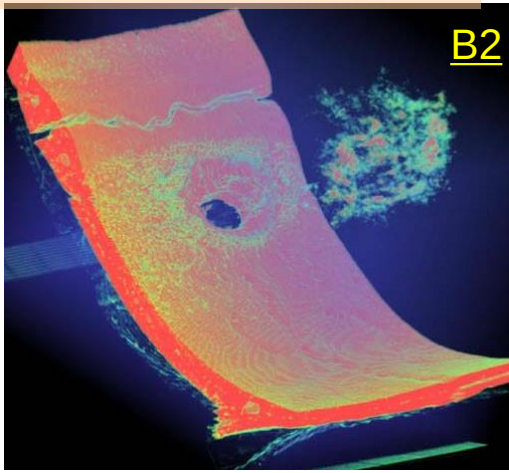

Rat 706: Metastasis spread in the spine

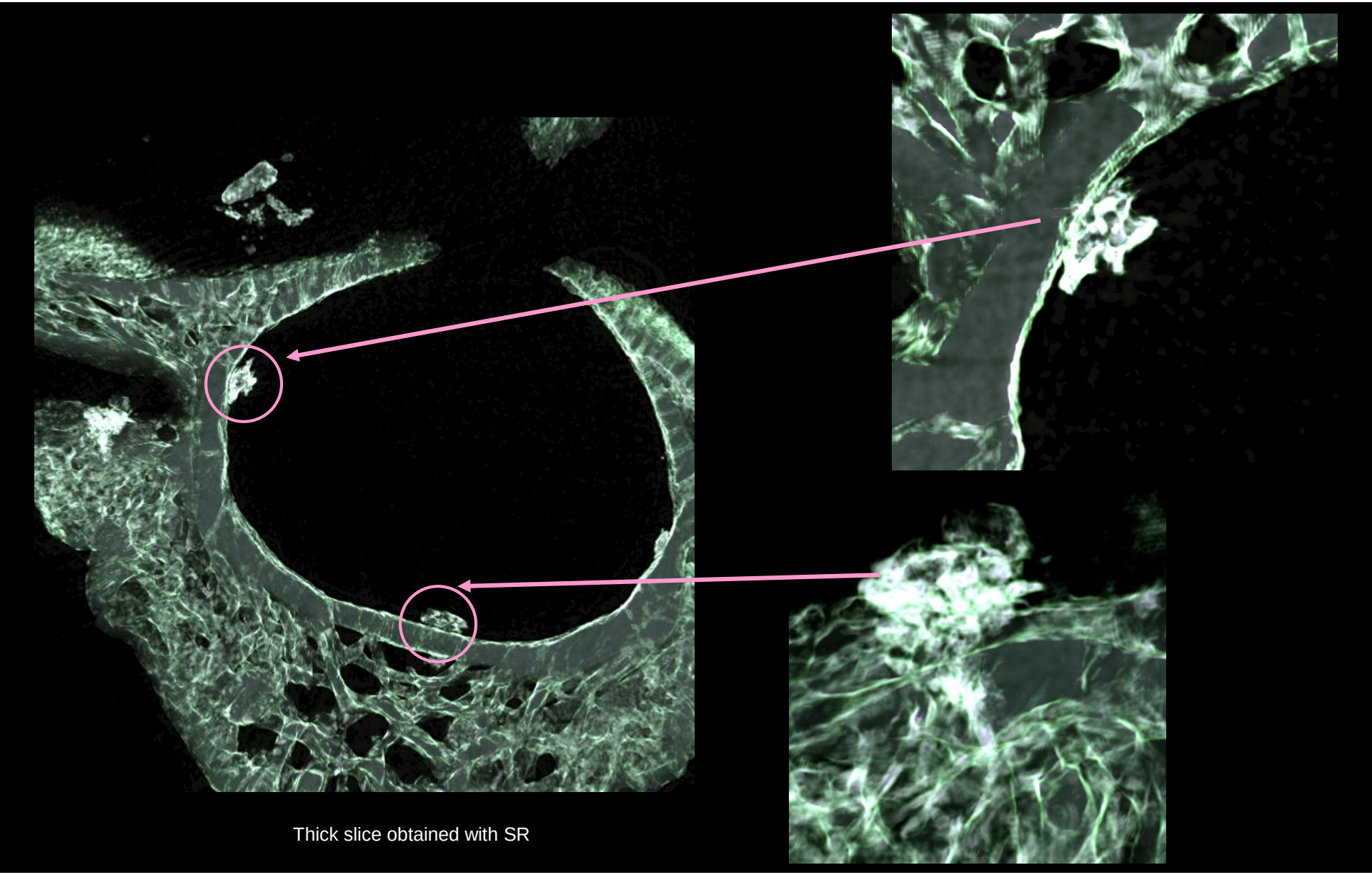

Thick slice obtained with SR

Elettra Sincrotrone Trieste

In-vivo study at low dose

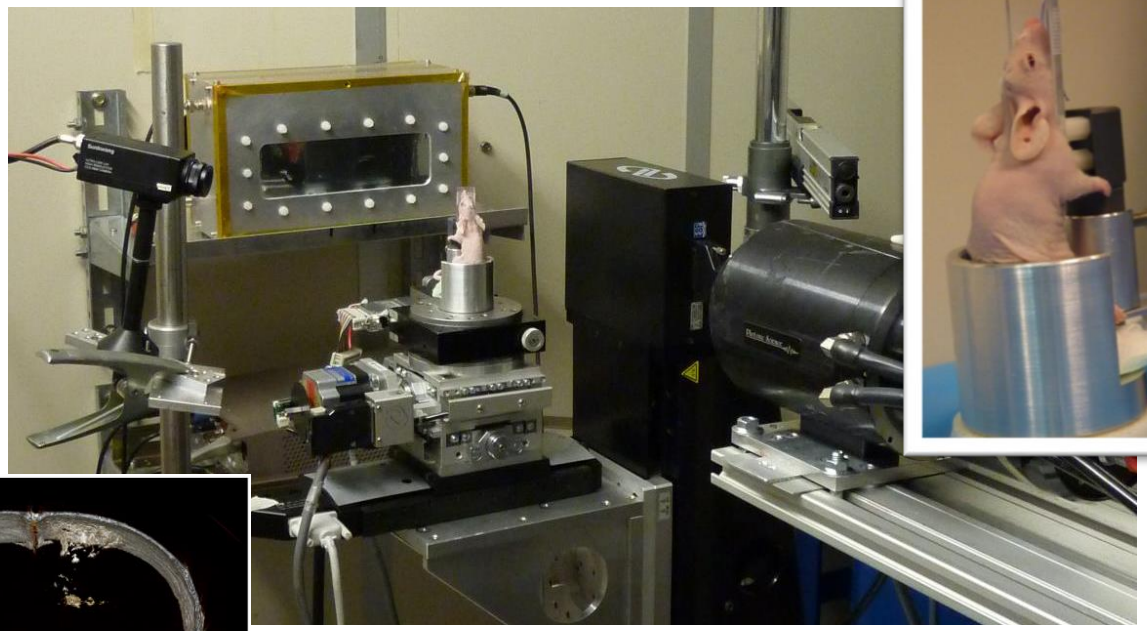

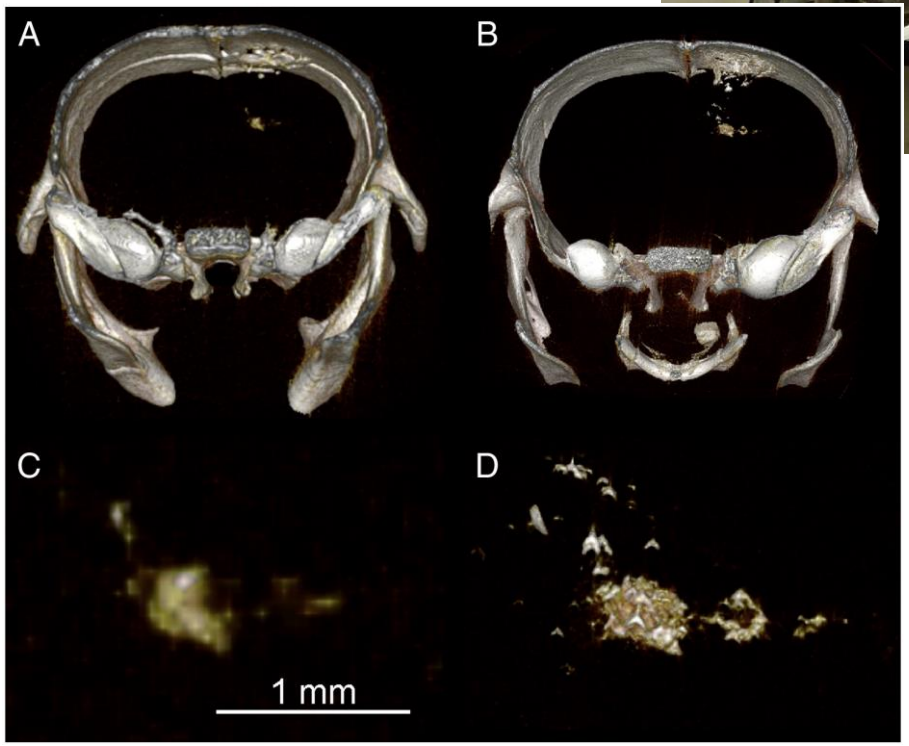

Comparison of two 3D renderings of a CT of a mouse injected with 100,000 GNP-loaded F98 cells depicts:

(A–C) - low x-ray dose *in vivo* data

(B–D) the high x-ray dose *ex vivo* data

The images in panels C and D are enlargements at full system resolution of the developed tumor depicted in panels A and B, respectively.

First experiment *in vivo*: lesions are visible also at low doses

A. Astolfo et al., Nanomedicine: Nanotechnology, Biology and Medicine, Vol. 9, Issue 2013

Clinical applications

- potential studies with patients

- *Need to **limit** radiation dose. Strict research protocol for selected patients. Find best compromise between dose and image quality, pixel sizes : 50 – 100 µm*

  - Breast imaging
  - ABI potentials for imaging of cartilage and joints
  - Feasibility study for low dose Phase contrast lung CT

Elettra Sincrotrone Trieste

Clinical trial at SYRMEP: Breast imaging

Azienda Sanitaria Universitaria Integrata di Trieste

UNIVERSITÀ DEGLI STUDI DI TRIESTE

INFN Istituto Nazionale di Fisica Nucleare

Outcomes of first protocol

Clinical images with SR have:

- *higher specificity,*
- *better agreement with the golden standard (biopsy),*
- *improved image quality,*
- *strong reduction of X-ray doses.*

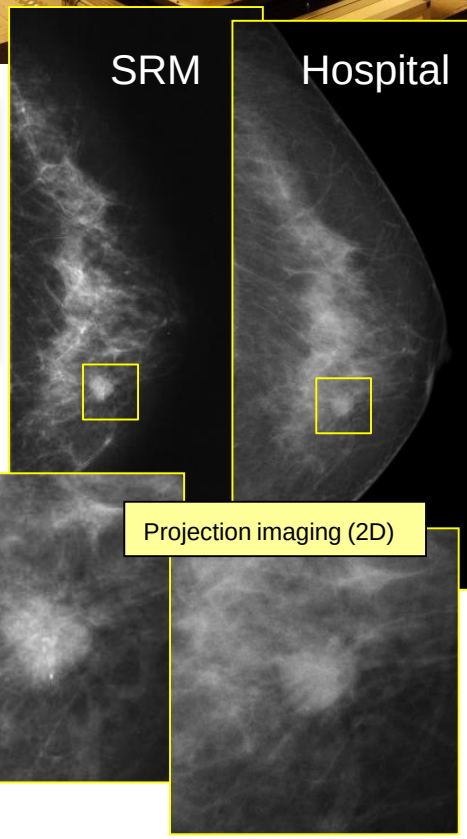

Next step: 3D imaging: Low dose phase contrast breast CT protocol

Slice

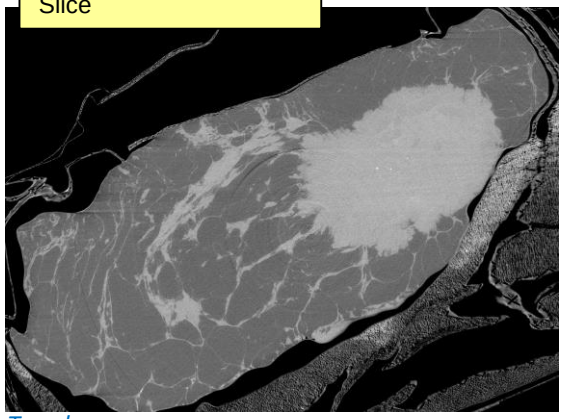

Different CT views

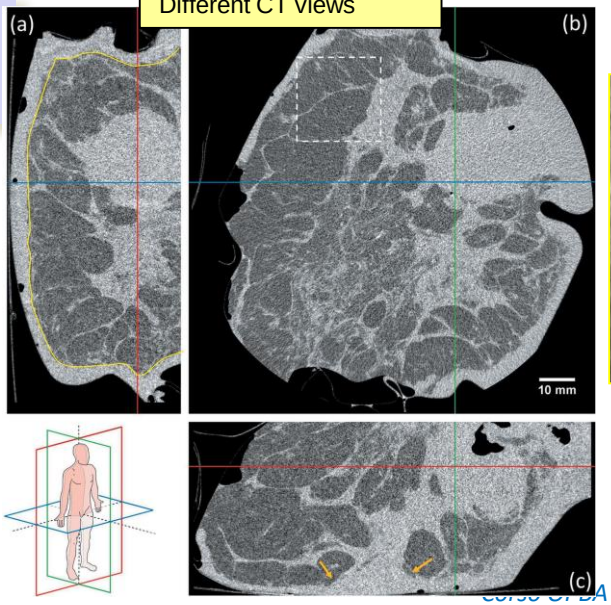

ABI studies of Cartilage and bone interface

Osteoarthrosis (OA) is a disease characterized by the progressive degeneration of articular cartilage and the development of altered joint congruency. It has a high incidence in the adult population. Affecting mainly the elderly population, it is one of the main causes of disability worldwide. Conventional radiography detects only **important osseous changes**, at advanced OA or RA stages, when therapeutic strategies are less effective. **Early changes** in the **cartilage** and other **articular tissues** are **not** directly visible. MRI imaging works better but the maximum achievable spatial resolution is not always adequate.

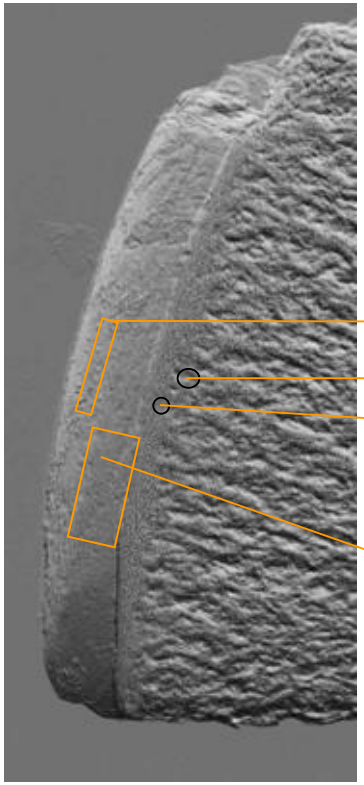

Need to study:
- cartilage
- cartilage-bone interfaces
- changes in the bone structure

Superficial Layer (Zone of horizontal collagen fibers with flat cells)

Subchondral Bone Plate (**Important for diagnostic purposes in OA**)

Tidemark (Border between normal and mineralized cartilage)

Transitional and Deep Layer (round cells, collagen fiber switches from horizontal to vertical orientation, increasing stiffness and material density)

Aim: detect the architectural arrangement of collagen within cartilage and evaluate how the cartilage degeneration affects the underlying subchondral and trabecular bone.

Femur head core cuts: collagen arcades structure

- The ABI technique allows to visualize the discontinuities in the sample and the inner structures invisibles by means of conventional X-Ray imaging.
- The transition bone-cartilage is emphasized.
- The articular cartilage striations are well visible due to X-ray diffraction at edges of fibers

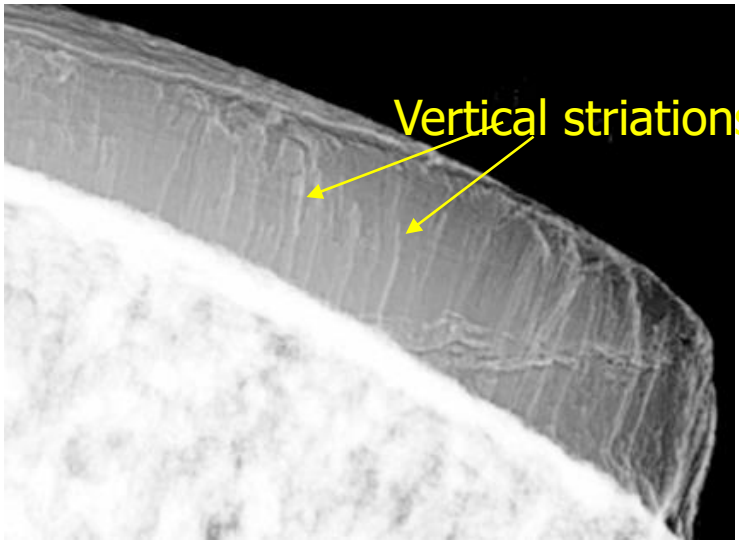

Apparent absorption image

Refraction image

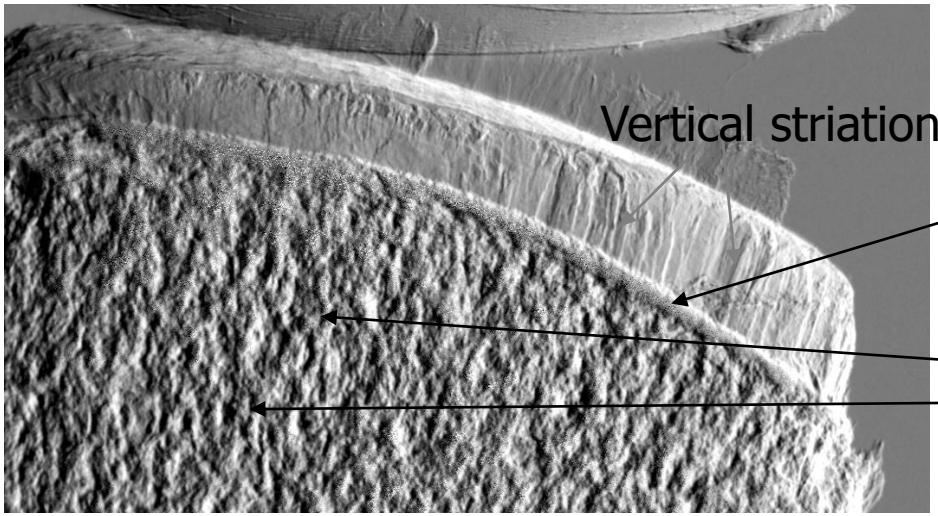

Elettra
25 keV

Muehleman C et al., J, Osteoarthritis and Cartilage 12 (2): 97-105, 2004

Femur head core cuts: comparison with MRI

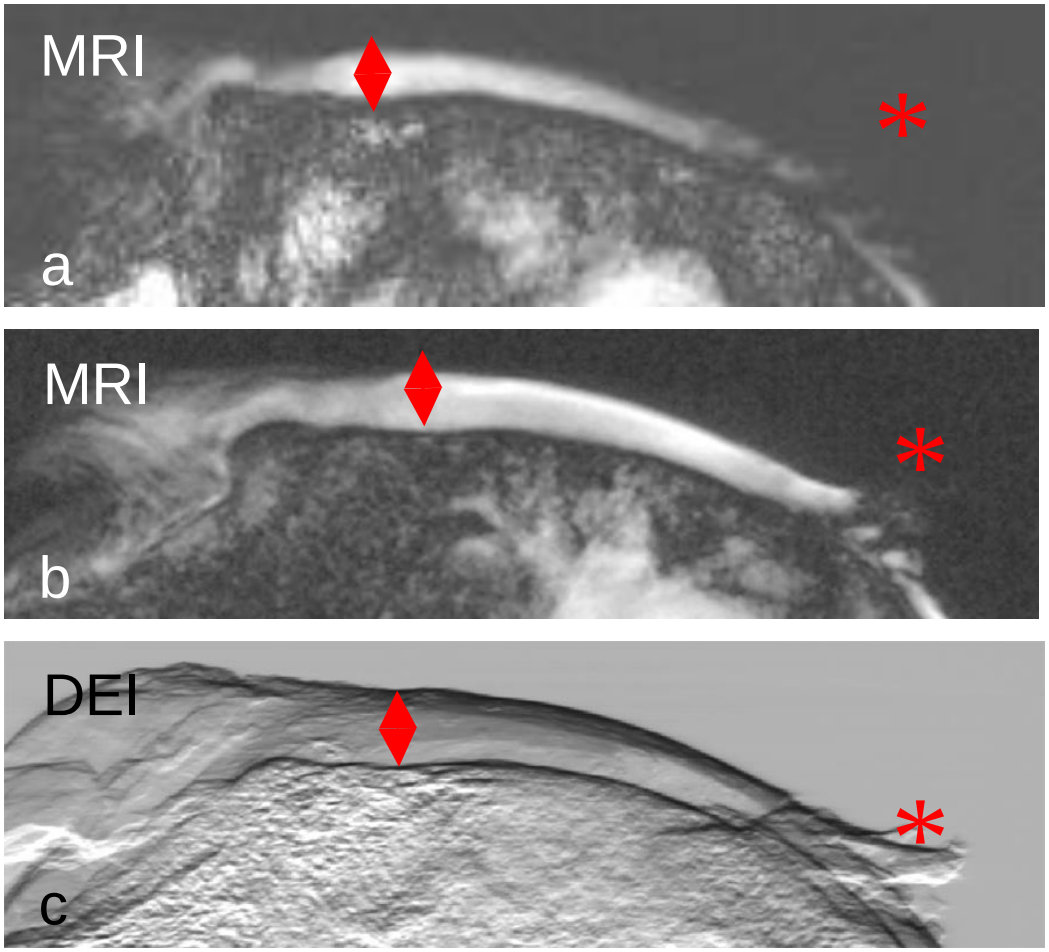

5 sec

150 sec

A.Wagner et al., Nucl. Instrum. Methods A 548, 47 (2005).

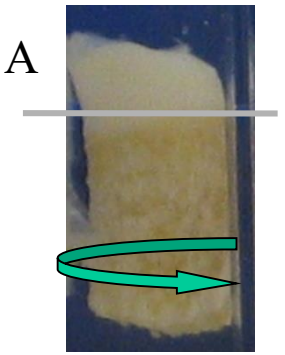

Specimen of normal cartilage (A), Coronal plane extracted from the reconstructed CT volume (B), Magnified portion identified by the ROI (C), Corresponding section from histologic preparation (D).
E = 26 keV, pixel size = 8 x 8 μm^2.

ABI in planar and tomographic modes was performed *in vivo* on articular joints of guinea pigs. Images showed the potential of technique in revealing initial lesions. Images with high spatial resolution and with an acceptable radiation dose.

Coan, P., et al., Invest. Radiology, 45(7), 437-444 (2010)

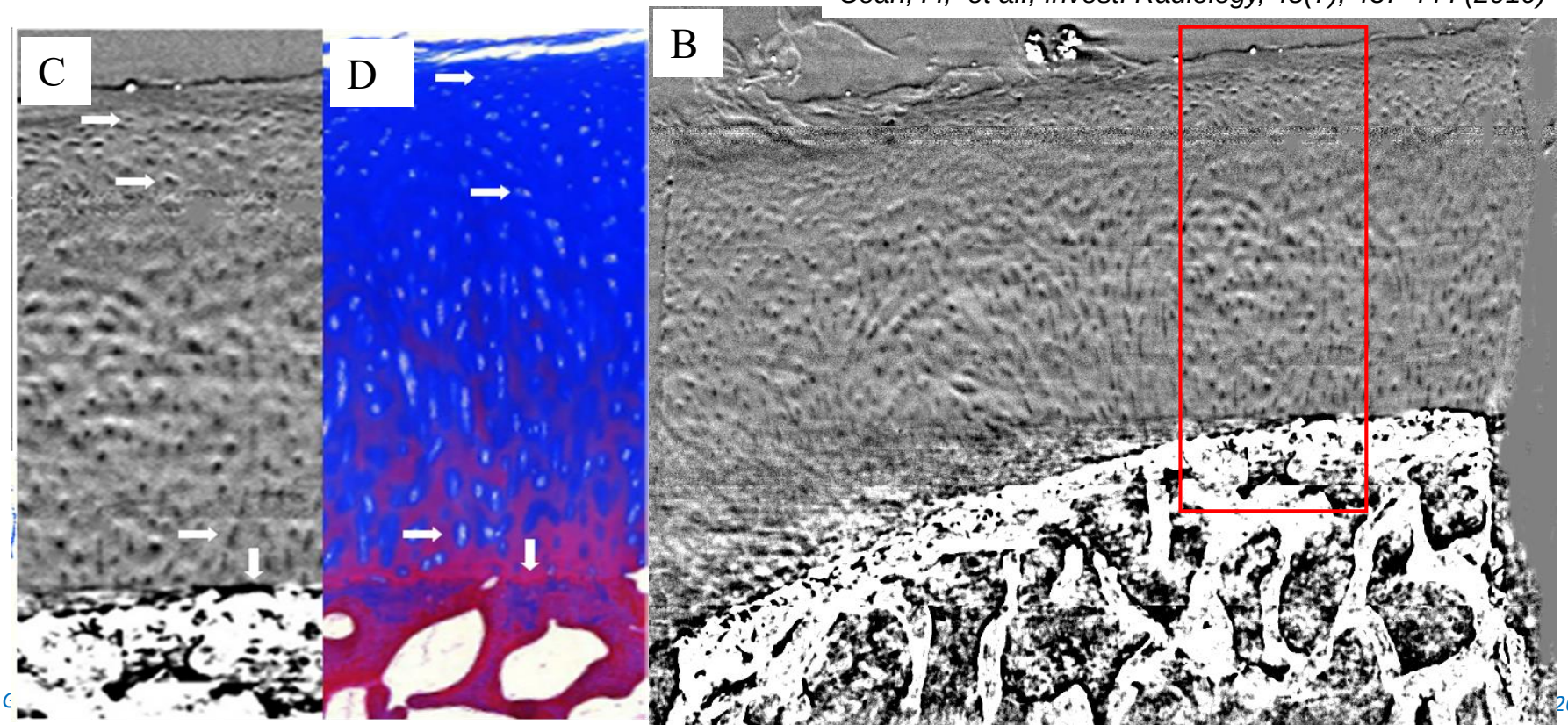

ABI studies of the finger joint

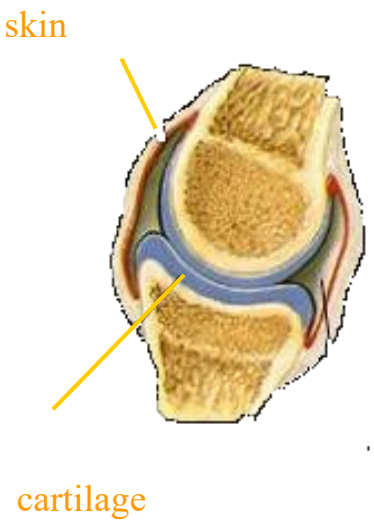

Conventional radiograph

Apparent absorption image @ 20 keV
at ELETTRA

Lewis, R. A., et al., British J. Rad., 76(905), 301-308 (2003)

Index finger proximal interphalangeal joint

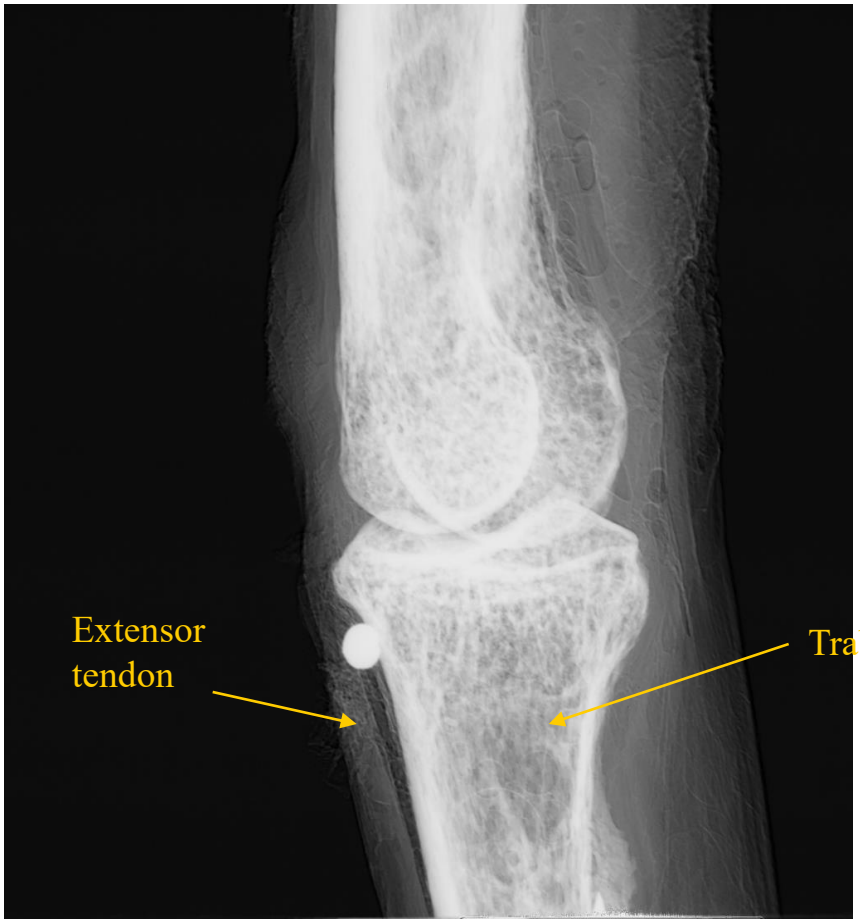

Apparent absorption Image

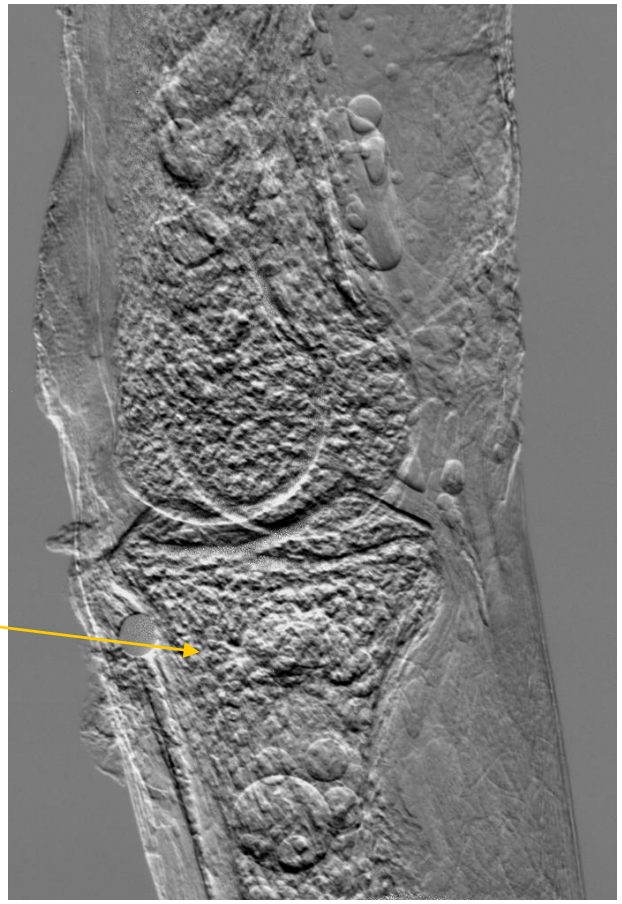

Refraction Image

Lewis, R. A., et al., British J. Rad., 76(905), 301-308 (2003)

Index finger proximal interphalangeal joint

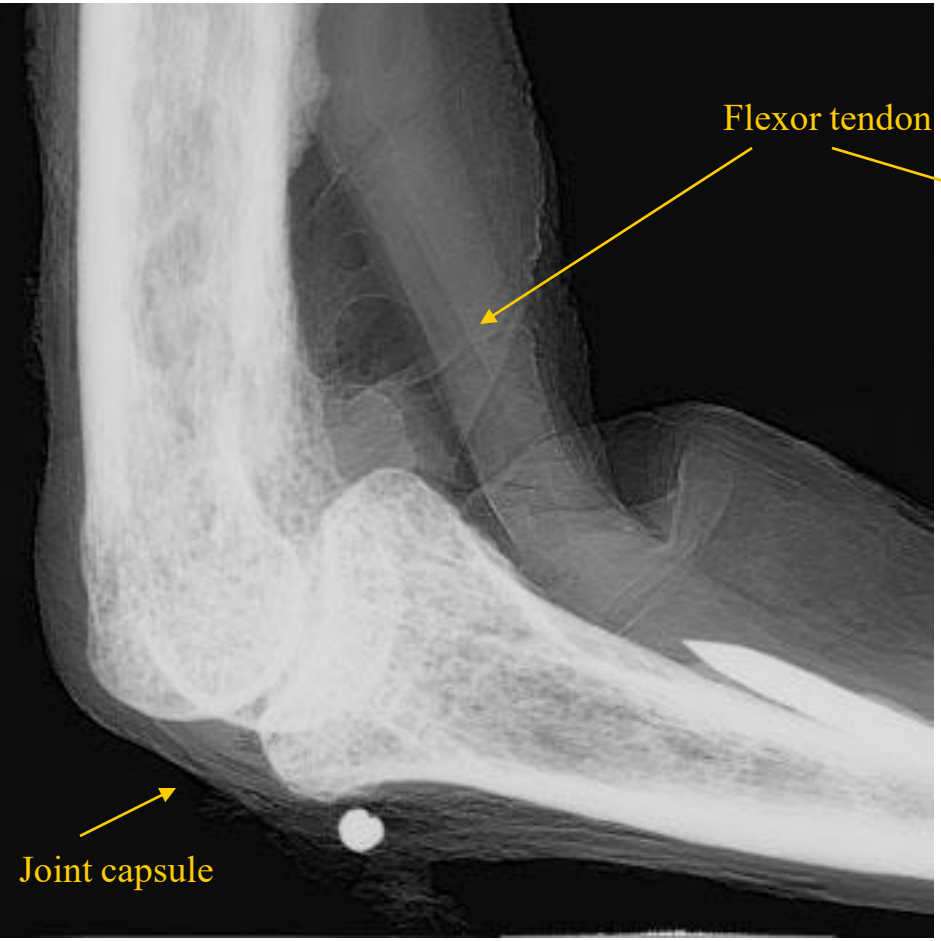

Apparent absorption Image

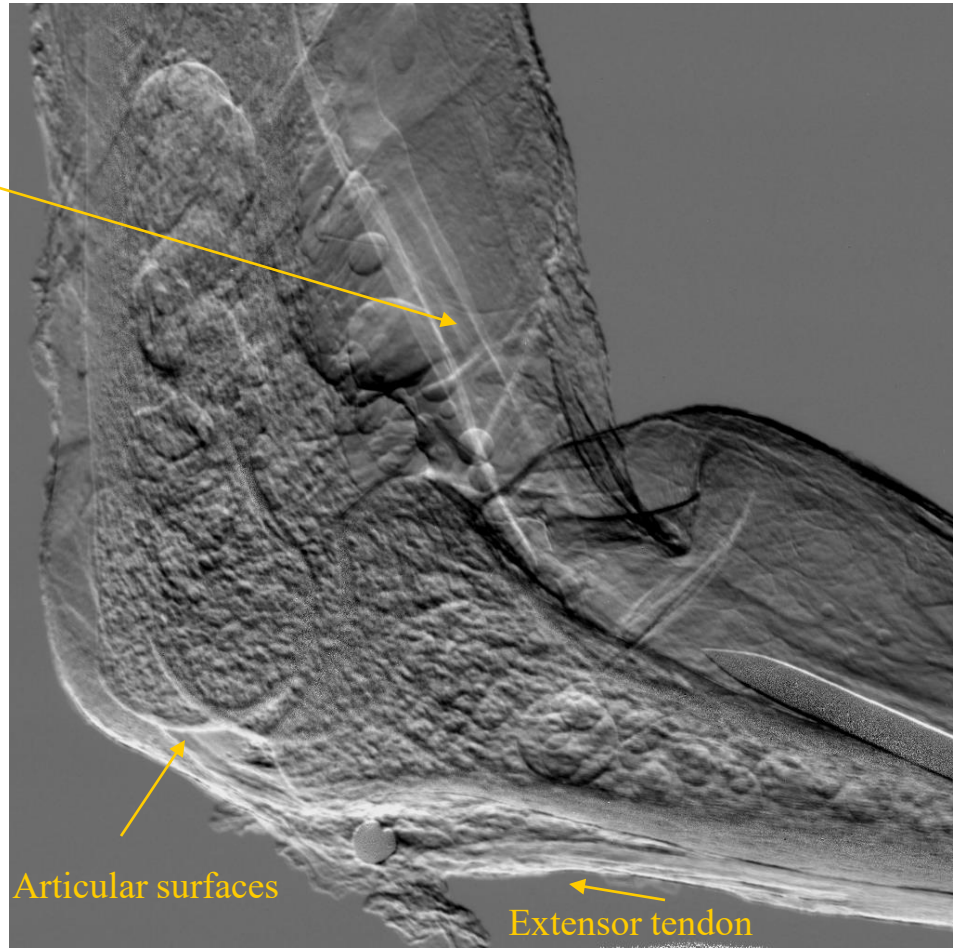

Refraction Image

Lewis, R. A., et al., British J. Rad., 76(905), 301-308 (2003)

Low dose phase contrast Lung CT - proof-of-principle study on porcine lungs

Aim: evaluate the potentials of lungs CT in humans

- samples: porcine lungs in the artiCHEST training phantom
- SR imaging: E = 40 keV, prop dist = 2.5 m, air entrance dose ~ 13 mGy
- Reconstruction: conventional FBP, phase retrieval pre-processing

SYRMEP beamline

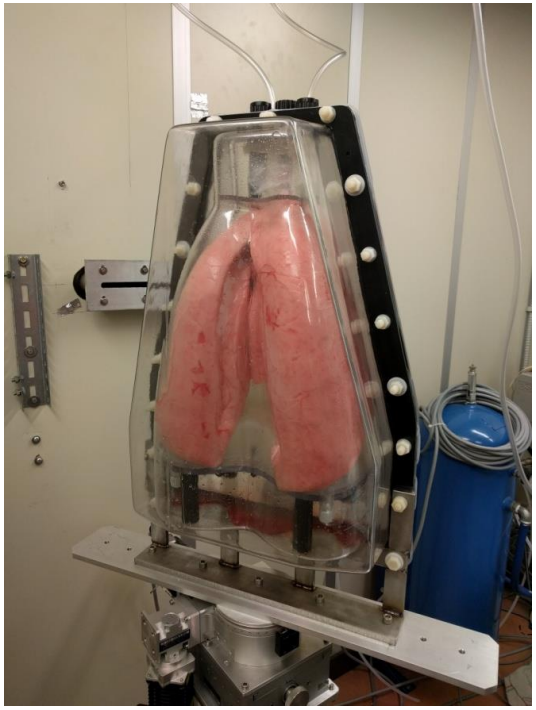

Cattinara hospital Trieste

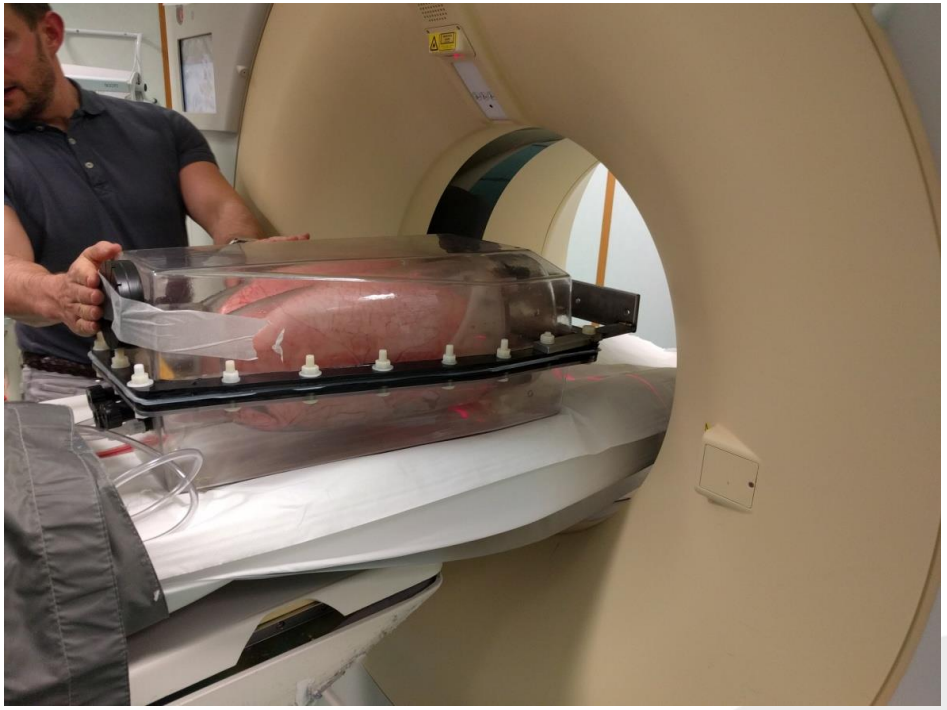

W.Wagner et al.: J.Synchrotron Rad. 25, (2018)

Elettra
Sincrotrone

Conventional CT slice

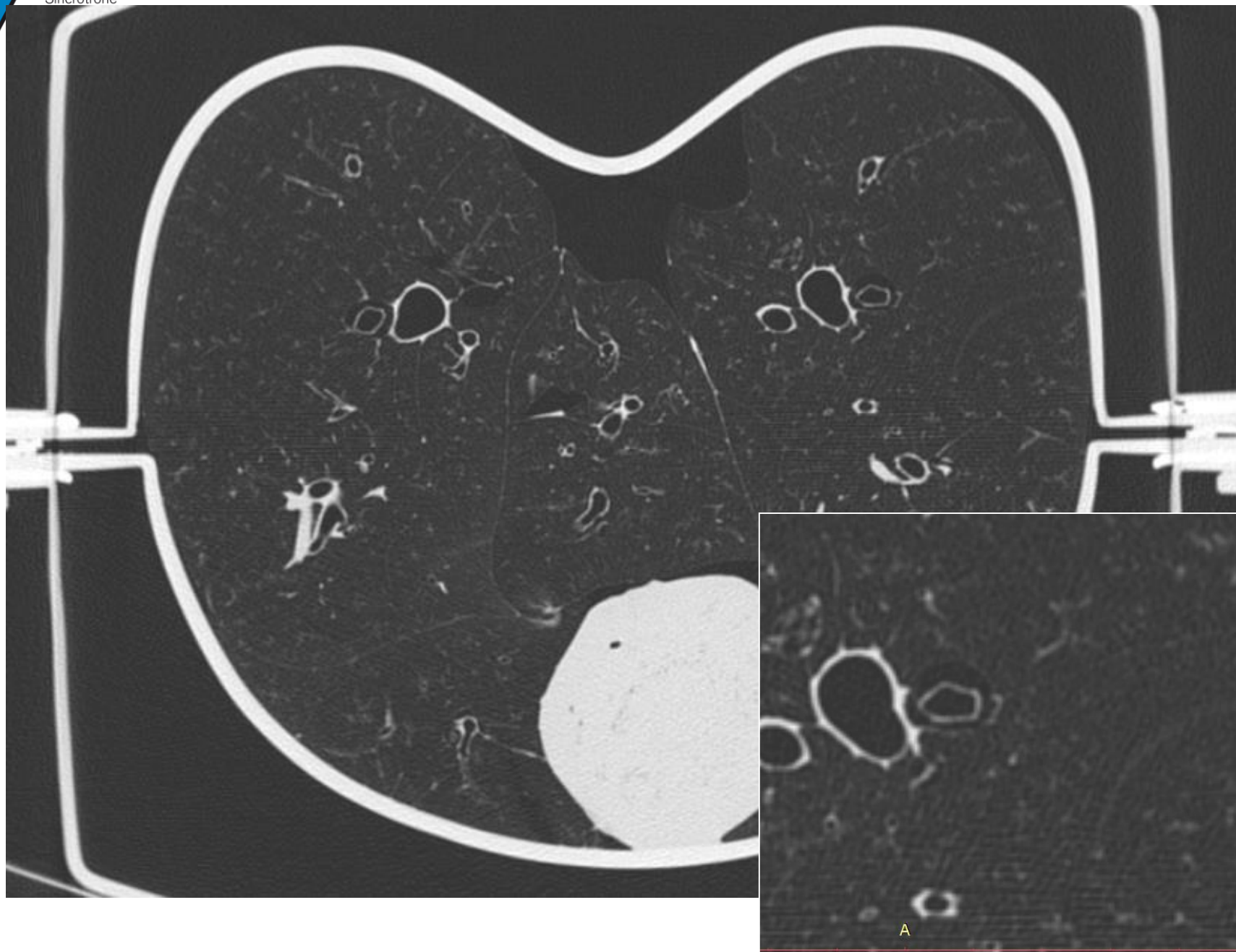

SR CT slice

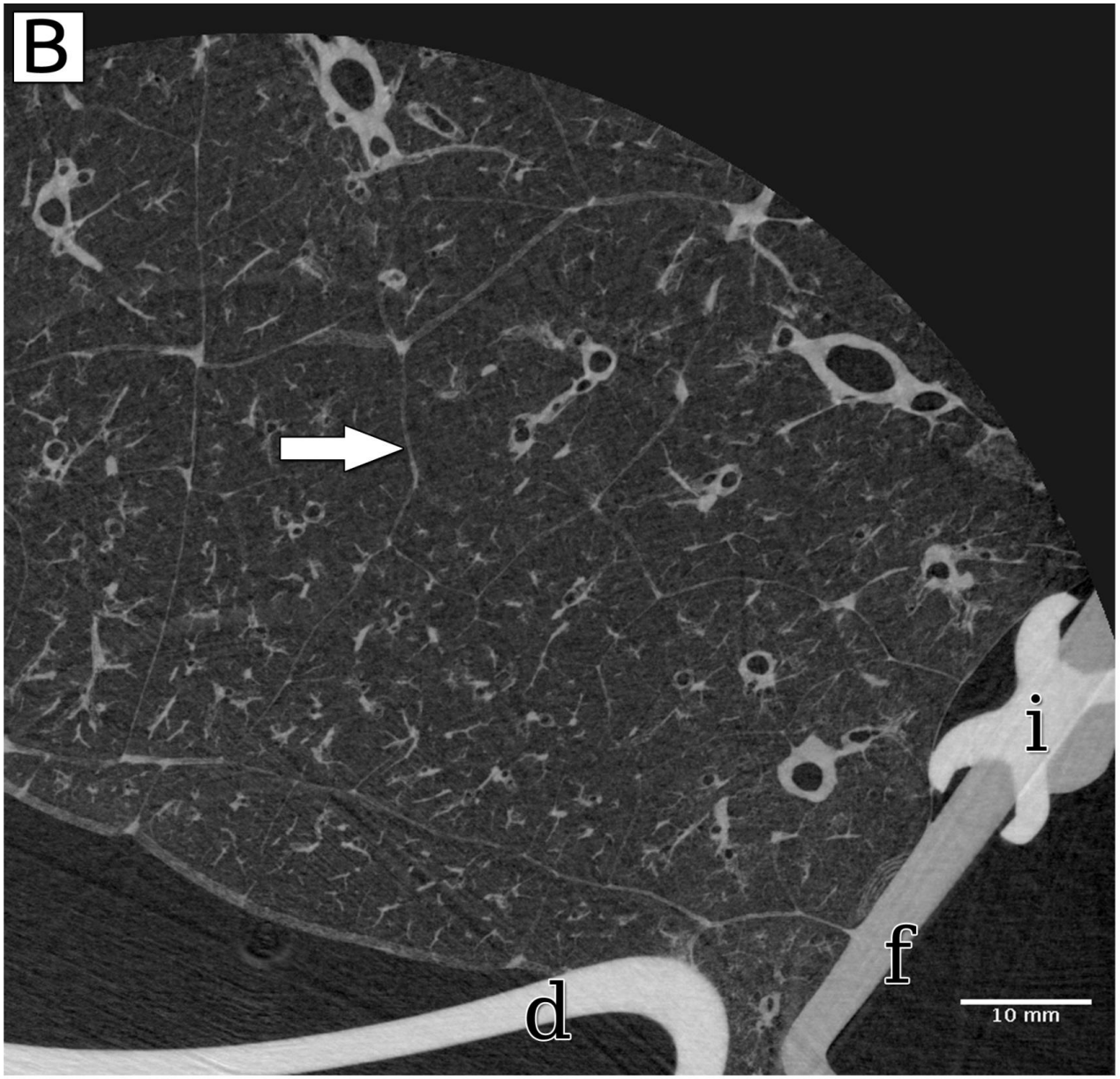

Lesions visualization

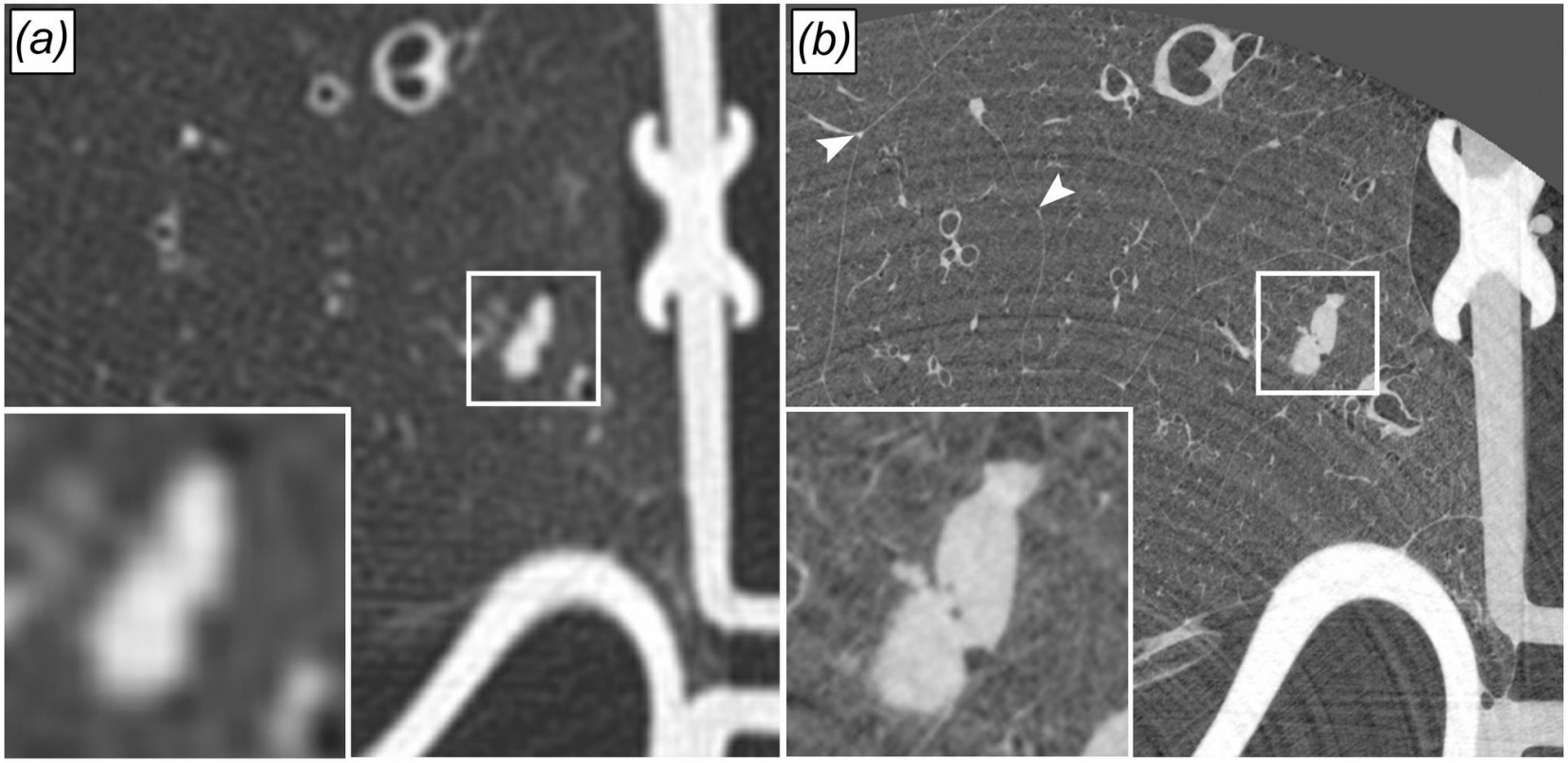

(a) clinical HRCT - air kerma ~ 33 mGy, voxel size 0.45 x 0.45 x 0.9 mm^3
(b) SYRMEP - air kerma ~13 mGy, voxel size 0.1 x 0.1 x 0.1 mm^3

W.Wagner et al.: J.Synchrotron Rad. 25, (2018)

Lesions density assessment

- Artificial nodules created by injecting in lungs of agarose at different concentrations
- Without phase retrieval no density difference between the nodules can be detected (RAW). Phase retrieval (PHR) allowed the differentiability between the nodules density.

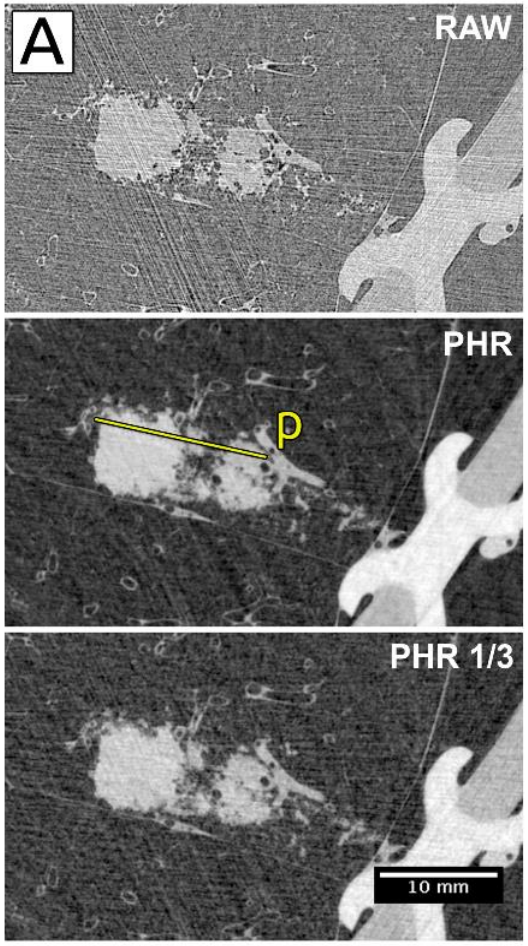

B

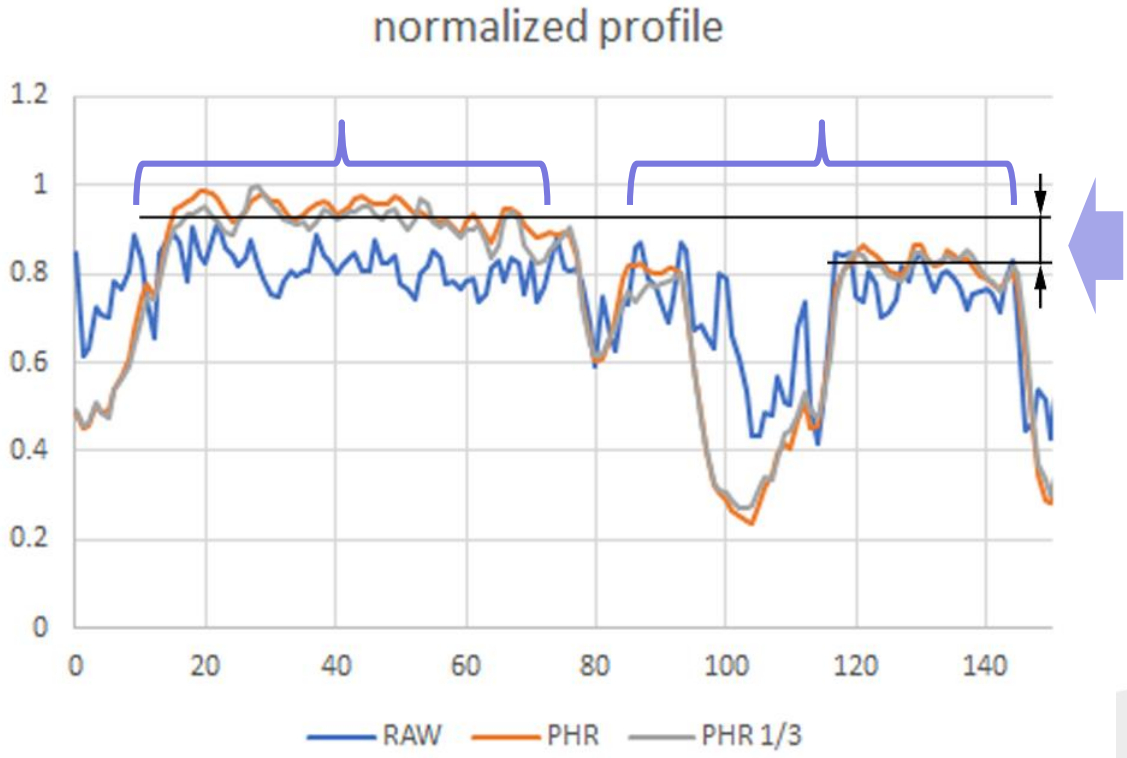

W.Wagner et al.: J.Synchrotron Rad. 25, (2018)

Quantitative analysis

Pore3D: a software tool for **3D image processing** and **analysis**

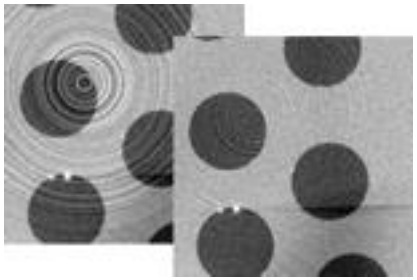

Filters
Basic (mean, median, gaussian, ...)
Anisotropic diffusion
Bilateral
Ring artifacts reduction
Binary (median, clear border, ...)

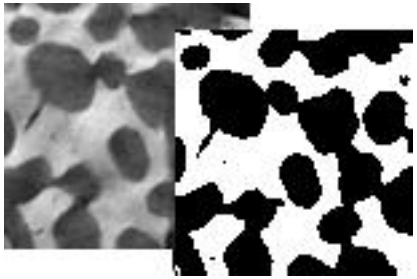

Segmentation
Automatic thresholding (Otsu, Kittler,..)
Adaptive thresholding
Region growing
Multiphase thresholding
Clustering (*k*-means, *k*-medians, ...)

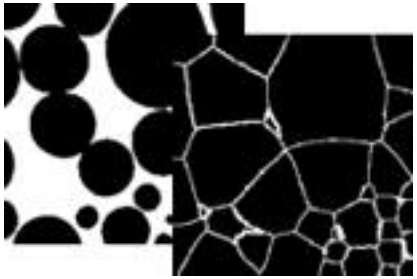

Morphological processing
Dilation and erosion
Morphological reconstruction
Watershed segmentation
Distance transform
H-Minima filter

Skeleton extraction
Thinning
Medial axis (LKC)
DOHT
Gradient Vector Flow
Skeleton pruning
Skeleton labeling

Analysis
Minkowski functionals
Morphometric analysis
Anisotropy analysis
Blob analysis
Skeleton analysis
Textural analysis (fractal dimension, ...)

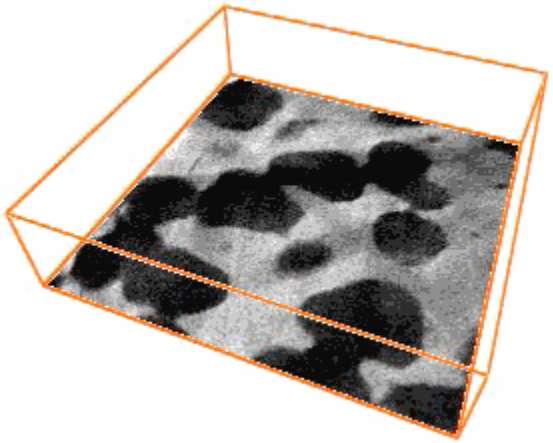

http://ulisse.elettra.trieste.it/uos/pore3d

F. Brun et al., NIM A, 615 (2010) 326–332

Bone turnover in mice exposed to micro-gravity conditions

- 3 wild type (WT) mice and 3 pleiotrophin-transgenic (PTN-Tg) mice in a special payload (MDS - Mice Drawer System). The transgenic mouse strain over-expressing pleiotrophin (PTN) in bone was selected because of the PTN positive effects on bone turnover.
- **91 days in the International Space Station (ISS) by NASA: Aug. - Nov. 2009.**
- Controls:
  - mice on Earth in the same special payload MDS (*ground* mice)
  - mice in common cages (*vivarium* mice)
- SR µ-CT experiments were performed on femurs and spines
- Being non-destructive, µ-CT is very attractive for these rare specimens

University of Genova

Elettra Sincrotrone Trieste

Università Politecnica delle Marche

University of Trieste – Dept. of Engineering

http://www.nasa.gov/mission_pages/station/research/experiments/MDS.html

Analysis of the microarchitecture of the trabecular bone in femurs

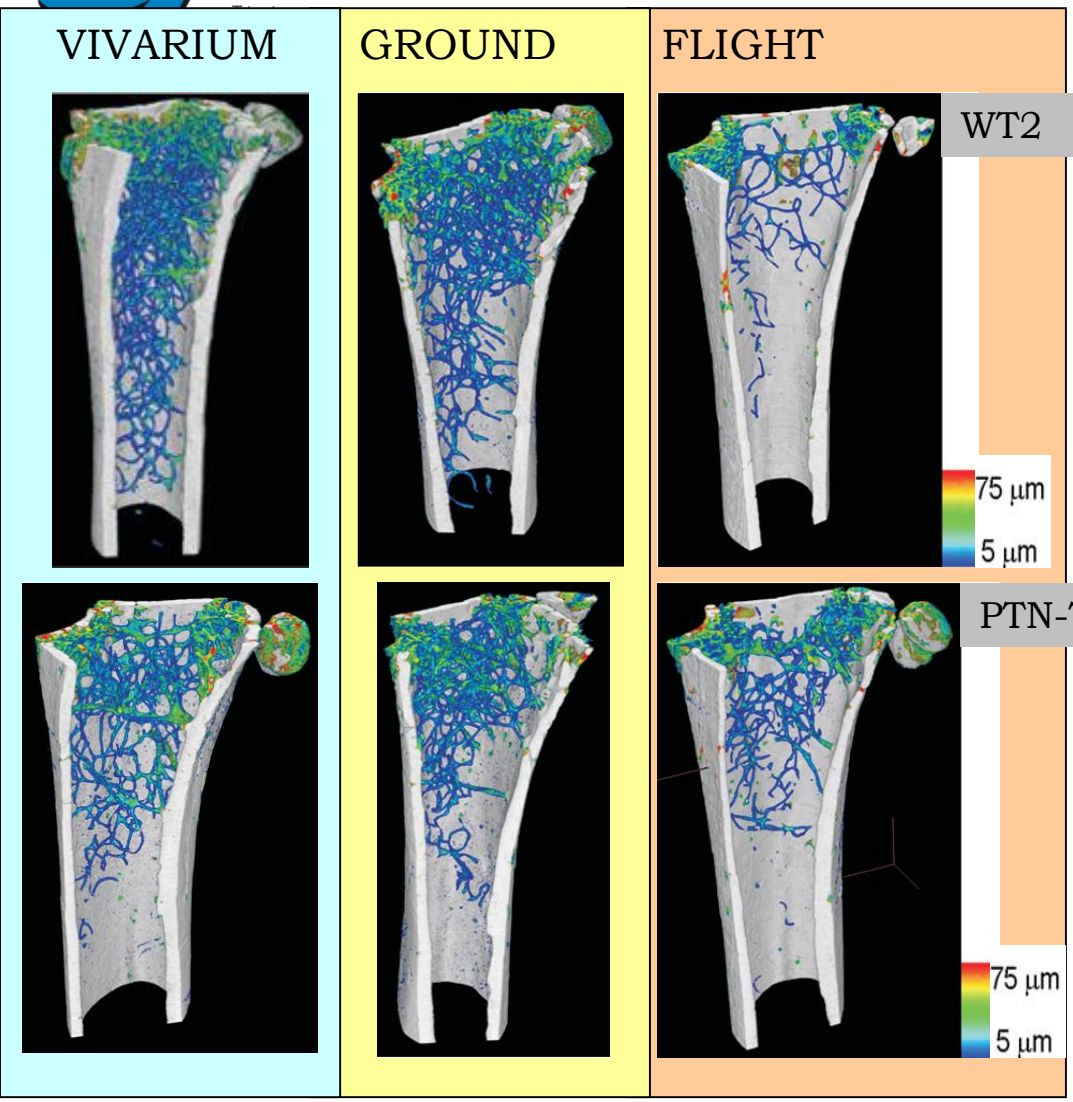

Revealed:

-a **bone loss** during spaceflight in the weight-bearing bones

-a **decrease** of the trabecular number

-an **increased** mean trabecular separation

-no significant change in trabecular thickness.

-No effects on not weight-bearing bones.

E = 19 keV
Pixel size = 9 mm
N. Proj = 900
Distance sample-ccd= 3 cm

Comparison WT vs.PTN-Tg2:

- PTN-Tg exposed to normal gravity has a poorer trabecular organization than WT mice

- the expression of the PTN gene during the flight resulted in some protection against microgravity's negative effects.

Color map represents bone trabecular thickness distribution in the femur (red = 75 µm, blue = 5 µm)

S. Tavella et al "*Bone Turnover in Wild Type and Pleiotrophin-Transgenic Mice Housed for Three Months in the International Space Station (ISS)*", *PlosONE, March 2012.*

Elettra Sincrotrone Trieste

New challenges: dynamic studies and multiscale micro-CT

- Dynamic CT studies (4DCT): repeated series of scans performed at sequential time lapses, to provide information about the microstructure evolution.
  - Application in entomology
  - First in-vivo low dose CT studies of mice lung at Elettra

- Multiscale micro-CT combines different resolution modalities on the same sample
  - Visualization of Vascular and neuronal network
  - Mise lungs visualzation at cellular level

4DCT: *in vivo* X-ray microscopy with projection-guided gating

- Visualizing fast micrometer scale internal movements of small animals
- Application of phase contrast microCT (~ 3.3 μm voxel size) with retrospective, projection-based gating
- 20 CT scans selected through the 150 Hz oscillations of the blowfly flight
- It is a key challenge for functional anatomy, physiology and biomechanics

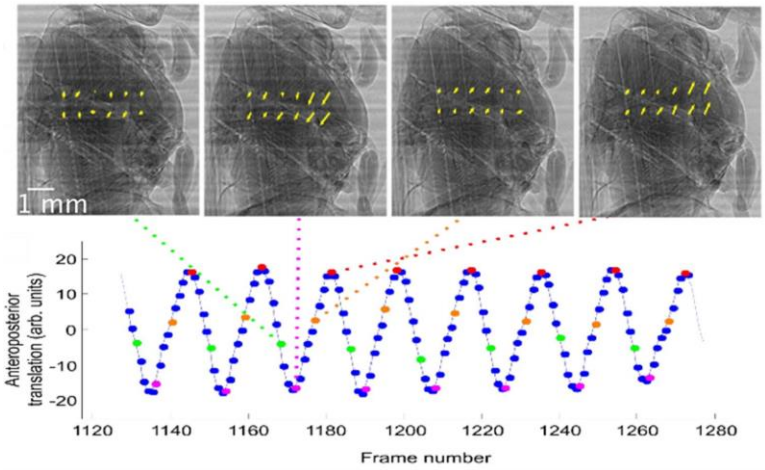

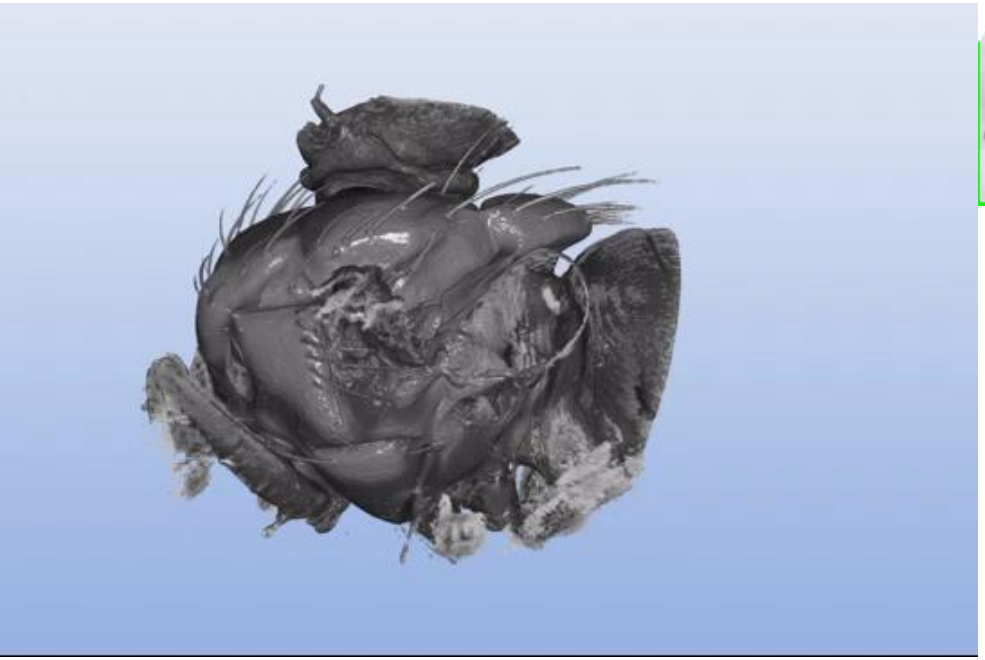

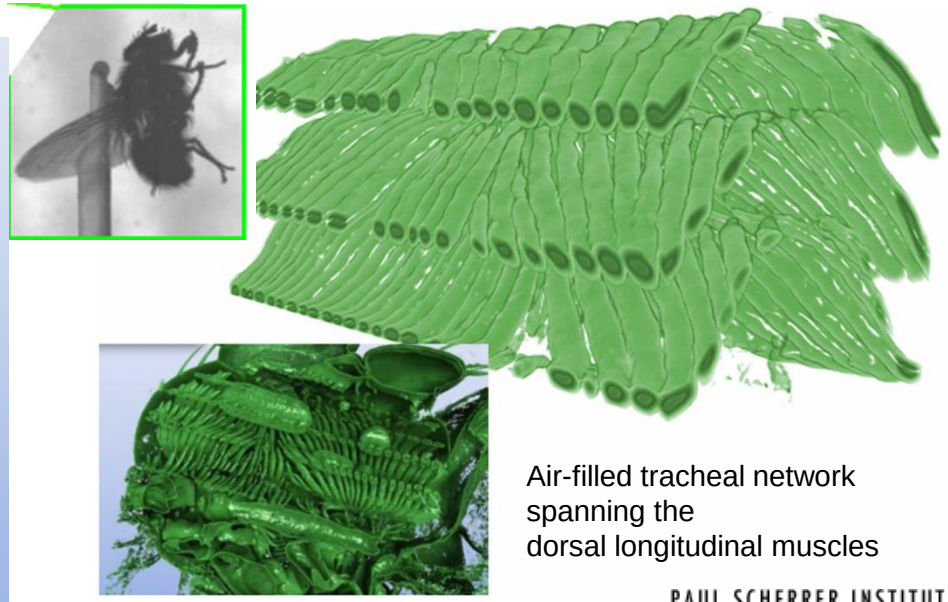

Air-filled tracheal network spanning the dorsal longitudinal muscles

Rajmund Mokso et al.: Sci. Rep. | 5 : 8727 | (2015)

Elettra Sincrotrone Trieste

Dynamic measure of **X-ray Absorption function** (Xaf) XAFs of a healthy control mouse (**blue**), an asthmatic mouse (**red**) and a dexamethasone treated mouse (**green**).

UNIVERSITÄTSMEDIZIN GÖTTINGEN : UMG

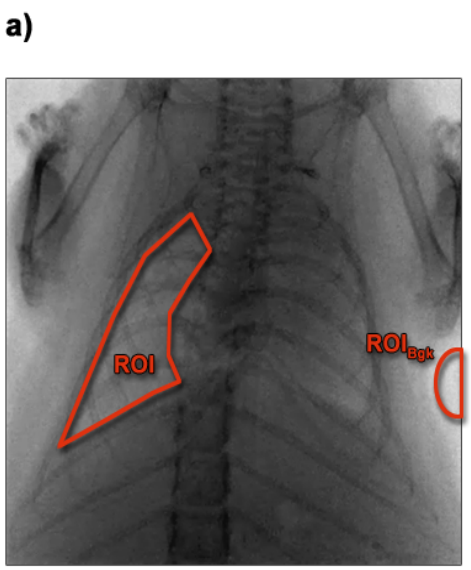

radiograph of the mouse chest

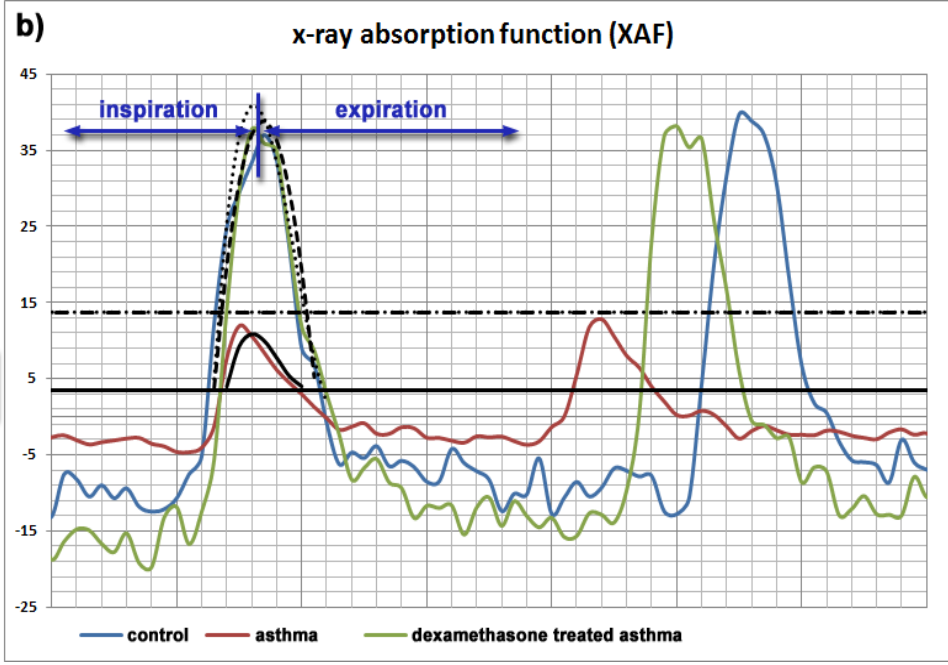

C. Dullin, et al.:, Scientific Reports | 6:36297 | 2016

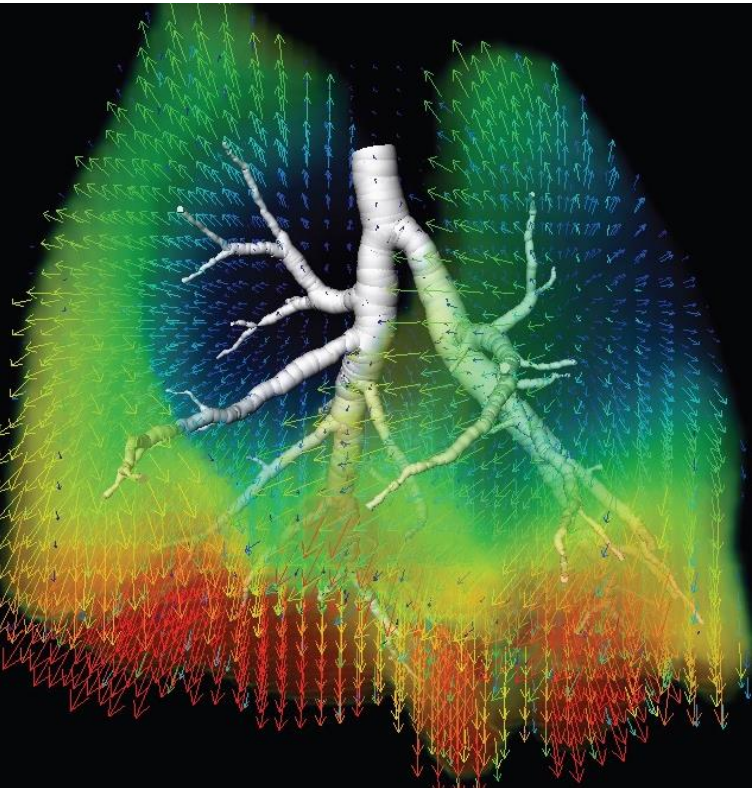

Measure of Lung function

X-ray velocimetry - 3D map of mouse lung tissue velocity during inspiration. The vectors represent tissue velocity direction, and the colours represent velocity magnitude.

SPring-8

S. Dubsky, A. Fouras, Advanced Drug Delivery Reviews 85 (201

Elettra Sincrotrone Trieste

First *in-vivo* low dose propagation based imaging in a mouse model of allergic airway inflammation

(Preliminary data – experiment performed in October 2019)

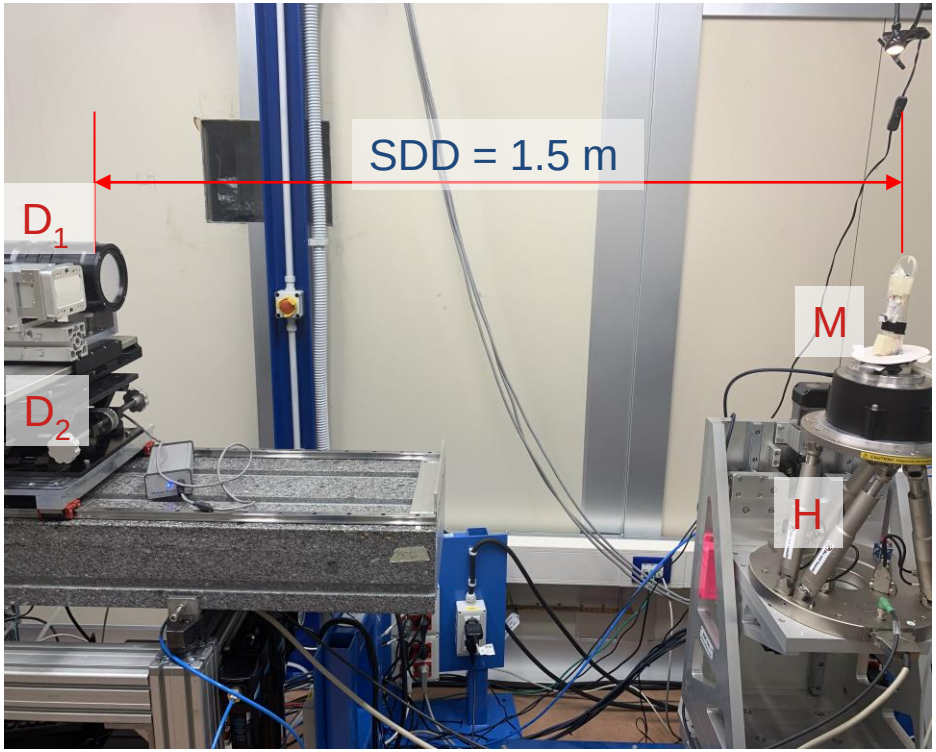

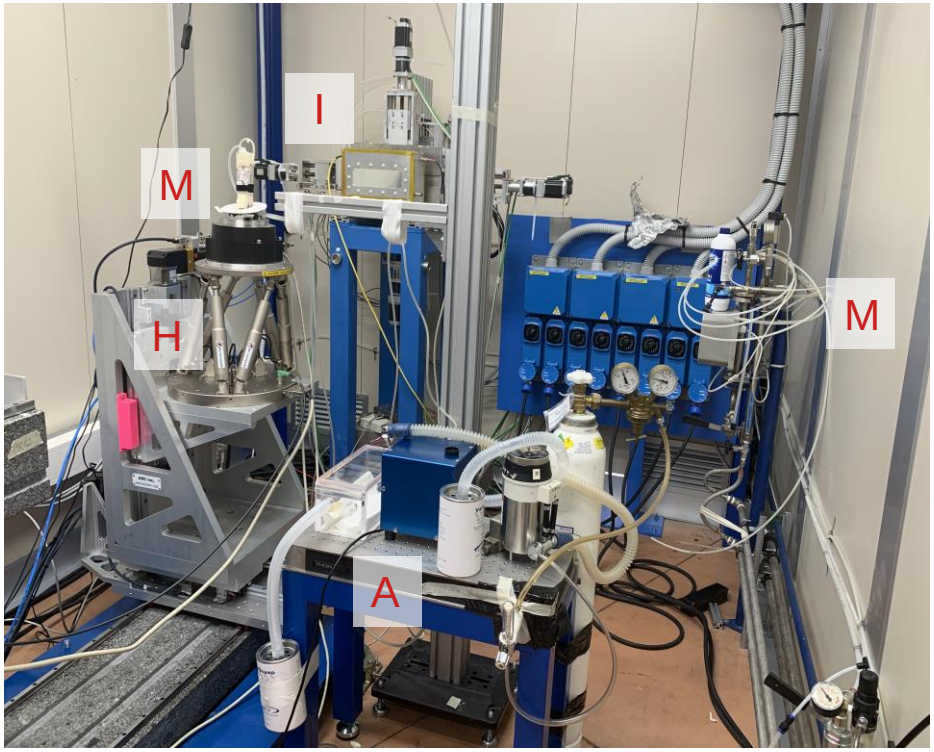

(D_1) Photonics detector, (D_2) Mönch detector, (I) Ion chamber, (A) gas anesthesia setup, (H) hexapod for positioning, (M) mouse holder with living mouse
Energy = 22 keV

⇒ 2D movies for **lung function** measurement, CT data sets for **quantification of anatomical changes**

Dullin C, Tagat A, Albers J, di Lillo F, Alvares S, Tromba G, Bergamaschi A, Alves F

UNIVERSITÄTSMEDIZIN GÖTTINGEN UMG

Preliminary Results – Photonics detector

Photonics detector - sCMOS detector by GSENSE 400 assembled by Photonic Science, 33 µm equivalent pixel
Measure of lung function and low dose CT

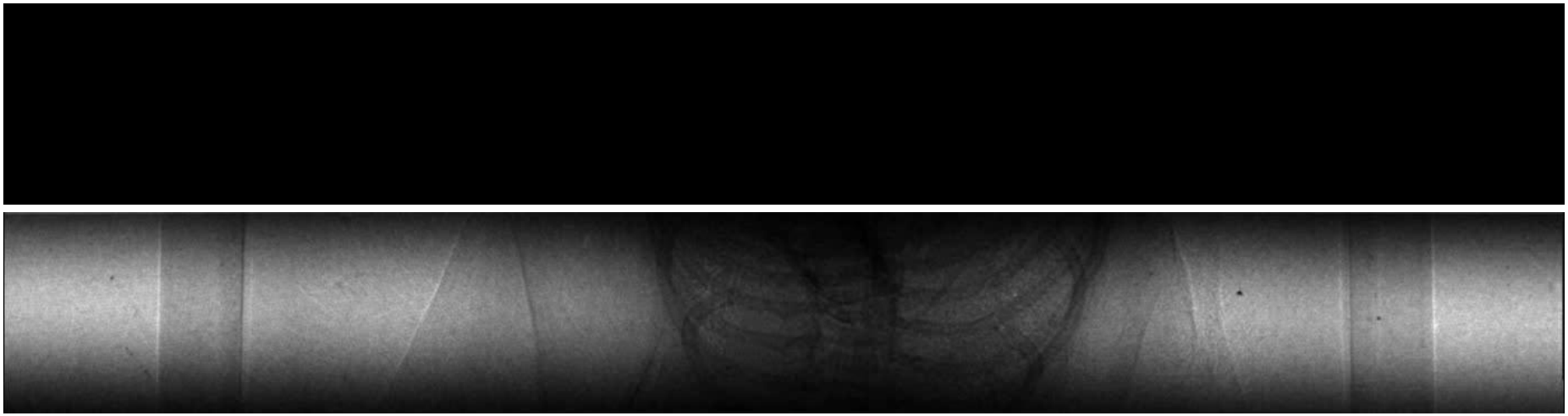

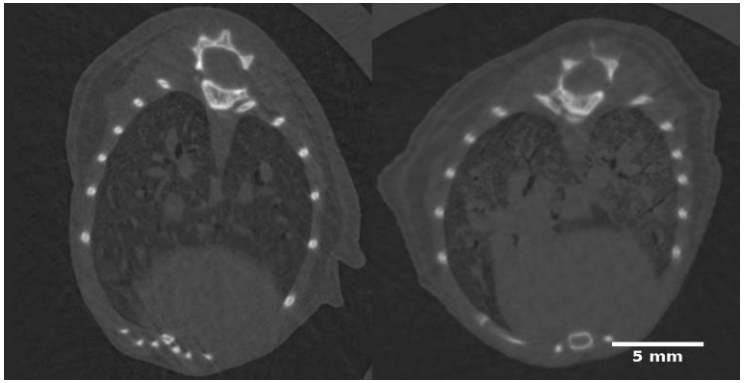

32µm, 40Hz,
56mGy, 1min

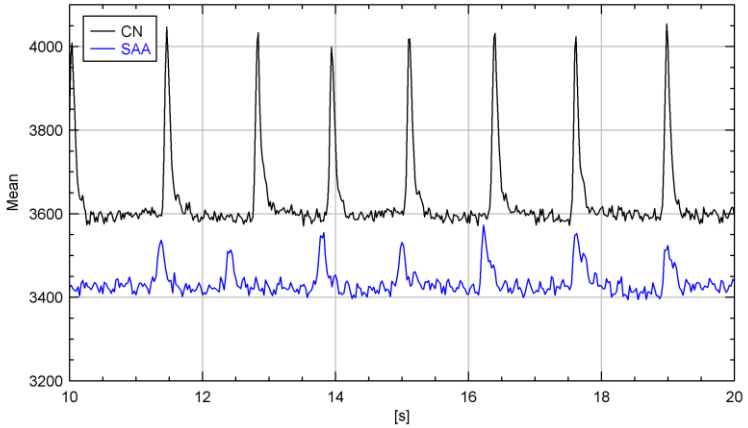

Dullin C, Tagat A, Albers J, di Lillo F, Alvares S, Tromba G, Bergamaschi A, Alves F

Preliminary Results – Monch detector

Mönch detector - (PSI), a hybrid pixel detector with charge-integrating architecture , pixel pitch = 25 µm (Dinapoli et al., J. Instrum. 9, 2014,C05015).
Measure of lung function and low dose CT

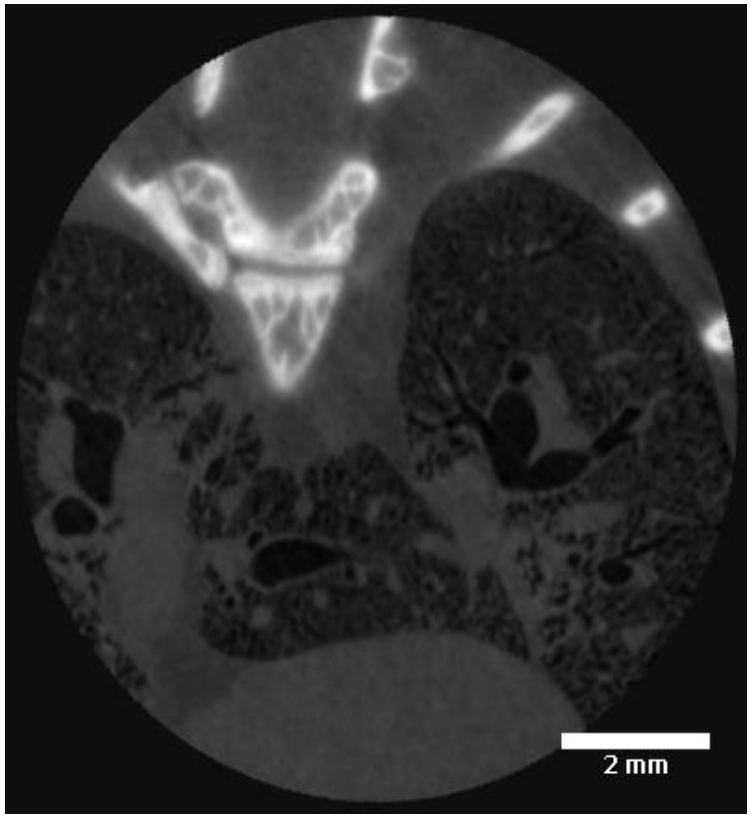

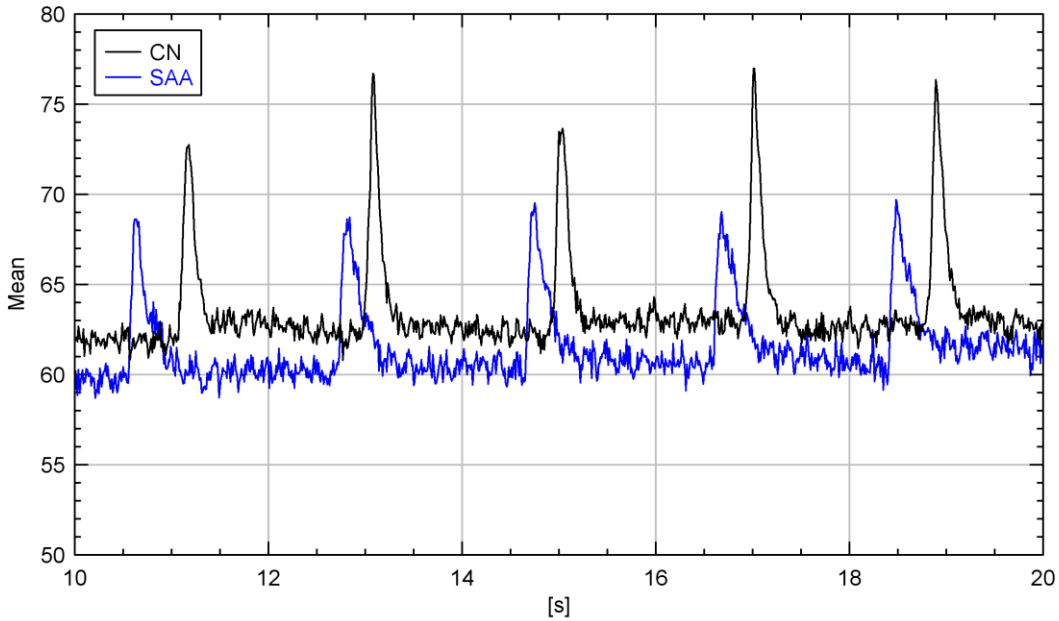

typical asymmetric shape in breathing pattern of asthmatic mice

25µm, 100Hz, 56mGy, 1min

⇒ Better spatial resolution
⇒ Higher temporal resolution
⇒ Better anatomical and functional analysis

Dullin C, Tagat A, Albers J, di Lillo F, Alvares S, Tromba G, Bergamaschi A, Alves F

Phase contrast multiscale-microCT

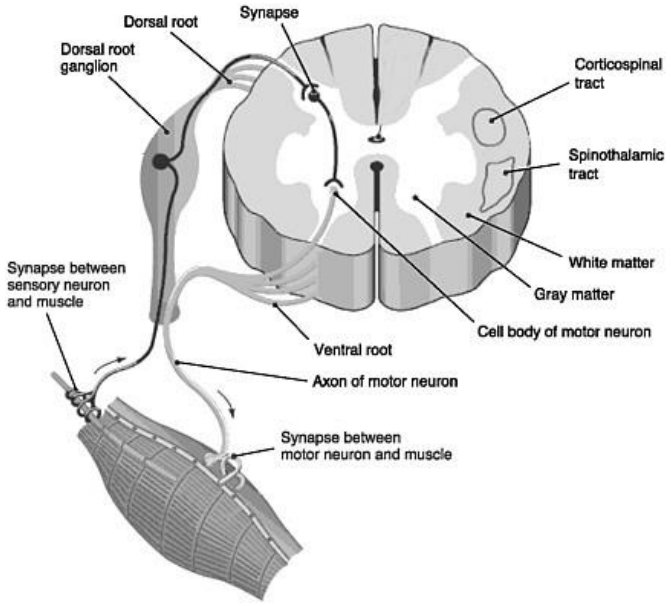

Aim:

Simultaneous 3D visualization of the vascular network (VN) and neuronal network (NN) of *ex-vivo* mouse spinal cord.

Motivation:

Pre-clinical investigation of neuro-degenerative pathologies

Reveal relationship between VN and NN

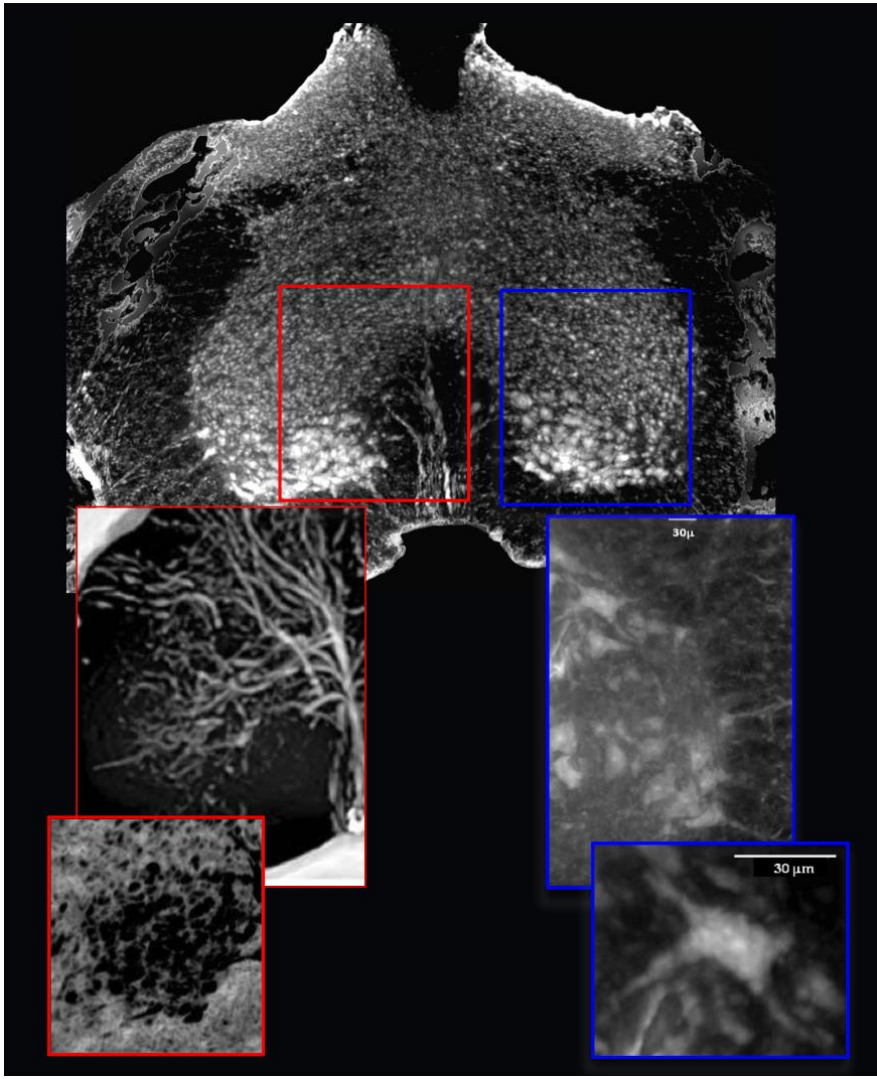

Vascular network

Neuronal network

Fratini, M. et al. (2014) Sci. Rep., | 5 : 8514 | (2014)

Multi-resolution CT: Zoom CT

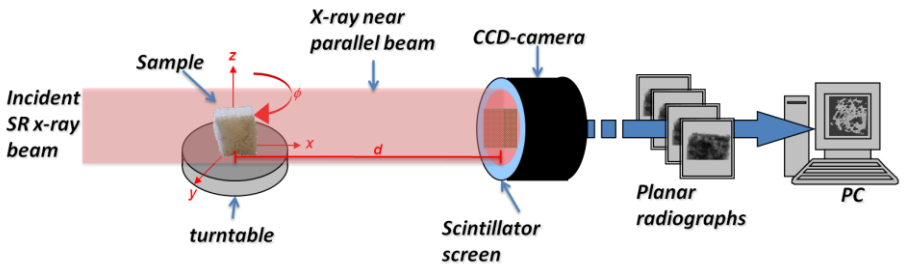

Agarose embedded mice

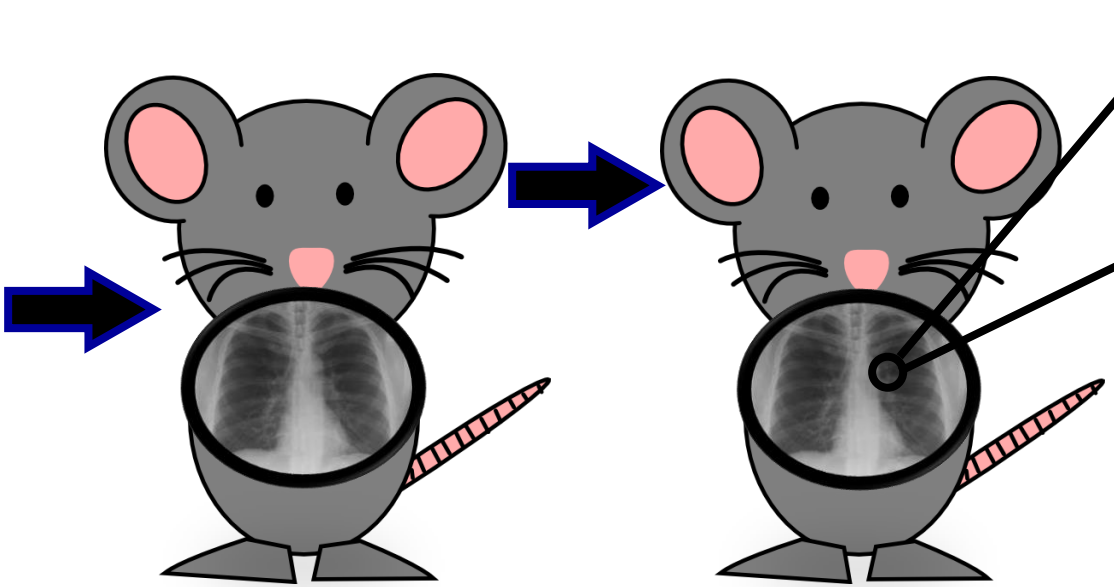

9 µm voxel size overview scan

1-2 µm voxel size region of interest scan

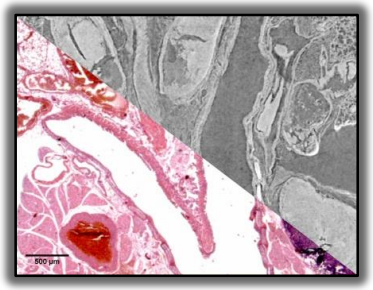

Combined CT / histology analysis

Zoom CT - Visualization of lung methastasis in mice

E = 22 keV,
pixel size = 9 μm
Slice of the entire lung

Lesion produced by cancer cells labeled by Ba np injected in blood stream

Pink beam,
pixel size = 2 μm
Phase retrieval,
δ/β = 1950

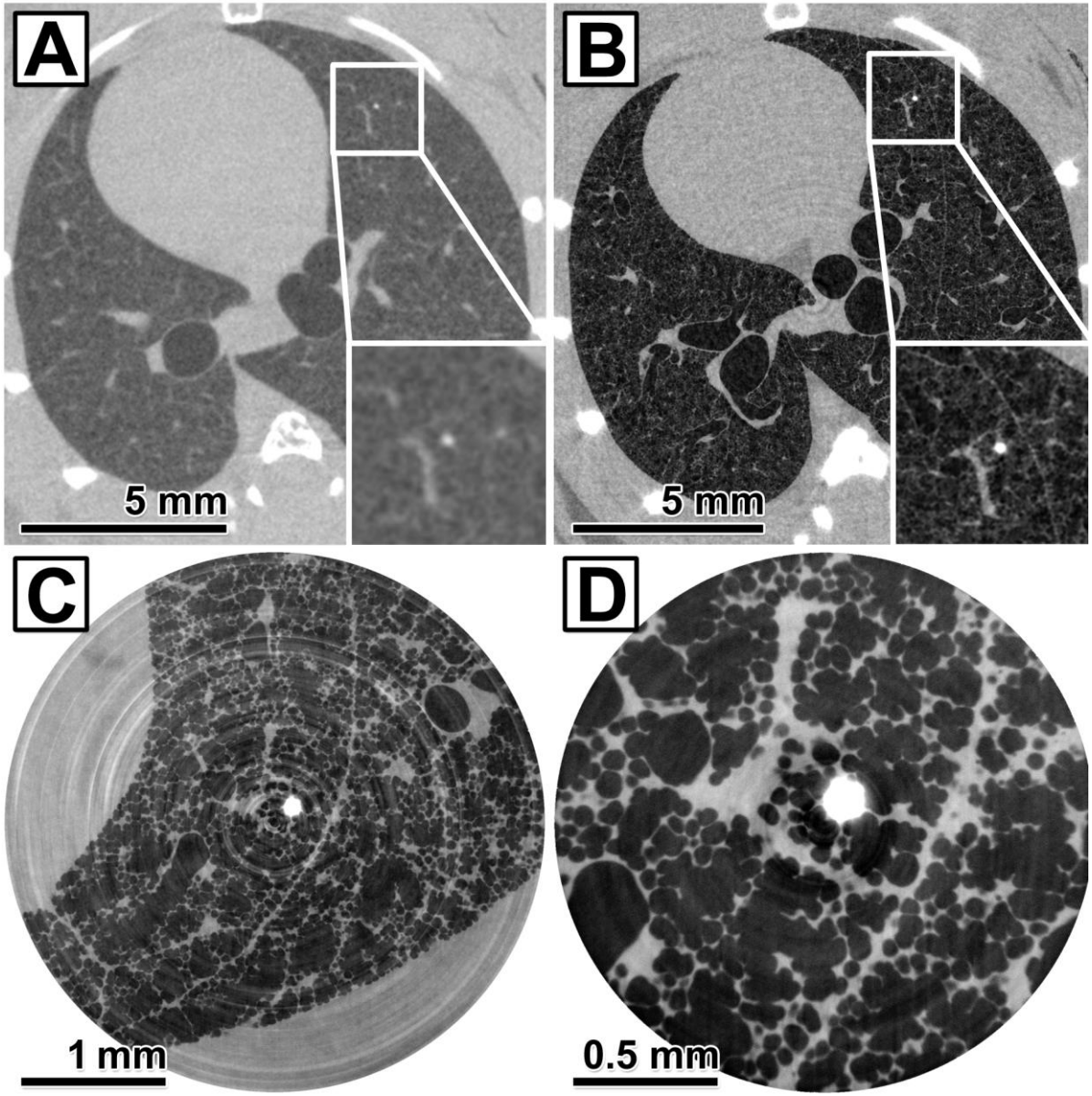

E = 22 keV,
pixel size = 9 μm
Phase retrieval,
δ/β = 1950

Pink beam,
pixel size = 1 μm
Phase retrieval,
δ/β = 1950

(Courtesy of J. Albers)

Zoom CT - Volumes

pixel size = 9 μm

pixel size = 1 μm

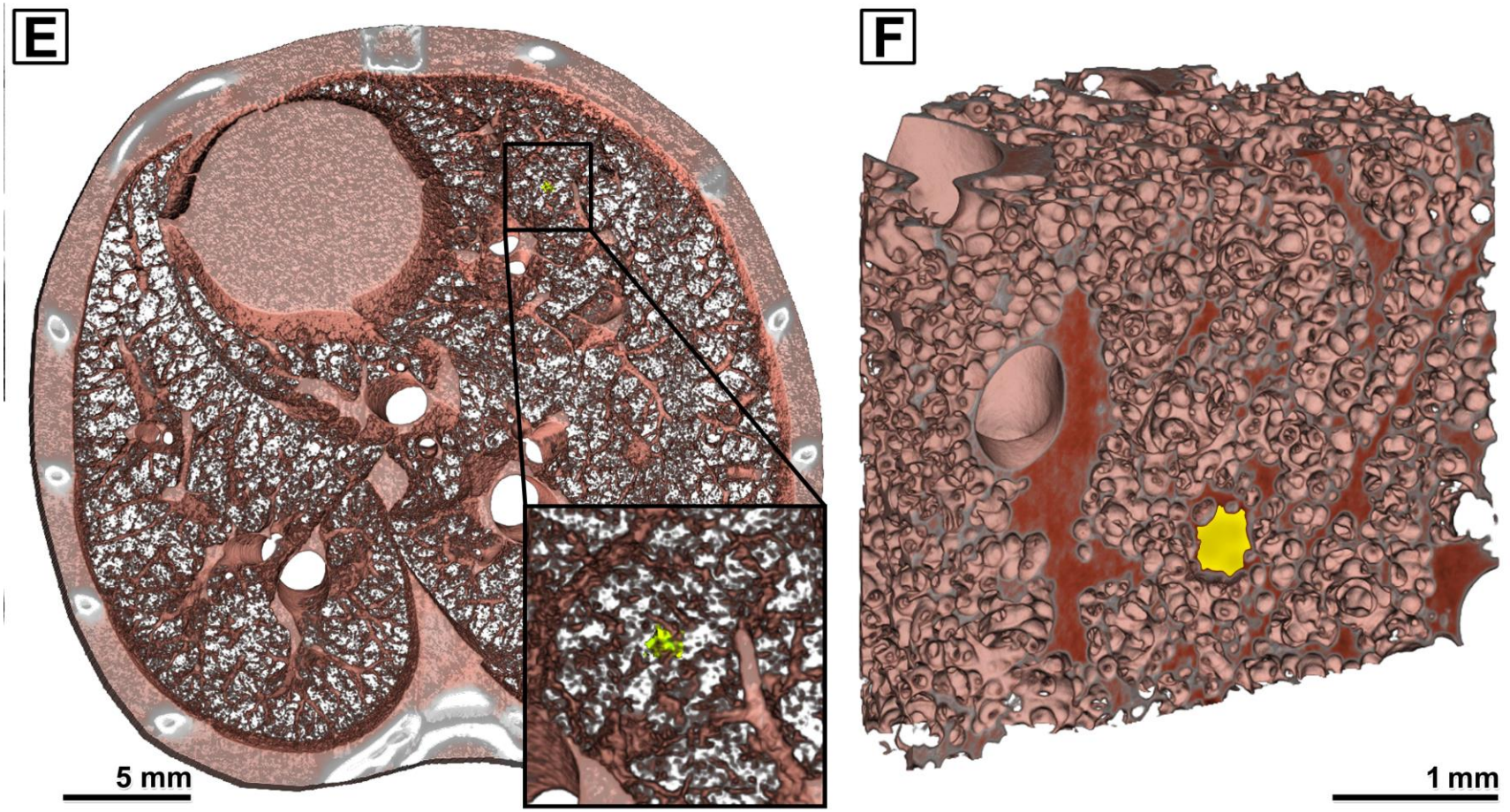

pixel size = 2 μm

UNIVERSITÄTSMEDIZIN GÖTTINGEN UMG

(Courtesy of J. Albers)

Contact: **giuliana.tromba@elettra.eu**